

# 1 Hyperbolic navigation systems

## 1-1 Introduction

A navigation system in which two transmitting stations transmit certain specified types of radio wave, according to the rated time sequence, and in which a user of the system finds his position by measuring the difference in distance between him and the two transmitting stations, is called a "hyperbolic navigation system". Under such system, the locus of the points having a certain difference in distance forms a hyperbola, and the user determines two of such hyperbolas (which are referred to as "line of position") from the two pairs of transmitting stations he selects, to fix his position at the point of intersection between these two hyperbolas.

The Decca Navigator system, Loran A system and Loran C system are representative of the hyperbolic navigation systems.

### 1) Phase difference and difference in distance

Supposing that the frequency of the radio wave transmitted from the transmitting station is 100 KHz and the propagation speed of the radio wave is  $3 \times 10^8$ m (in actual cases this speed alters according to the condition of propagation path), the wave length of this radio wave would be 3000 metres, that is, the radio wave of 100 KHz would propagate 3,000m during one cycle. Since the phase angle changes from  $0^\circ$  through to  $360^\circ$  during the one cycle, the radio wave of 100 KHz would propagate 3,000m during the time the phase angle of  $360^\circ$  changes. Figure 1-1 shows the state of this propagation. If the frequency and propagation speed of a radio wave are given, as in the above case, the distance may be replaced by the wave length or phase of radio waves. A difference in the distance from the two transmitting stations can be measured as phase difference of the radio wave transmitted by the transmitting stations.

Suppose radio waves are transmitted continuously on the same frequency and at the same time from Point A and Point B in Fig. 1-2 so as to make the phase of the transmitted waves from A and B identical (this is called "phase synchronization"), the phase of the radio waves from both stations would be completely identical at Point P which is situated at an equal distance from points A and B. There is no phase difference and this indicates that no difference in distance at this point. However, as seen from this figure, there are many points other than Point P, at which the phase difference becomes zero, and therefore some method should be worked out to select a single point wanted (this will be explained further in the paragraph of "Lane identification").

If point P in Fig. 1-2 moves to Point P', the phase of the radio waves from Point A would be  $270^\circ$  and the phase from Point B  $90^\circ$ , and since the phase difference is  $180^\circ$  in this case, the difference in distance would be known to be 1,500m. Further, the phase difference at Point Q is  $360^\circ$  and the difference in distance is therefore 3,000 m.

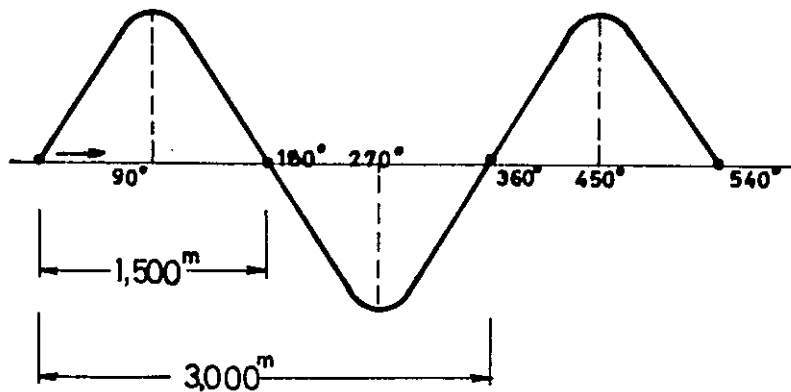


Fig. 1-1 Phase and Distance

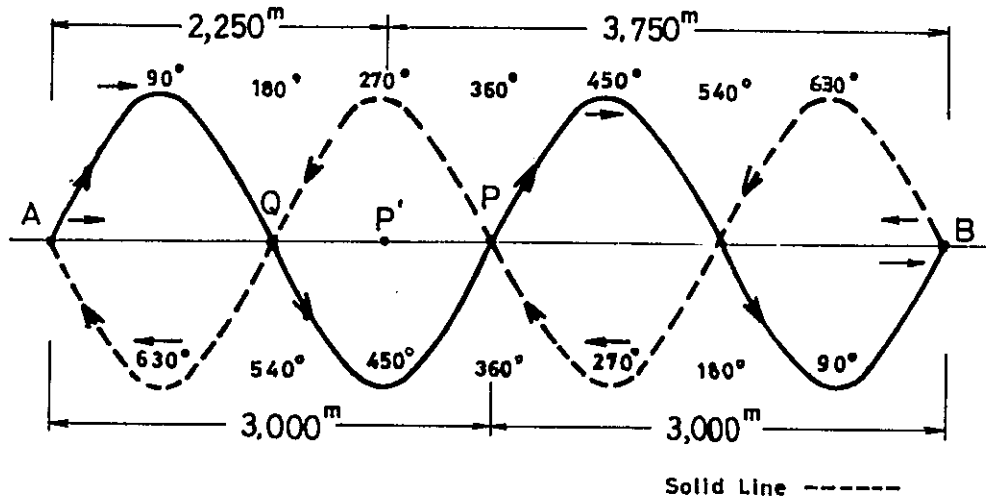


Fig. 1-2 Difference in Distance and Phase Difference

1-2 Decca Navigator system

1-2-1 Principle of Decca system

The effect of transmitting signals of equal frequency from the master and slave is achieved by assigning harmonically-related values to the two frequencies so that multiplying circuits in the receiver can derive from each a common harmonic. Thus in the red hyperbolic pattern, for example, the master and slave signals are multiplied to a common frequency of  $24f$ , where  $f$  is a non-transmitted fundamental value of about 14 kHz, and their phase is compared at this common frequency. The master transmits a signal of frequency  $6f$  and the slave  $8f$ , the respective channels in the receiver being followed by 4 and 3 multiplier stages; geometrically the system behaves as if the common frequency  $24f$  (about 340 kHz) were radiated from the two sites. The purple and green hyperbolic patterns are generated in a similar manner by using different frequency values and multiplication factors as indicated in Table 1-1. The basic arrangement of the receiver is shown in Fig. 1-3.

Nearly all Decca navigational chains have three slave stations disposed around the central master and thus provide three inter-



secting hyperbolic patterns; in practice the user selects the two lines giving the best angle of cut at his location and rejects the third. Table 1-1 also shows typical values for lane width on the interstation baselines. A lane is the name given to the space bounded by two adjacent hyperbolic position lines having the same phase-difference value, so that in crossing a lane the receiver records one complete cycle of phase difference. Interpolation of one-hundredth of a lane can be realized in practice and corresponds to a change of position of the order of 5 metres along the baseline where the lanewidth is narrowest.

Table 1-1 Typical values for radiated and comparison frequencies and wavelength

( $f = 14.16 \text{ kc/s}$ )

Stations	Harmonic	Frequency kc/s		Wavelength m
		Radiated frequencies		
Master	6f	85.000		3521
Red slave	8f	113.333		2640
Green slave	9f	127.500		2347
Purple slave	5f	70.833		4225
		Comparison frequencies		
Red	24f	340.000		880
Green	18f	255.000		1174
Purple	30f	425.000		704
		Lane-width on baselines assuming a velocity of 299250 km/s		
		metres		yards
Red		440.074		481.28
Green		586.765		641.70
Purple		352.059		385.02

Fig. 1-4 is a drawing representing the position-line patterns produced by a chain of stations and showing the red and green decometer readings that will be obtained on board a ship at the position indicated. The lanes of each pattern are subdivided into zones, the latter being identified by letters of the alphabet. The lanes are numbered, using a notation which prevents confusion between the three patterns, and there are respectively 24, 18 and 30 red green, and purple lanes per zone. Each lane is numbered in such a way as 0 through 23 for the red station, 30 through 47 for the green station and 50 through 79 for the purple station. The zones have the same width for each pattern (approximately 10 km on the baseline) and their width is such as to correspond to a phasecomparison frequency of the fundamental value  $f$ . In each decometer the basic phase-meter drives a fraction pointer which makes one revolution per lane, and the successive lanes are counted by an appropriately geared pointer which makes one revolution per zone. The zone letters are indicated by a dial, viewed through an aperture below the centre of the instrument, which is driven by a further set of gearing.

The effectiveness of a Decca lane identification system proves that it will be sufficient if the ship's position is known within less than half a zone, when starting a journey or when entering the coverage, and then her precise position within this zone can be obtained from the LI meter and decometers. According to the aforesaid information, the lane and zone indicators on the decometers are then set in a manner similar to the adjustment of the hands of a clock, thereafter, so long as reception is uninterrupted, the ship's movement through the patterns will be continuously recorded by the decometers, and readings may be taken from them at any time and plotted on the hyperbolic chart.

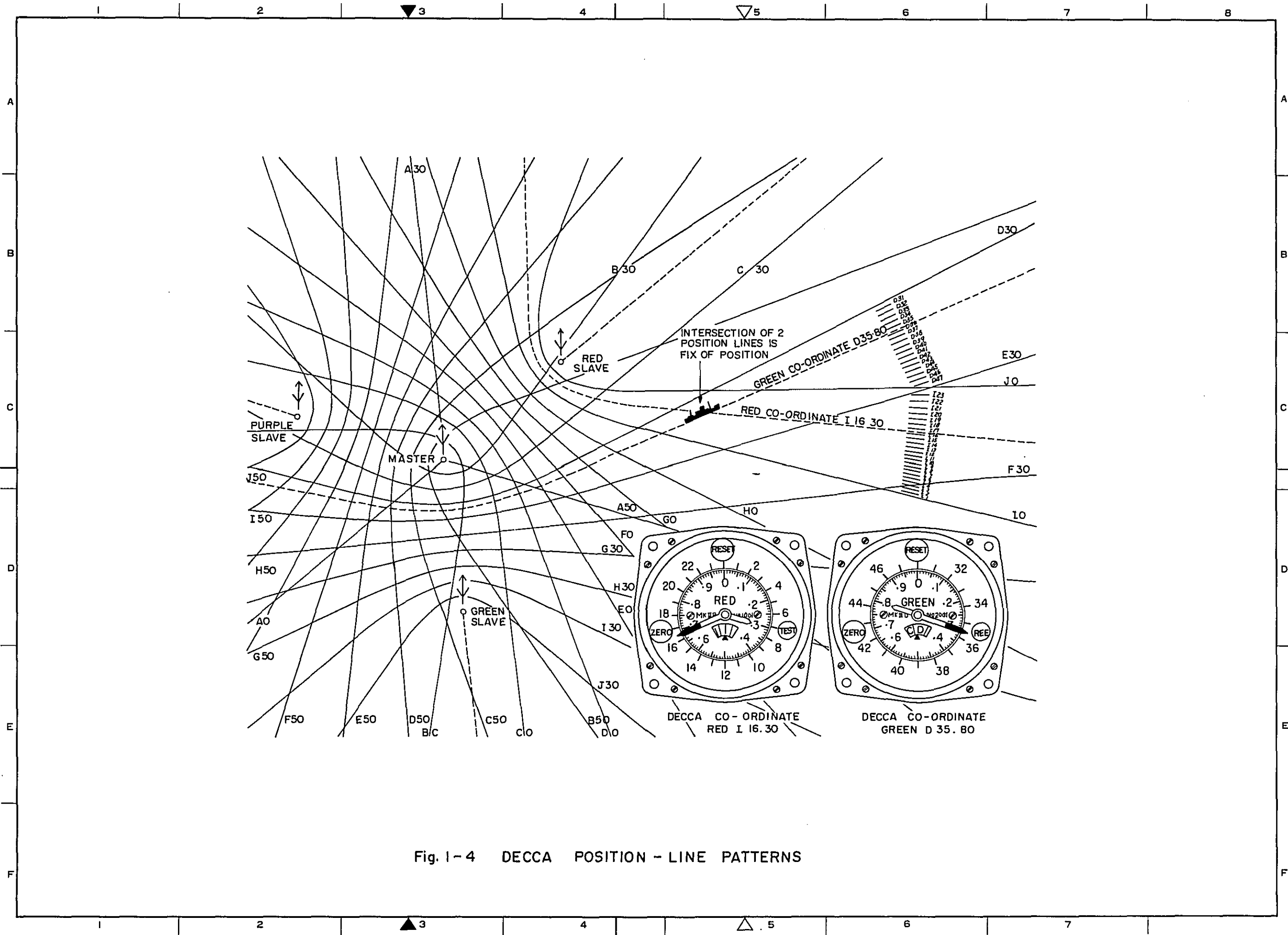


Fig. 1-4 DECCA POSITION - LINE PATTERNS

## 1-2-2 Decca charts

The Decca position lines are plotted on charts in the colours accepted at standard for the patterns: red, green and purple. The lines are numbered according to the convention adopted for the decometer dials, i.e. the lanes in each zone are numbered 0 - 23 for red, 30 - 47 for green and 50 - 79 for purple as shown in Fig. 1-4. A transparent rule carrying a number of different-sized decimal scales is issued for the purpose of interpolating fractional values within a lane. In a few charts of very large scale, the lanes are subdivided into fractional position lines, e.g. every 0.5 lane. The zone boundaries are printed more boldly than the lanes and are lettered A - J. In patterns containing more than ten zones, zone J is followed A, B, etc.



### 1-2-3 Lane identification

The function of a Decca receiver in the Decca Navigator system is to accurately measure the phase difference between a pair of signals from the master and a certain specified slave station and display the phase difference on the decometer. There is a decometer for each of the combinations of master/red slave, master/green slave and master/purple slave, and they are called red decometer, green decometer and purple decometer respectively.

The decometer automatically displays, immediately upon the switch-on of the receiver, so long as it is within the effective area of a transmitting station, the width of a lane in a hundred equal parts. The Decca pattern produced by the master and a slave station includes many lanes and everytime the receiver crosses a lane within this pattern, the decometer's pointer records the number of lanes automatically. In normal use, the decometer continues to indicate correct value at all times during the equipment is in operation, if the value of the zone and lane is set, precisely prior to the starting of the decometer. If, for some reason, the action of the equipment is interrupted while the vessel is underway, the decometer will fail to indicate correct value, in which case the decometer should be reset. This resetting of the decometer at sea is called "lane identification".

The lane identification is necessary in order to:

- 1) Set the value of zone and lane to its original position;
- 2) Correct the decometer when service is interrupted for some reason.

In the Decca system, it is designed that the zone widths are so sufficiently wide that the navigator will find it unnecessary to carry out zone identification. The zone widths are more than 10 km long on the baseline. Accordingly, Decca marine receivers have no function for carrying out zone identification.

The widths of lanes are, on the other hand, not very wide which makes it imperative for a vessel to know in which lane she is. To conduct lane identification is nothing less than allowing the person who carries out such lane identification to find at what point in a zone he is now situated. As stated before, the zone means an interval between the two adjoining points where the phase difference is zero, of the basic frequency  $1f$  (about 14 KHz). Lane identification is thus possible by making a phase comparison of  $1f$  of the signal from the master station and one of the slave stations and indicating the value produced by the comparison on the indicator.

The multipulse system (Mark 10 transmission system) is the latest system for transmission capable of setting up automatic lanes and providing zone identification for airborne receivers. The lane identification pattern is a coarse  $1f$  pattern which is effectively superimposed on each of the three normal patterns in turn. The  $1f$  pattern is generated by a brief transmission of the normal pattern frequencies  $5f$ ,  $6f$ ,  $8f$  and  $9f$  from each of the stations in turn, transmissions from the other three stations being suppressed at these items.

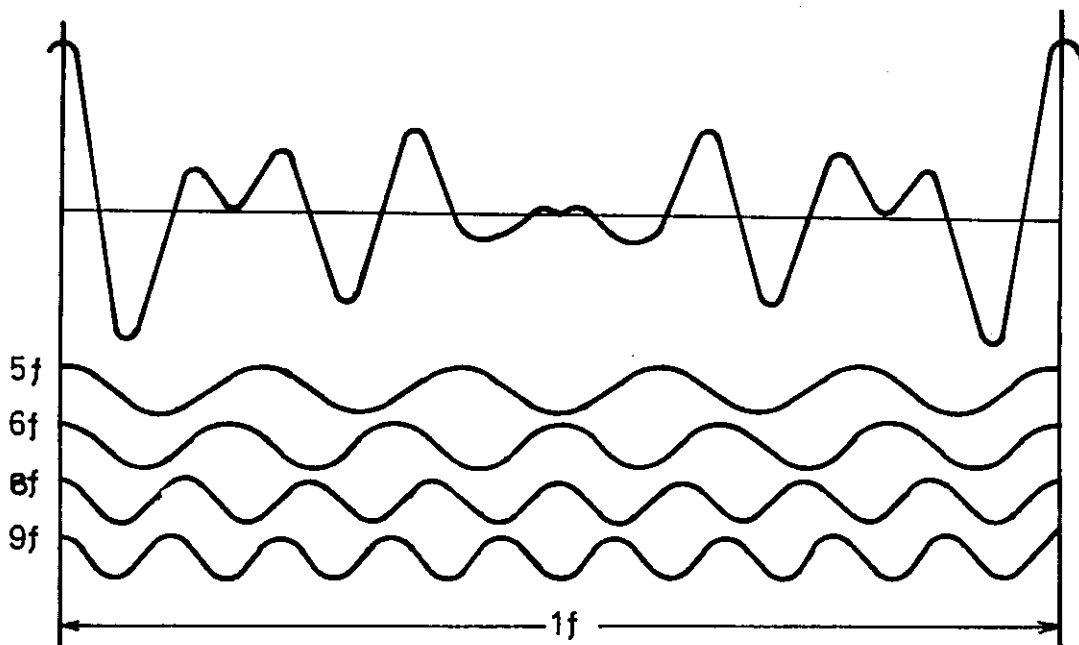


Fig. 1-5 Identification Pulses of Mark 10 System

These "multipulse" transmissions are carefully phased at the transmitting station, and the resultant waveform, shown in Fig. 1-5, provides a 1f pulse component. It can be shown that individual variations in phase of the four component frequencies forming the pulse will give rise primarily to amplitude variations in the resultant phase signal and, only when there are very large phase variations, to the production of a false pulse displaced in phase with respect to the wanted one.

Just prior to the multipulse transmissions, each station radiates a guard transmission for a short period on a frequency of  $8.2f$  to initiate switching in certain types of receivers in the field. The master guard transmission is also used a zero time synchronising signal by the slave station. The multipulse transmission sequence is initiated three times a minute as shown in Fig. 1-6.

#### 1-2-4 Frequency channels

The frequency bands of 70 to 90 KHz and 110 to 130 KHz are approved for the 3rd district for the Decca Navigator system under the International Telecommunication Convention.

On the basis of this, sixty-three frequency channels are provided for the Decca Navigator system under the standards shown in Tables 1-2 and 1-3 in the following pages:

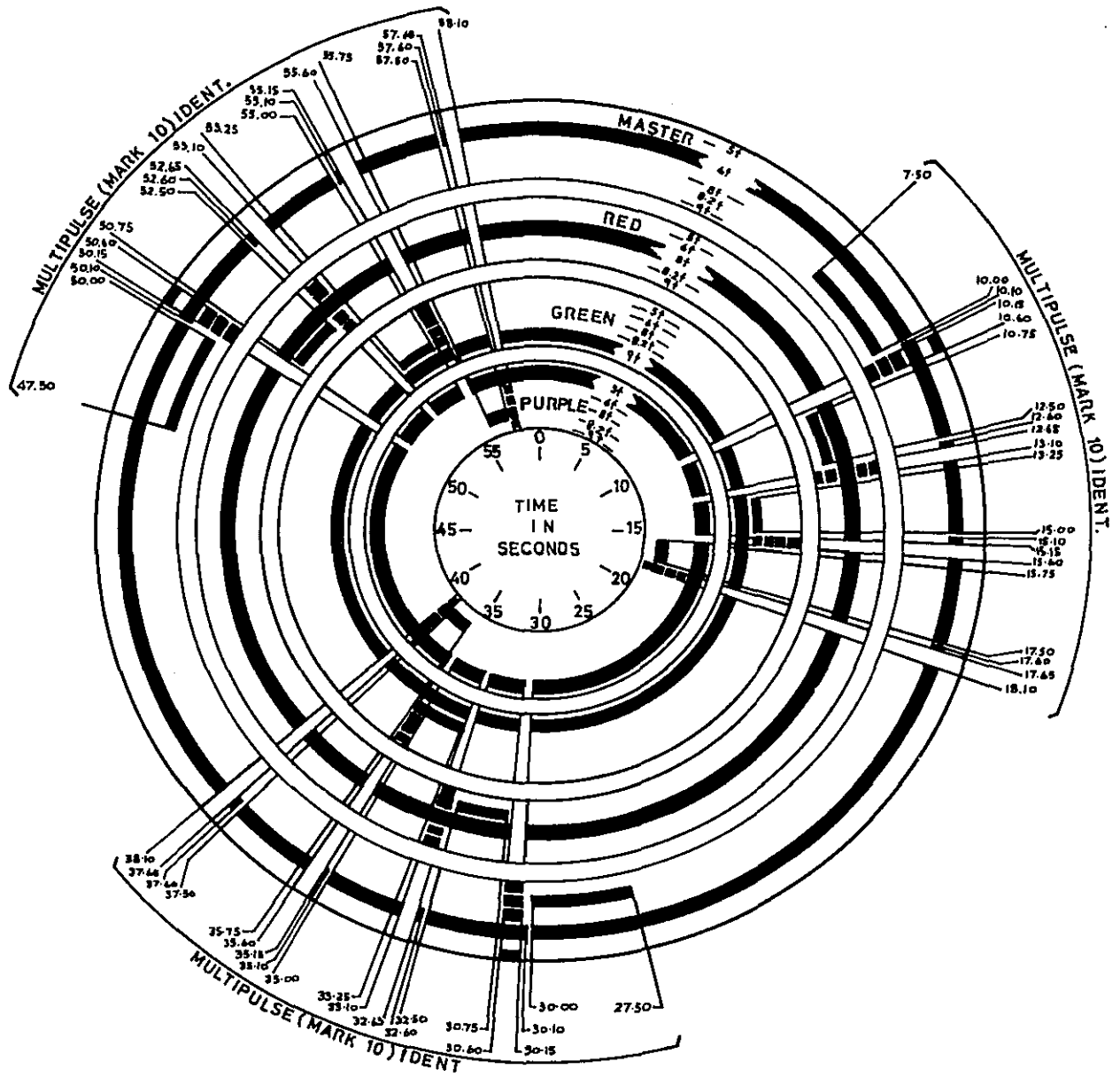


Fig 1-6 60-second transmission cycle for 4-station chain

Table 1-2

Decca chain frequency grouping in kc/s

Nominal frequency (B) and 'half frequency' (E) groups

Decca Frequency Code	Master 6f	L.I. Signalling 6f + 60c/s	6f - 60c/s	Red 8f	Green 9f	Purple 5f	Orange 8.2f
0 B	84.105	84.165	84.045	112.140	126.1575	70.0875	114.9435
0 E	84.195	84.255	84.135	112.260	126.2925	70.1625	115.0665
1 B	84.280	84.340	84.220	112.373	126.420	70.233	115.183
1 E	84.370	84.430	84.310	112.493	126.555	70.308	115.306
2 B	84.460	84.520	84.400	112.613	126.690	70.383	115.429
2 E	84.550	84.610	84.490	112.733	126.825	70.458	115.552
3 B	84.645	84.705	84.585	112.860	126.9675	70.5375	115.6815
3 E	84.735	84.795	84.675	112.980	127.1025	70.6125	115.8045
4 B	84.825	84.885	84.765	113.100	127.2375	70.6875	115.9275
4 E	84.915	84.975	84.855	113.220	127.3725	70.7625	116.0505
5 B	85.000	85.060	84.940	113.333	127.500	70.833	116.167
5 E	85.090	85.150	85.030	113.453	127.635	70.908	116.290
6 B	85.180	85.240	85.120	113.573	127.770	70.983	116.413
6 E	85.270	85.330	85.210	113.693	127.905	71.058	116.536
7 B	85.365	85.425	85.305	113.820	128.0475	71.1375	116.6655
7 E	85.455	85.515	85.395	113.940	128.1825	71.2125	116.7885
8 B	85.545	85.605	85.485	114.060	128.3175	71.2875	116.9115
8 E	85.635	85.695	85.575	114.180	128.4525	71.3625	117.0345
9 B	85.720	85.780	85.660	114.293	128.580	71.433	117.151
9 E	85.810	85.870	85.750	114.413	128.715	71.508	117.274
10 B	85.900	85.960	85.840	114.533	128.850	71.583	117.397

Table 1-3

Sample group of Decca frequencies

Showing relationship of A-B-C-D-E-F spot frequencies (in kc/s)  
for one complete numerical group

Decca Frequency Code	Master 6f	L.I. Signalling 6f + 60c/s	Red 8f	Green 9f	Purple 5f	Orange 8.2f
5 A	84.995	85.055	113.327	127.4925	70.829	116.159
5 B	85.000	85.060	113.333	127.500	70.833	116.167
5 C	85.005	85.065	113.340	127.5075	70.837	116.1735
5 D	85.085	85.145	113.447	127.6275	70.904	116.283
5 E	85.090	85.150	113.453	127.635	70.908	116.290
5 F	85.095	85.155	113.460	127.6425	70.912	116.2965

1-2-5 Service area

The service area of the Decca Navigator system is determined by the following two limitations:

- (1) Limitations of effective range signal-to-noise ratio at a given receiving location
- (2) Limitations of range by skywave at night

A detailed description of this is given in the paper appended hereto.

The effective range of a Decca chain to be established in the Southeast Asian area by the radiation power of 200W (transmitter power 1.2 kw and umbrella type aerial 110m tall will be used) stated in the present report, will be 400 km during both daylight periods and nighttime.

### 1-3 Operation of Decca transmitting equipment

#### 1-3-1 Phase control equipment

There are two types of phase control equipment, one is for the master station and the other for a slave station. The systems of their respective operation are shown in Fig. 5-4-19 and Fig. 5-4-20.

The phase control equipment for the master station produces the signals that would become a frequency standard of a Decca chain, by the crystal oscillator of the main oscillating unit of the duty rack. To be more precise, the frequency of Rubidium oscillator is divided up to  $0.2f$  by the frequency synthesiser to drive the transmitting driving unit of each radio wave. Then the radio wave is transmitted from the aerial via the transmitter. The aerial current is feedback to the transmitter's driving unit and so controlled as to coincide the phase of the aerial current with that of the  $0.2f$  signal. Part of the feedback signal, on the other hand, impresses even the transmitter's driving unit of the spare rack and controls so as to make the phase of the  $0.2f$  signal of the rack coincide with the phase of the duty rack.

The output signals of the driving unit of the transmitter are in wave form switched by switch circuit of the transmitter's driving unit by the signals consistent with time schedule of the Mark-10 transmitting system in the time signal generating unit.

The phase control equipment for a slave station monitors by the  $6f$  receiver the phase of signals transmitted from own station to insure that the phase coincide with that of the master station at all times, and controls by difference of signal's output. And the time sequence itself should be corrected by the zero time signal of the  $8.2f$  receiver's output because its reference point must coincide with the master station. The operation of other equipment for a slave station is similar to that of the master station.



### 1-3-2 Switching equipment

The monitoring and switching equipment is a device by which to monitor the operating conditions of the transmitting equipment, to rate the serviceability of the three sets of phase control equipment above-mentioned, and, immediately upon detection of any abnormality, to switch over automatically to the phase control equipment of high serviceability. The system of this equipment is shown in Fig. 5-4-21.

Abnormalities of the three sets of phase control equipment in the phase synchronisation, in the operation of the master oscillator and in the time synchronisation are input in the fault ratio detector to calculate the ratio of faults to time. The output is then input in the automatic selector and led the selected signal to the switching unit. The switching is performed by sending out the switching signals to the control unit by command from the switching unit. Switching can be done both automatically and manually, and when it is done manually, artificial alarm is produced from the test keyboard and an operational test of automatic selection can be performed. The operational condition of the phase control equipment by automatic selection can be monitored by the display unit.

Each slave station has a receiver to monitor the phase synchronisation between the master and slave stations in the basic frequencies of  $1f$  and  $0.2f$ . This receiver is of superheterodyne system, in which the monitoring of synchronisation is carried out by the display of the decommeter. If this phase synchronisation is stepped out, phase control is done by the remote control from the central monitoring equipment.

Following is an outline of the functions of the monitoring and switching equipment:

- a) During its normal operation, the phase control equipment is switched over to another phase control

equipment every 24 hours, and the switching over is done in the order of No.1, No.2 and No.3 equipment.

- b) The amplitude, phase and time of the transmitted radio waves are compared with those of each phase control equipment and the automatic monitoring and switching equipment, and the serviceability of the equipment is classified into the following four stages in accordance with the number of troubles to time ratio of each phase control equipment.

OK, Dubious, Suspect and No vote

The "No vote" is a case where troubles are detected more than once during four minutes; the equipment is not in operable condition.

- c) At a slave station, abnormalities caused by such factors outside the slave station as failures in the equipment at the master station and faults in radio wave propagation are discriminated by the anti-static circuit, thereby restricting the switching of equipment in the receiving system in an abnormal condition.
- d) With this monitoring and switching equipment, it is possible to cut the automatic switching system off and to switch over to manual handling and check the operating condition of the equipment by simulation.

### 1-3-3 Transmitter

The transmitter comprises five racks of equipment having identical functions, and each rack has a different frequency. The system of the transmitter is as shown in Fig. 5-4-22.

In the pre-input mixing circuit of the transmitter, the input from three racks of phase control equipment is distributed and impressed in four exciting units, opening the gate only for the rack

designated for the duty transmitter and amplified and divided into eight parts by the coupling transformer. Then twelve pieces of power amplifier units are excited. The output of each power amplifier unit is 100W which is composed at the output transformer to make an output of 1.2kw. There are tap changers in the output transformer, and the equipment can be operated by half or low power output as occasion demands. In the event of failure in the blower unit, the equipment can be operated, reducing the power automatically to half power. And the output voltage is fed back to the exciting unit, cause it to perform ABC operation, and the output fluctuatuion is diminished. The blower unit has a circuit separately incorporated to detect troubles in the exciting unit, power amplifier and fan motor, displays the abnormalities on its panel and outputs signals for remote monitoring.

#### 1-3-4 Aerial coil assembly

The aerial coil assembly is a device to feed the aerial with power for five waves sent from the transmitter without mutual interference and with high degree of efficiency.

Power for the five radio waves from the transmitter is supplied through a feeder (coaxial cable) into the aerial coil assembly normally 200m to 300m away from the transmitter. The power is first supplied to the feeder collector unit, and after setting the electric delay angle by the feeder at a certain degree ( $\lambda/4$ ) for the five waves, is input to an independent matching unit for each frequency via the ATAM equipment. These high frequency signals are adjusted to the impedance of the aerial tuning unit by the matching unit, and the signals are effectively fed into the aerial tuning unit, where the reactance parts of the aerial impedance is compensated, and radio waves are transmitted on five frequencies from the aerial.

The ATAM equipment (Automatic Tuning And Matching) is a system to detect change in the phase and absolute value of load impedance on the transmitter side to cope with the change in aerial impedance caused by the change in the weather conditions, and drive the aerial tuning system and matching unit to make the optimum load automatically.

The return of the aerial tuning unit is earthed through the phasing loop unit and aerial current meter. One of the signals detected by the phasing loop is fed back to the phase control equipment to control the phase of the signal and another signal is sent to the monitoring and switching equipment to monitor the aerial current.

#### 1-3-5 Central monitoring equipment

The central monitoring equipment is a device set up in the master station to monitor the phase and level of the radio waves transmitted from the other stations. It also monitors the operational condition of the equipment in the master and slave stations. Remote control is carried out as occasion demands in order to insure normal transmission of the radio waves at all times.

The remote control console is composed from its functions of a monitoring unit to monitor the radio waves transmitted from the other stations and of a control unit to control the operation of equipment at the stations. The radio waves from the master and slave stations are received at the monitor site some dozen kilometres away from the master station. The signals thus received are made into codes and monitored via UHF link at the monitoring unit of the remote control console.

This central monitoring equipment also has the data logger which records the major state of performance in the overall system operation, analysing the operation of a Decca chain as a whole and which makes a detailed "diagnosis" of the troubles in the equipment, etc. in the stations.

## 2 Outline of Loran C system

### 2-1 Loran C transmitting equipment

#### 2-1-1 Principle of Loran C system

Loran is the designation for a family of radio position fixing systems which operate on the principle of measuring the difference in time of arrival of pulse signals from a number of transmitting stations. A pair of loran transmitting stations produces a family of lines of position uniquely determined in space. These lines of position of lines of equal time difference are hyperbolae, hence the name hyperbolic for this type of system. The name Loran was derived from the words LOnG RAnge Navigation.

Loran A is the standard Loran system operating on a frequency of about 2000. The difference readings are obtained by matching the envelopes of the transmitted pulses.

Loran C is the logical extension of Loran A; the two major characteristics by which they differ are transmission frequencies and time difference measurements.

To take advantage of the stable propagation characteristic and long range of the LF band, 90 - 110 kHz frequency band was chosen as allocated internationally for long distance radionavigation systems.

Time difference measurements are made by utilizing both the pulse envelope and the phase of the carrier within the envelope, and the envelope match produces a coarse time difference reading and the cycle match produces the fine time difference reading.

It is this additional fine reading and longer baseline between stations which give Loran C its increased coverage and higher accuracy compared with previous Loran A system.

#### (1) Configuration of transmitting stations

Loran C chains are comprised of master transmitting station, two or more secondary transmitting stations and, system area

monitor (SAM) stations. In Fig.2-1 is shown a typical configuration of Loran C stations. The transmitting stations are located such that the signals from the master and at least two secondary stations can be received throughout the desired coverage area. For convenience, the master station is designated by the letter "M" and the secondary stations are designated W, X, Y, or Z. Thus, a particular master-secondary pair and the TD which it produces can be referred to by the letter designations of both stations or just that of the secondary (e.g. MX time difference or TDX.)

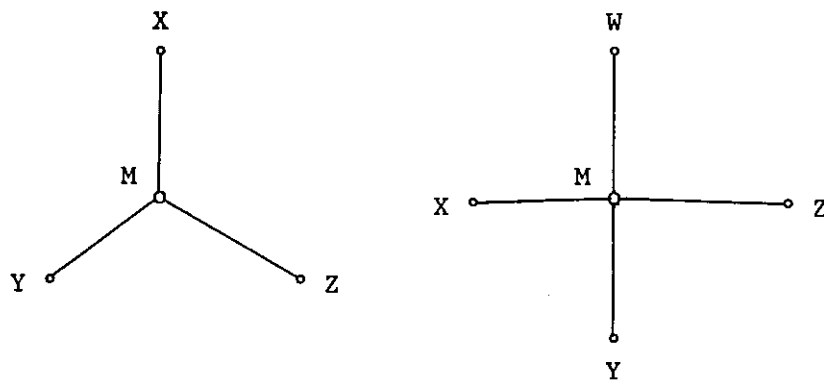


Fig. 2-1 Configuration of LORAN C stations

(2) Method of transmitting radio waves

The transmitting stations of a Loran C chain transmit groups of pulses at a specified group repetition interval (GRI). Each pulse has a 100 kHz carrier and is of the shape described in Figure 2-2. For each chain a minimum GRI is selected of sufficient length so that it contains time for transmission of the pulse group from each station (10,000 microseconds for the master and 8,000 microseconds for each secondary) pulse time between each pulse group so that signals from two or more stations cannot overlap in time anywhere in the coverage area. (See Figure 2-3.) Thus, with respect to the time of arrival of the master, a secondary station will delay its own transmissions for a specified time, called the secondary coding delay. The minimum GRI is therefore a direct function of the number of

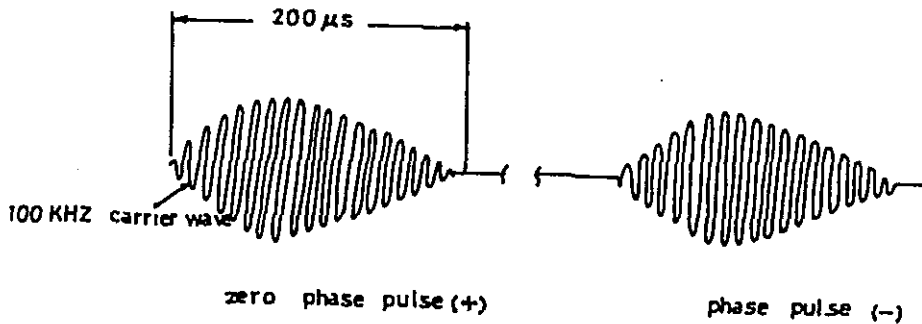


Fig. 2-2 Pulse waveform

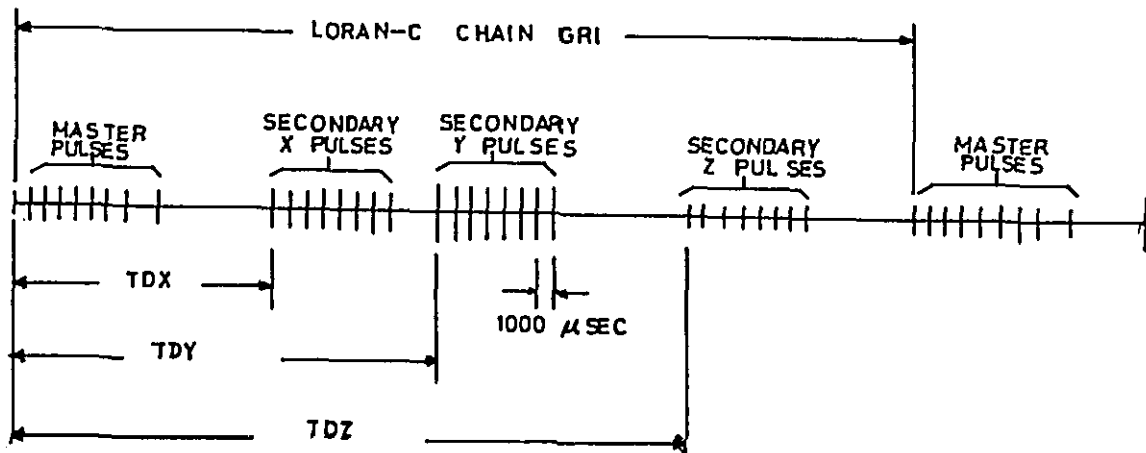


Fig. 2-3 Example of repetition synchronisation of Loran-C system

stations and the distance between them. A GRI for the chain is then selected so that adjacent chains do not cause mutual (cross-rate) interference. Possible values for GRI are listed in Table 2-1. The GRI is defined to begin coincident with the start of the first pulse of the master group.

Each station transmits one pulse group per GRI. The master pulse group consists of eight pulses spaced 1,000 microseconds apart, and a ninth pulse 2,000 microseconds after the eighth. Secondary pulse groups contain eight pulses spaced 1,000 microseconds apart.

As shown in Fig. 2-2, there are two different types of pulse; zero-phase pulse and phase pulse. Transmission of radio waves is performed using the combination of these different types of pulses as shown in Fig. 2-3.

	Stations	
GRI	Master	Secondary
A	+ + - - + - + - +	+ + + + + - - +
B	+ - - + + + + + -	+ - + - + + - -

Fig. 2-4 Phase code of Loran C pulse

Table 2-1 Pulse repetition period of Loran C

Special repetition period	Basic repetition period $\mu$ s					
	SS	SL	SH	S	L	H
0	100,000	80,000	60,000	50,000	40,000	30,000
1	99,900	79,900	59,900	49,900	39,900	29,900
2	99,800	79,800	59,800	49,800	39,800	29,800
3	99,700	79,700	59,700	49,700	39,700	29,700
4	99,600	79,600	59,600	49,600	39,600	29,600
5	99,500	79,500	59,500	49,500	39,500	29,500
6	99,400	79,400	59,400	49,400	39,400	29,400
7	99,300	79,300	59,300	49,300	39,300	29,300

The phase pulses or codes are used in the receiver in identifying the master and secondary stations and in automatic search at the master station and automatic synchronisation to the master station. An example of the phase code is shown in Fig. 2-4, and pulse repetition synchronisation is given as shown in Table 2-1.

(3) Loran C transmitting station equipment

Fig. 2-5 shows the composition of Loran C station equipment. The Cesium oscillator is used as standard oscillator of frequency to supply reference signal to the timer which generates the standard repetition pulse of Loran C. The



pulse generators (PGEN's) are driven by the trigger pulse the timer output, and thus the standard Loran C pulse signal can be obtained. The PGEN can adjust manually the amplification of the eight cycles of 80  $\mu$ s among the first building-up time of the standard Loran C pulse. It can also change the whole level of driving pulses of the transmitter.

As it is given the output of PGEN, the transmitter amplifies the power of high frequency energy straight forwardly to produce the required output at the final stage and feed the aerial with it. There are two transmitters; one is a duty transmitter and the other a stand-by equipment. In the event of failure of the duty transmitter, the transmitter automatic controller (TAC) can switch it over automatically to the stand-by equipment.

The aerial coupler has a loading coil which matches the aerial with the transmitter, and the duty and stand-by transmitters are so designed as to be switched over to each other as occasion calls by the aerial/dummy change-over switch. Part of the output fed into the aerial is picked up and led to the above-mentioned TAC or electrical pulse analyser to perform the monitoring of output wave form and the measurement of required parameters, and to display the operational condition of the transmitter by means of the alarm unit.

There is in the Loran C system a monitor station to monitor the transmitted wave form from the master and secondary stations in order to ensure the normal operation of the system. Should any abnormality be detected in the transmitting station, such abnormality is controlled by the teletypewriter placed in the monitor station. The remote control interface is a device to perform this and other functions.

At a secondary station the radio wave should be made synchronised to that of the master station set at the required coding number and for this reason signals from the master station is received by the Austron timing receiver to set the timer of the secondary station or blinking at the master station is detected here to produce alarm signal.

2-1-2 All functions and features of the transmitter equipment

- (1) Dual transmitter configuration: Automatic switchover to the standby transmitter in the event of a failure of the duty transmitter.
- (2) Water-cooled amplifier for the final output stage of transmission
- (3) Solid state high voltage power supply utilises SCR regulation
- (4) Features of all solid-state LRE
  - 1) Control of Loran C pulse shape and amplitude
  - 2) Automatic switching of Loran C transmitter
  - 3) Loran C alarm indications centralised
  - 4) Digital Loran C pulse shape analysis
  - 5) Remote control of important matters relating to power source, transmitting equipment, sending of unusable signal

2-1-3

Composition of transmitting equipment

The composition of the transmitting equipment is as shown in the following table:

Table 2-2 Components of Loran C transmitting equipment  
(In the case of 3 secondary stations)

Name of unit	Master station	Secondary station (each station)	Monitor station	Remarks
Transmitter	2 sets	2 sets	-	
Aerial coupler	1 set	1 set	-	
Dummy load	1 set	1 set	-	
Cesium frequency standard rack	1 set	1 set	-	One set consists of 3 Cs standard OSC's
Timer set	1 set	1 set	-	Pulse monitor, Pulse generator, etc.
Transmitter control set	1 set	1 set	-	
Auxiliary rack	1 set	1 set	-	Status alarm unit, Austrom timing receiver, etc.
Recorder rack	1 set	1 set	-	
Remote control interface unit	1 set	1 set	1 set	
Teletypewriter	1 set	1 set	1 set	
Monitor station receiver	-	-	1 set	

The whole figure of the system, an outer appearance of each component and the system drawing are shown in Fig. 2-5 through 2-12.

2-1-4

Main ratings of the transmitting equipment

- (1) Transmitting frequency: 100 KHz
- (2) Band width: 20 KHz (90 ~ 110 KHz)

- (3) Type of emission: Pulse
- (4) Emission power: 400 Kw (Peak value)

2-1-5 Cesium frequency standard oscillator

This constitutes the frequency (phase) standard of a Loran C transmitting station and is composed of the following components:

- (1) Cesium oscillator 3 units
- (2) Phase microstepper
- (3) Phase adjuster
- (4) Distributing amplification
- (5) Phase recorder

2-1-6 Timer equipment

This is a unit to generate Group repetition interval that is most important in the Loran C equipment, and is composed of the following equipment:

- (1) Loran timer 2 units
- (2) Timer switching unit 1 set
- (3) Power unit

2-1-7 Transmitter control set

This is a device to produce standard Loran C signals to drive the transmitter by the trigger signals of the timer. In addition, it has such other functions as the monitoring of output wave form of the transmitter and the switching over to the stand-by transmitter in the event of failure of the duty equipment.

Main functions of transmitter control set are as follows:

- (1) Pulse generator (PGEN)
  - 1) The PGEN develops a transmitter drive wave form (TDW) from the timing pulse received from the timer set.
  - 2) Generation of standard pulse wave form  $(t^2 \exp(-t^2/65))$
  - 3) Correction of distortion of transmitting pulse wave form

(2) Transmitter automatic controller (TAC)

This is a controlling equipment to monitor the wave form of "On air", and in case of a fault in the duty transmitter, switch it over automatically to the stand-by equipment.

(3) Electrical pulse analyser (EPA)

- 1) Precise and unambiguous Loran C pulse shape and amplitude measurements
- 2) The measurements of envelope-to-cycle difference (ECD) of the first pulse
- 3) The EPA generates a "reference envelope wave form",  $t^2 \exp(-2t/65)$ , which is used in conjunction with an oscilloscope.

(4) Components of transmitter control set are as shown in the following table:

Table 2-3 Transmitter control set components

Name of unit	Quantity	
	Master station	Secondary station (each station)
Emergency stop panel	1 set	1 set
Transmitter automatic controller	1 set	1 set
Electrical pulse analyser	1 set	1 set
Pulse generator No.1	1 set	1 set
Pulse generator No.2	1 set	1 set

2-1-8

### Auxiliary rack

This incorporates status display and alarm of the transmitting equipment and an Austron timing receiver for setting the "control number" of secondary stations.

Main functions of auxiliary rack are as follows:

(1) Status alarm unit (SAU)

When the equipment is in normal operation, only the green light shows. In the event of any abnormality, the location of trouble is indicated in red letters and at the same time the emergency buzzer rings. That is to say, the red colour display indicates that the equipment is in some sort of troubles.

(2) Austron timing receiver

- 1) This is a controlling receiver for synchronisation to the master station and setting of the "control number" of a neighbouring station.
- 2) To detect unusable signal of the master station and transmit warning signal
- 3) To monitor other pair of a master and secondary stations.

2-1-9

### Composition of the auxiliary rack

The composition of the auxiliary rack is as shown in the following table (This is a case where the number of secondary stations is three)

Table 2-4 Composition of auxiliary rack

Name of unit	Quantity	
	Master station	Secondary station (each station)
Austron timing receiver	-	1 set
Status alarm unit	1 set	1 set
Digital voltmeter	1 set	1 set
Synchro scope	1 set	1 set

2-1-10 Remote control interface unit

The Loran Replacement Equipment (LRE) is controlled by the system monitor station by teletypewriter through this remote control interface unit.

The main features of remote control interface are as follows:

- (1) Interface to perform local phase adjustment through remote control
- (2) Instruction and stoppage of blinking for the master and secondary stations
- (3) Cabling out of and instructions to transmitting station monitoring personnel

2-1-11 Main actions of the transmitter

- (1) The peak current of 700A and peak radiated power of 400 KW are fed into the 625 foot toploaded monopole aerial (TLM).
- (2) At the final stage, the equipment is operated as forced water cooling system and B-class straight line amplifier, and the second intermedilage amplifier drives with cathod follower at the final stage.
- (3) Ample band width is provided for each stage so that the standard Loran C pulse signals may be amplified without any distortion.
- (4) Since the building-up waveform of the transmitter output gets blunted usually because of the high quality factor of the aerial system circuit, the transmitter input from the pulse generator is pre-emphasised.

2-1-12 Components of the transmitter

The transmitter is composed of the following units:

Table 2-5 Transmitter components

Name of unit	Quantity		Remarks
	Master station	Secondary station (each station)	
First stage power amplifier	1 set x 2	1 set x 2	
1st & 2nd intermediate power amplifier	1 set x 2	1 set x 2	
Final power amplifier	1 set x 2	1 set x 2	AC 208V: 225 KVA
Power supply	1 set x 2	1 set x 2	AC 460V: 300 KVA

2-1-13 Aerial coupler

The main part of an aerial coupler is a loading coil unit for matching of the aerial with the transmitter.

- (1) The aerial loading coil network is provided to perform matching the aerial base impedance with the required feeder line impedance on the side of the transmitter output.
- (2) The aerial current transformer is provided on the earth side of aerial circuit to measure the input signals of the transmitter automatic controller (TAC) circuit and aerial current.
- (3) There is a high tension vacuum switch to change No.1 and No.2 transmitter over to the aerial and dummy equipment.



2-1-14 Composition of aerial coupler

The components of the aerial coupler are as shown in the following table:

Table 2-6 Aerial coupler components

Name of unit	Quantity	
	Master station	Secondary station
Aerial loading coil	1 set	1 set x 3
Aerial current transformer	1 set	1 set x 3
Vacuum tube relay for aerial dummy changing	1 set	1 set x 3

2-1-15 Electrical aerial dummy load

This is used as dummy load for adjusting the stand-by transmitter and its main features of Electrical aerial dummy load are as follows:

- (1) This dummy load is connected to the stand-by transmitter, which can be operated by full rated continuous load. Cooling is done by the forced air cooling system.
- (2) Non-inductive resistance units are connected series-parallel, which are of the value equivalent to the aerial base resistance at the dummy input extremity.

2-1-16 Composition of electrical aerial dummy load

The components of the electrical aerial dummy load are as shown in the following table:

Table 2-7 Electrical aerial dummy load components

Name of unit	Quantity	
	Master station	Secondary station (each station)
Non-inductive resistor	1 set	1 set
Blower for cooling	1 set	1 set

Reference literatures

1. G.R. Goodman and R.P. Oswitt: "Loran C Replacement Equipment (LRE)", Navigation, Vol.23, No.3, P.228 (Fall 1976)
2. H.T. Sherman and V.L. Johnson, "The Loran C Ground Station", Navigation, Vol.23, No.4, P.349 (Winter 1976-77)

## Loran C receiver

There is at present a wide variety of Loran C receivers for general (non-military) use, and those which are inexpensive ones are of the type utilising, just the pulse envelope curves and the accuracy they provide is not better than that of Loran A.

The receivers which conduct measurement by matching the carrier waves contained in the pulse, and this is a primary way of utilising the Loran C system, are rather expensive. and those sophisticated receivers for military use are extremely expensive, whose prices now amount to 100,000 US dollars.

There are no clear classifications or standards for both expensive and inexpensive ones, and the difference in the functions and other factors among the various types of receiver is very big. It is no easy matter at the present time to bring all of these under complete control and standardisation.

In Table 2-8 are shown some examples of high-class receivers for public use and in Table 2-9 is shown a comparison of their performance.

As seen from these tables, there is a considerable difference among the receivers in, for example, the time required for them to be stabilised, alone. According to the data published by the National Technical Information Service, some receivers could make correct selection only after 17 minutes of warm-up.

Table 2-8 Example of high-class Loran C receivers

Name of manufacturer and equipment	Automatic or semi-automatic	Display of hyperbola	Price	Remarks
EPSCO 4010-60	Semi-auto	by a pair	\$4,500	
SIMRAD LC-201	"	"	\$3,595	
SIMRAD LC-201	Auto	By two pairs simultaneously	\$4,650	
MICROLOGIC MC-200	"	"	\$4,195	
Decca DL-91	"	"	\$4,995	
TELEDYNE 601	"	by a pair	\$4,750	

Table 2-9 Comparison on performance of various types of high-class Loran C receivers

Name of equipment Classification	INTERNAV 204	Decca DL-91	MICROLOGIC ML-200
Range-ground wave	1200 n.m.	1000 n.m.	1400 miles
Range-skywave	2500 n.m.	Not specified	
Acquistition time	30 seconds	30 sec 0 db S/N 90 sec -6 db S/N	30 sec 10 db 90 sec -8 db
Setting time	5 seconds	400 sec 0 db S/N 600 sec -6 db S/N	200 sec 10 db 800 sec -8 db
Notch filter	2 systems incorporated	2 waves between 70 and 130 KHz. Capable of incorporating 4 waves in outer portion	4 waves between 65 and 155 KHz Depression: 26 db
R.F. Selectivity	6~7 KHz search 26KHz tracking	5 KHz search 23 KHz tracking	3 KHz search 16 KHz tracking

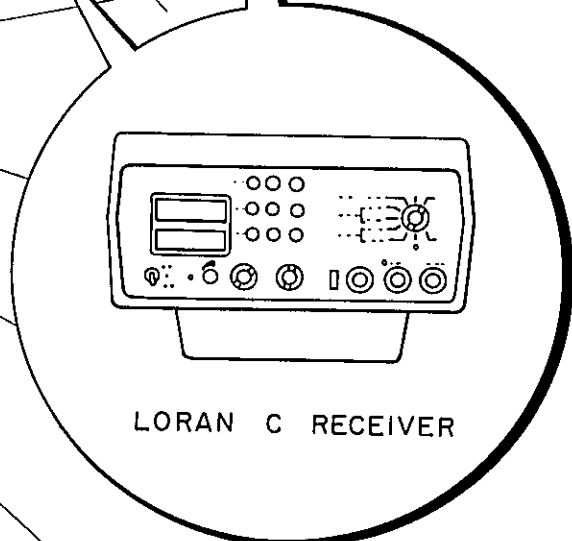
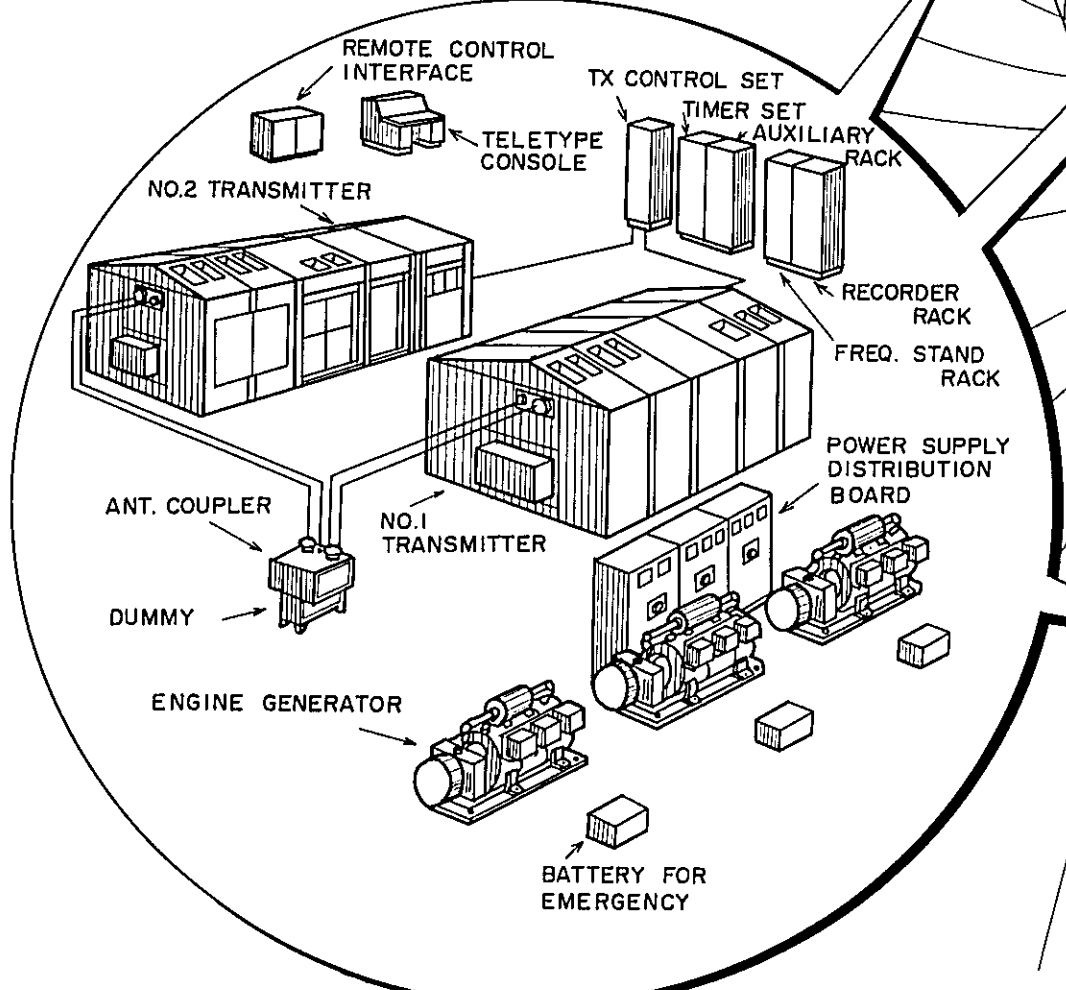
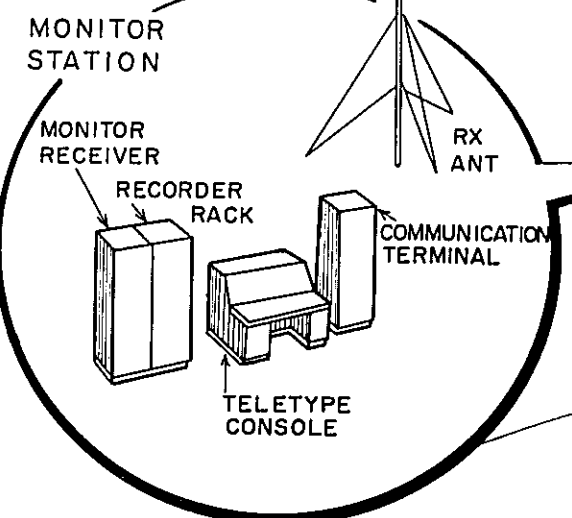
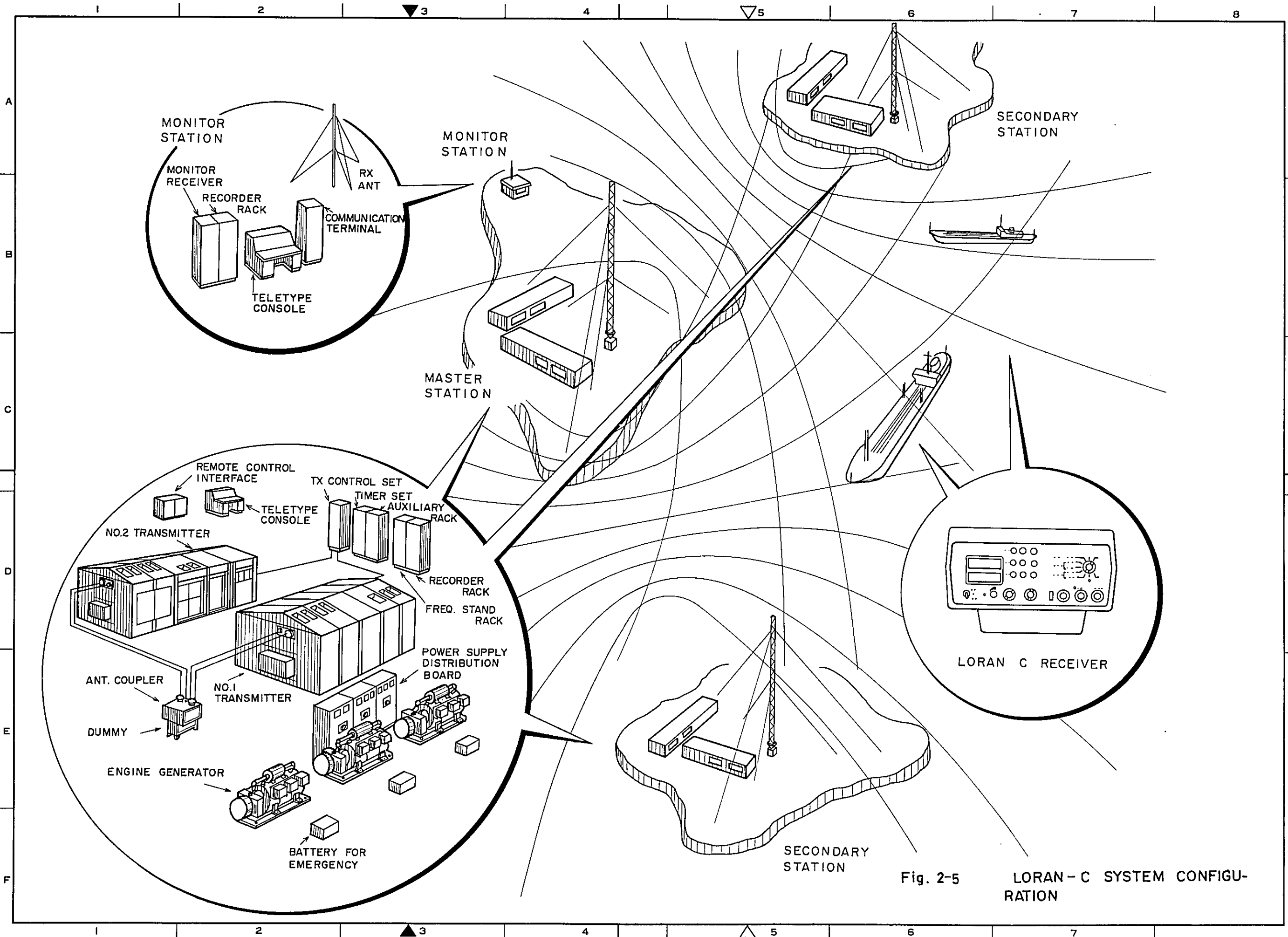


Fig. 2-5 LORAN-C SYSTEM CONFIGURATION

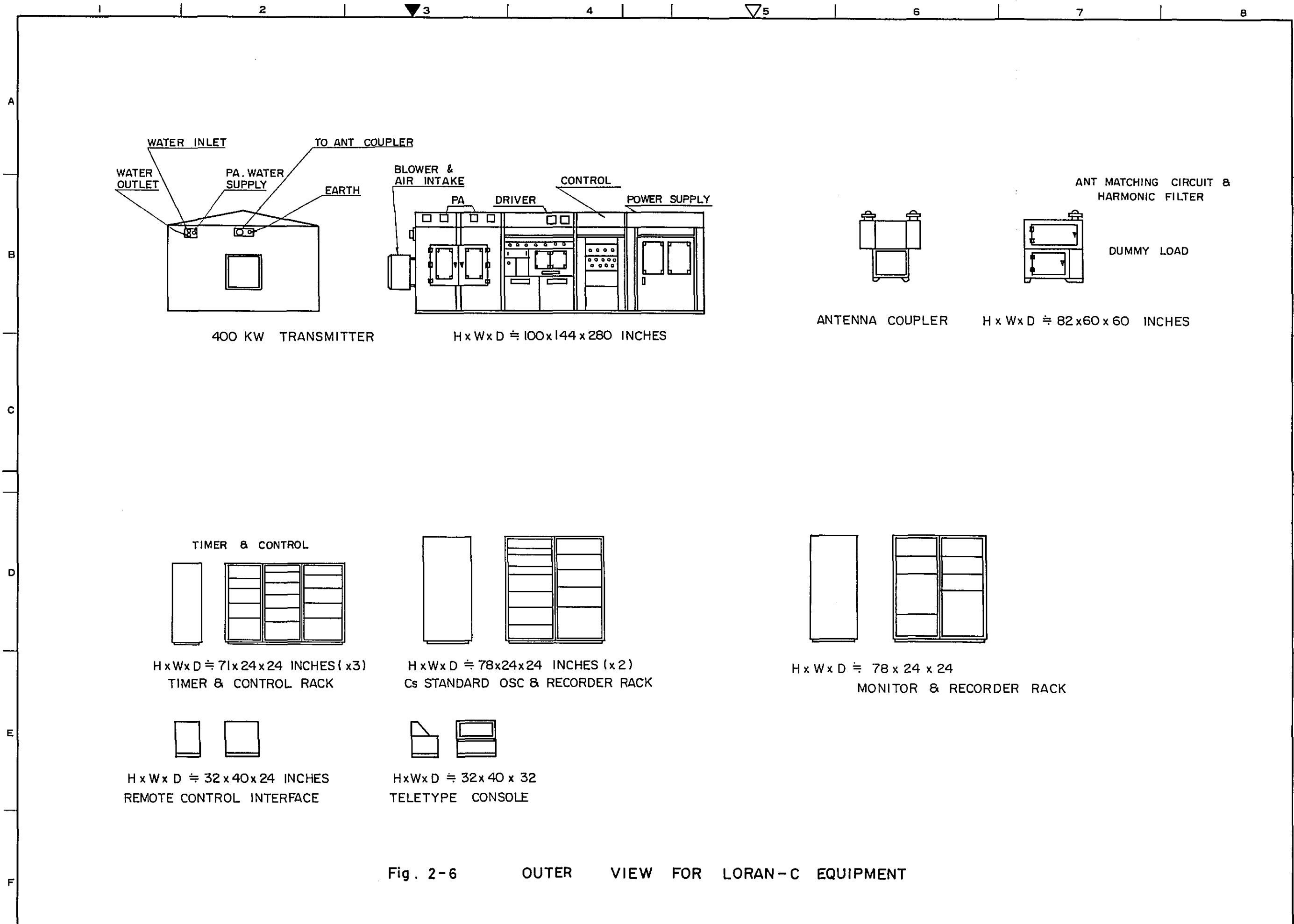
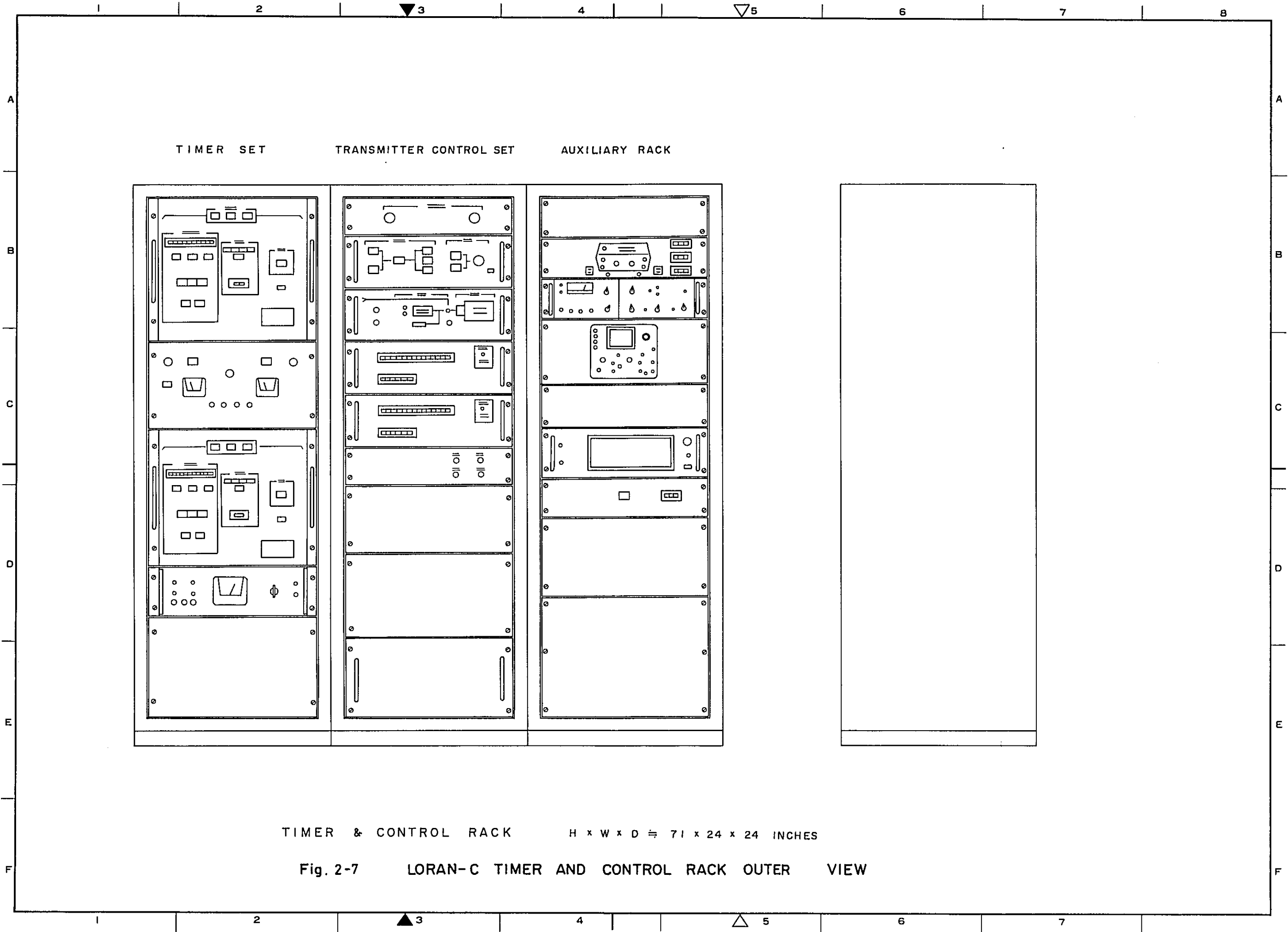


Fig. 2-6 OUTER VIEW FOR LORAN-C EQUIPMENT



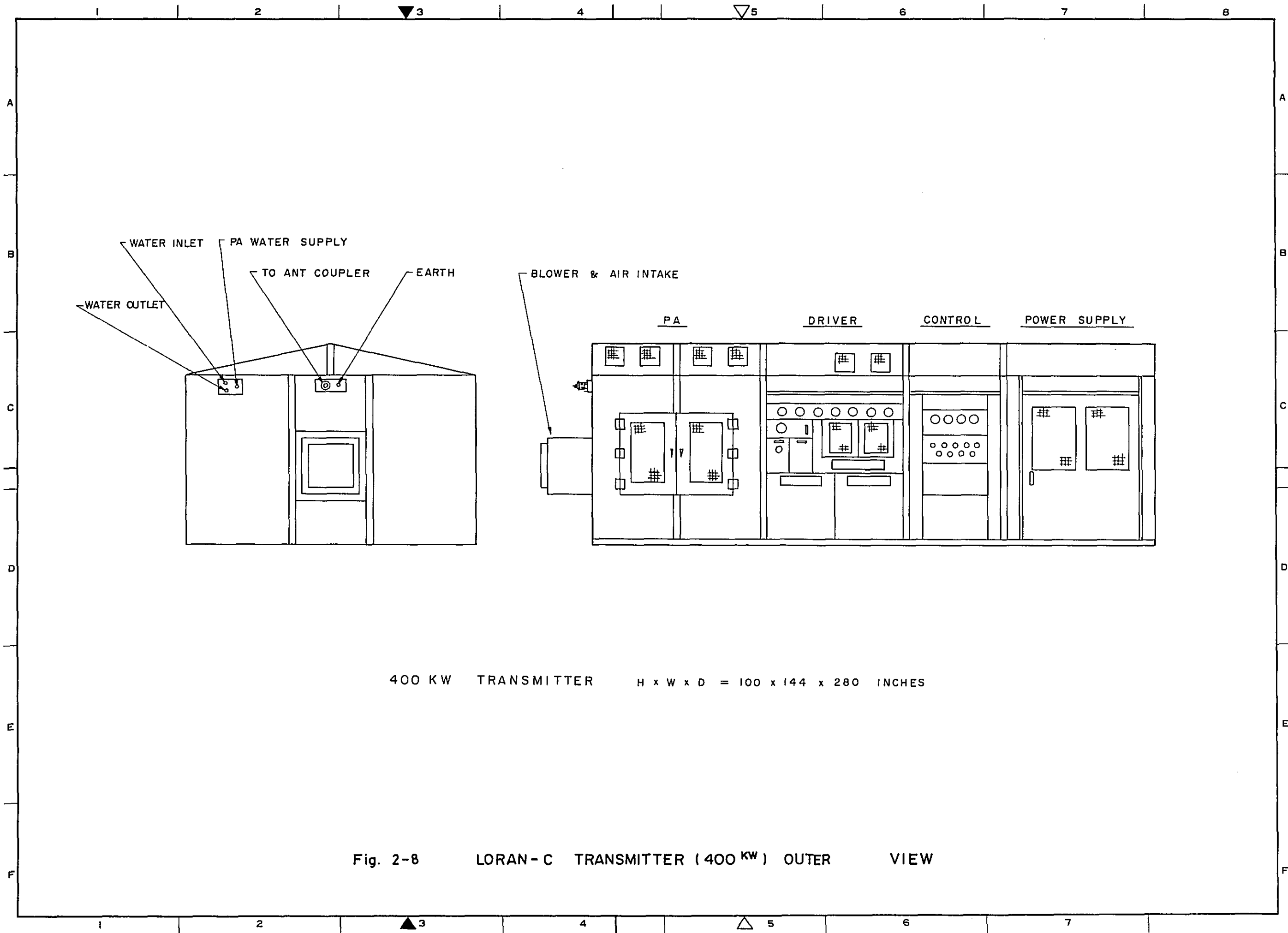
TIMER SET

TRANSMITTER CONTROL SET

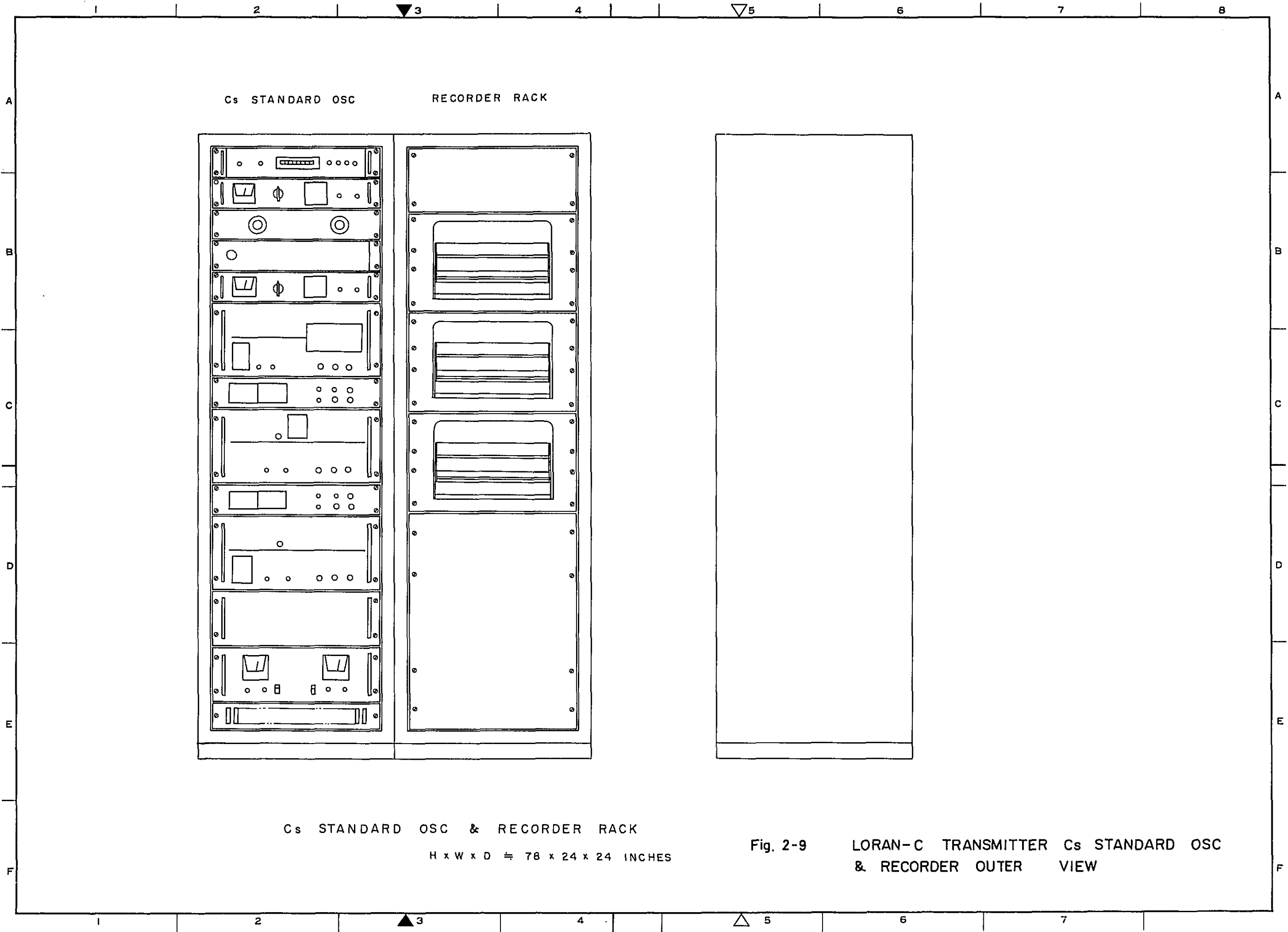
AUXILIARY RACK

TIMER & CONTROL RACK H x W x D = 71 x 24 x 24 INCHES

Fig. 2-7 LORAN-C TIMER AND CONTROL RACK OUTER VIEW







Cs STANDARD OSC

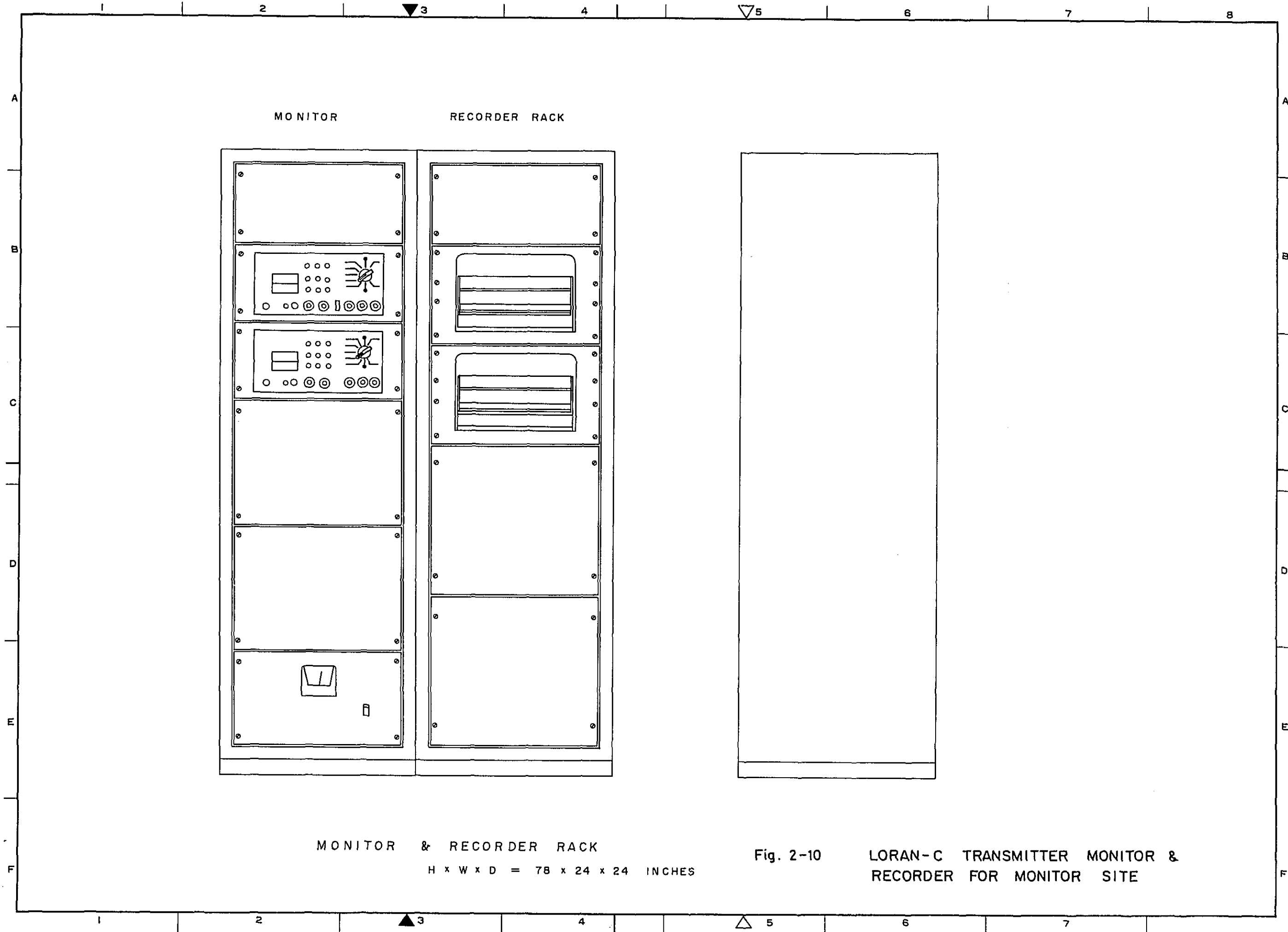
RECORDER RACK

Cs STANDARD OSC & RECORDER RACK

H x W x D ≈ 78 x 24 x 24 INCHES

Fig. 2-9

LORAN-C TRANSMITTER Cs STANDARD OSC  
& RECORDER OUTER VIEW



MONITOR

RECORDER RACK

MONITOR & RECORDER RACK

H x W x D = 78 x 24 x 24 INCHES

Fig. 2-10

LORAN-C TRANSMITTER MONITOR & RECORDER FOR MONITOR SITE

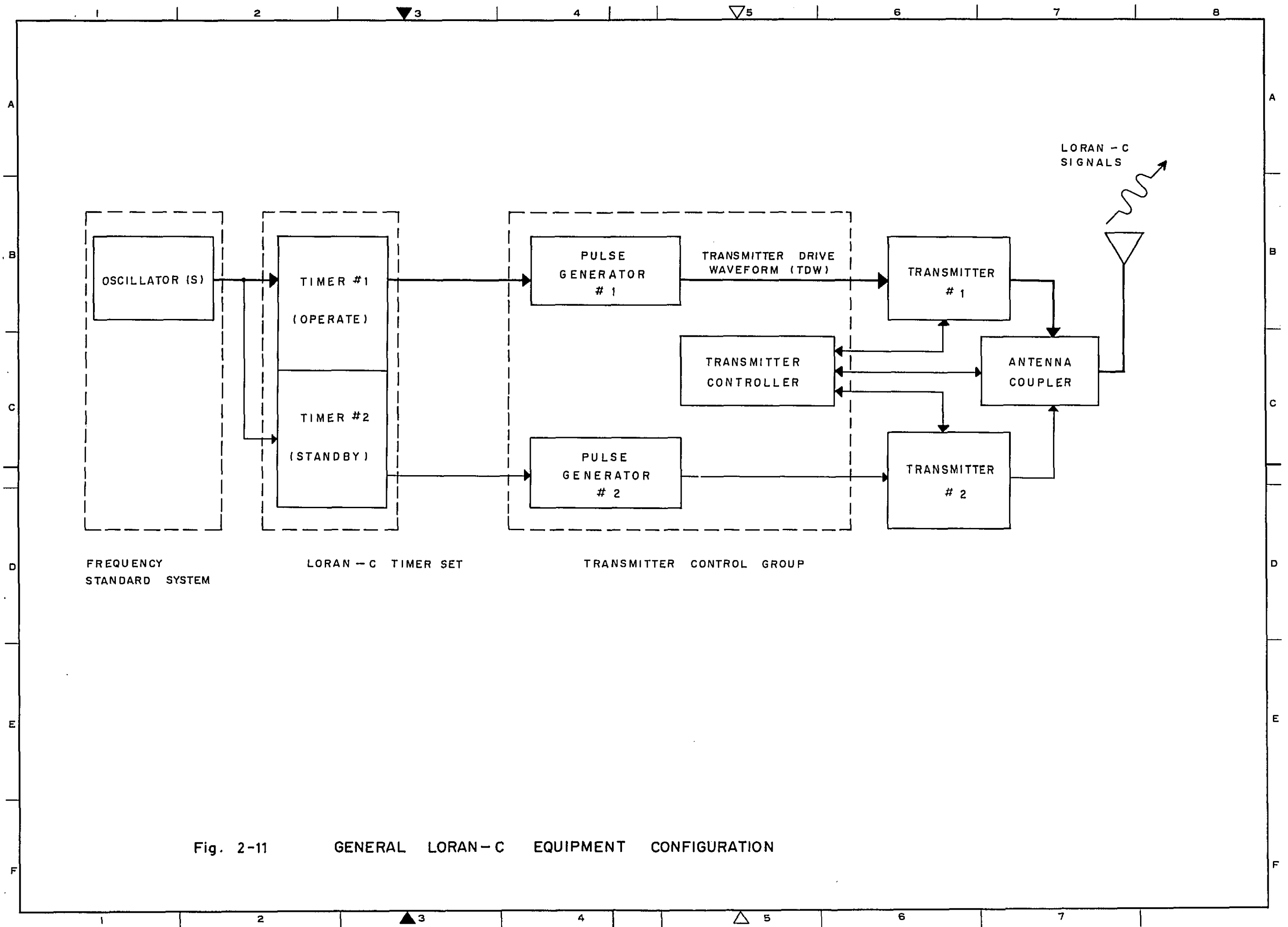


Fig. 2-11 GENERAL LORAN-C EQUIPMENT CONFIGURATION

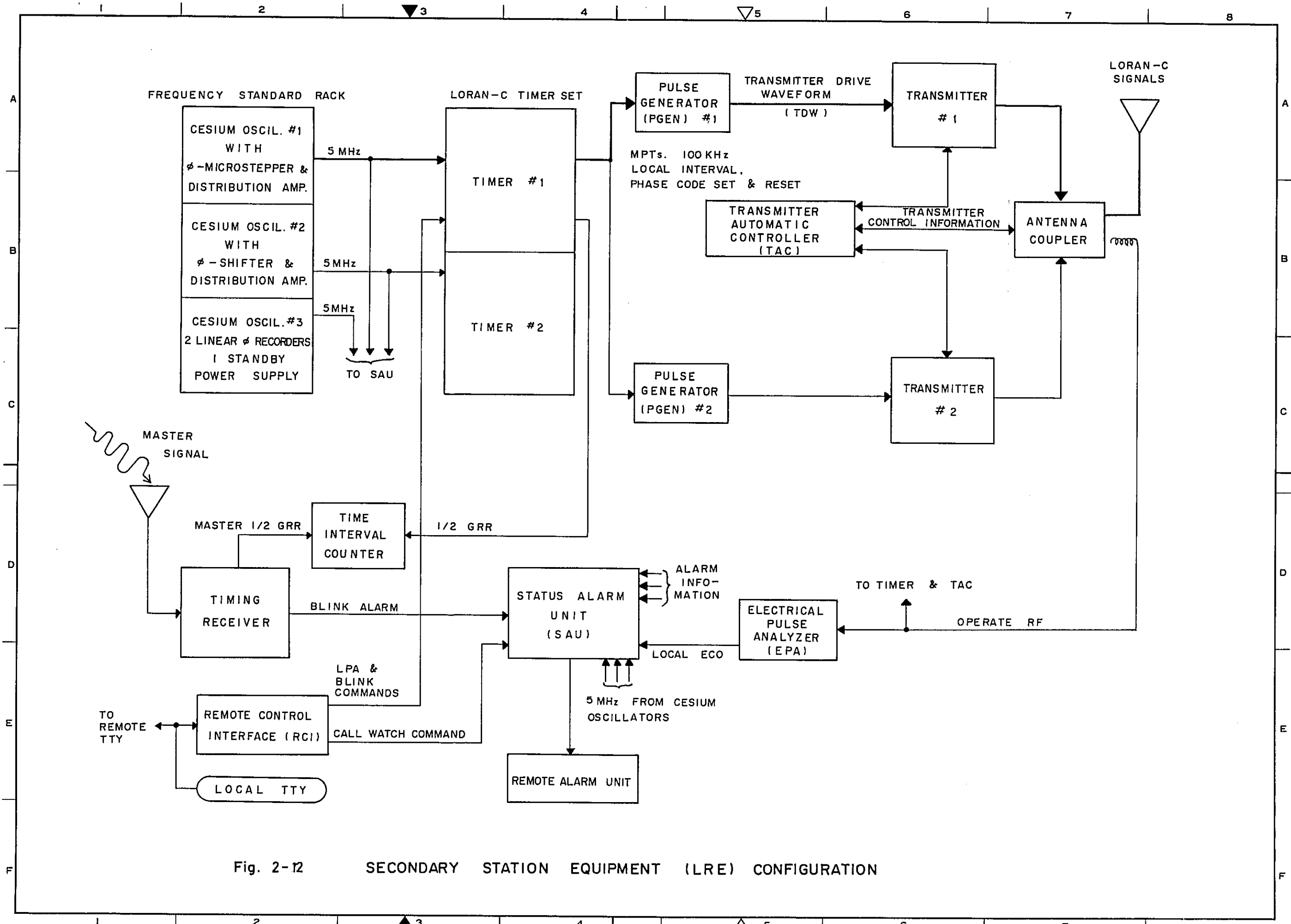


Fig. 2-12 SECONDARY STATION EQUIPMENT (LRE) CONFIGURATION

2-3 Power supply equipment for Loran C navigation system

2-3-1 Introduction

This power supply equipment is a device to supply power to the transmitting equipment, its ancillaries and other units for use with the Loran C station.

(1) The standards to be followed are as follows:

- 1) JIS Japanese Industrial Standards
- 2) JEC Standard of the Japanese Electrotechnical Committee
- 3) JEM Standards of the Japan Electric machine Industry Association

(2) The Environmental conditions are as follows:

- 1) Ambient temperature: 10 - 45°C
- 2) Relative humidity: 40 - 95%

2-3-2 Composition

This power supply equipment comprises the units enumerated below and the connection diagram is shown in Fig. 2-13. The skeleton diagrams are as shown in Figs. 2-14 and 2-15. The number of sets given below for a Loran C station.

(1) Engine generator 3 sets (Fig. 2-18)

A set of engine generator consists of the following units:

- |               |   |
|---------------|---|
| AC generator  | 1 |
| Diesel engine | 1 |

(2) Engine ancillary 1 set

(3) Generator control panel 1 set (Fig. 2-16)

The control panel composed of eight panels as follows:

Output switching panel	3
Automatic starter panel	3
Automatic change over panel	1
DC source panel	1
(4) Power distribution panel	1 set (Fig. 2-17)
(5) Spares and repair tools	1 set

2-3-3 Functions and ratings

(1) Engine generator

1) AC generator

° Type of protection:	Protected type
° System of excitation:	Brushless
° Output power:	300 KVA
° Voltage:	200 V
° Frequency:	50 Hz
° Phase:	3
° Revolutions:	1,000 rpm
° Poles:	6
° Power factor:	0.8 (lag)
° Rated:	Continuity
° Type of insulation:	Type F

2) Diesel generator

° Type:	Vertical, single acting, 4-cycles, pre-combustion chamber, water cooled type.
° Output:	300 PS
° Revolutions:	1,000 rpm
° members of cylinder:	6
° Starter:	Air starting
° Cooling system:	Water cooling with radiator
° Fuel:	Diesel oil or heavy oil
° Fuel consumption rate:	195g/PS/hr

(2) Generator control panel

1) Type of panel: Self stand, metal enclosed type

2) Functions of panel:

Functions of each panel are as follows:

- i) Output switching panel: On-off of output  
Automatic regulation of output voltage  
Monitoring of output
- ii) Automatic starter panel: Starting and stopping of the engine generator and other controls
- iii) Automatic change over panel: It performs automatic change over of three engine generator sets by parallel operation of the engine generator
- iv) DC source panel: It has two sets of storage battery 600AH - 12 cells and two sets of charger for use as control power source for the engine generator

(3) Power distribution panel

1) Type of panel: Self stand, metal enclosed type

2) Functions of panel: It receives output from automatic change over panel and supplies power to each load

## 2-4 Reliability of Loran C system

The Loran C system is extremely useful as a navigation system to cover a wide area, but it involves numerous problems when it is applied as it is in narrow channels where high degree of accuracy is required.

The factors or elements to influence the reliability of a system can be roughly divided into the following three items; radio wave propagation paths, transmitting equipment and receiving equipment. It is desirable that there is good harmony among these elements. In other words, it would be utterly meaningless if just the receiving equipment could be improved to almost perfection while the two other factors are dominant in lowering the reliability of the system. In the following paragraphs study will be made on the reliability according to the classified elements.

### 2-4-1 Propagation path

#### (1) Length of base line

The stability of propagation path is the key to determining the accuracy of a system. In order to maintain this stability, the base line should be as short as possible. In the case of the Loran C system which adopts transmission of pulses, high power and long base lines are inevitably required, and this gives rise to disturbances in the sky-wave. This danger increases when the length of the base line exceeds 1000 km.

Referring to this point, Mr. C.B. Jeffery of the Canadian Coast Guard indicates that when signal from the transmitting stations on the east coast of the United States was received, lane slip had already occurred at a point 300 miles away on the mixed land and sea propagation path (One lane slip corresponds to an error of  $10\mu s = 1500m$ ).

In other words, it can be said a system which cannot guarantee high reliability in the area 300 miles or more away. According to a report published by the National Technical Information Service (NTIS), the envelope-to-



cycle difference (ECD) sometimes changes by  $\pm 2.5 \mu S$  depending upon the difference of the propagation path. Further, it may change up to  $\pm 3 \mu S$  (error  $\pm 450m$ ) if the effect of the skywave is also taken into consideration. Unless Loran C adopts the differential system, the absolute accuracy (or geographic accuracy) would never be obtained in essence.

(2) Impulsive noise

The exclusive band width of the Loran C system is 20 KHz and therefore is susceptible to the influence of external noise. Particularly, the lightning impulsive noise at the time of thunderstorm falls completely in many cases from its energy distribution to within the Loran C transmission band width, and this is a defect in the L.F. band pulse transmission system.

(3) Inductive noise

In the cycle matching of the Loran C system the system is greatly affected by various noise sources in the vicinity of the receiving point. Noises from fluorescent lights, shipborne generators, radars, fish detectors, etc. all constitute causes of interference. Noises from cranes or other sources ashore while the vessel is getting alongside the wharf also become main causes of inductive noise, resulting in increasing lane slip.

(4) Interference of cross chain

According to a study made by Mr. D.A. Feldman and other Loran C experts of the U.S. Coast Guard, there is mutual interference between the existing chains. The South California Chain, for example, is seriously interfered by the Bering Sea Chain. This phenomenon will present itself all the more strikingly as Loran C chains increase in number. They warn that measures to counter such situation are urgently needed. The mere change of the

tracking rate is not sufficient as a counter-measure. Both phase code function (PCF) and group repetition interval (GRI) must be improved. This, however, will involve a large-scale improvement of transmitting chains, receivers and other equipment of the system, which will, in turn, present extremely serious problems, such as the obtaining of agreement on the part of the Governments, manufacturers and users, to say nothing of the international collaboration.

#### 2-4-2 Transmitting equipment

##### (1) Reliability of high power station

The scale of output of Loran C is a few figures larger than that of the Decca Navigator system. The base current of Loran C aerial amounts to as much as several hundred amperes at the peak value, making the base voltage go up, and this makes it necessary to work out measures to counter the corona discharge, thunderstroms and weather-proof peculiar to the tropical zone. This is a major factor to cause the deterioration of the system.

The operating hour percentage of the Decca chains in Japan attains over 99.9% throughout the year, and the system has been off-air just for a few minutes on an annual average. In the case of Loran C in the tropical zone, the percentage of operating hours is presumed to be very low, judging from the various factors mentioned above.

The mean time between failures (MTBF) and mean time to repairs (MTTR) in the modern Loran C station have already been published and are as shown in the table below. As seen from the figures, the off-air state should not take place even for a moment. The system can be said too coarse to be applied in the area in question.

Name of system	Fiscal year	MTBF (hour)			MTTR (minute)			Remarks
		Maximum	Minimum	Average	Maximum	Minimum	Average	
Loran C	'74	805	180	340	100	60	68	@ chain
	'75	1,913	180	366	510	60	134	@ chain

Note: Literature cited: "LF/VLF Navaid Signal Reliability in airborne applications "(Navigation,1976 Fall Vol 23, No.3)

In the above table the time of "off-air" includes only that of unexpected one, not off-air for the purpose of periodical maintenance check-up.

Failure occurs once every two weeks on an average.

(2) Pulse waveform of radiated power

In general, the height of a transmitting aerial in low frequency band is small as compared with the working wave length and therefore the radiation resistance is extremely low, quality factor (Q) is big and the band is apt to become narrow. For the Loran C system which uses pulse transmission, it is necessary to have matching circuit to conform to such type of transmission. In such cases, the aerial system can be easily affected by meteorological conditions by the fluctuation of various constants of Q, band width and the aerial of the aerial system due to the changes in earthing resistance and dielectric loss of the insulator. Particularly in the tropical zone where squalls or other sudden change in weather occur almost everyday, this presents a serious problem. With the fluctuation of the band width of radiation power comes the change in "rising time" of the pulse. To trim the rising waveform of pulses between the master and secondary stations in a chain, some special device would be needed not only in the aerial system, but in the whole transmitting system as well. It is however difficult for the system to maintain a high degree of accuracy.

(3) Control of envelope-to-cycle difference (ECD)

According to the data obtained from the U.S. Coast Guard, the width of  $\pm 5\mu S$  (error of approx.  $\pm 750m$ ) is accepted as the tolerance of ECD which constitutes the phase standard of transmitted wave. This means that the competent authorities themselves admit the extremely coarse and careless operation of their existing system. This problem has not been solved as yet. As compared with the Decca Navigator system, Loran C is originally a wide area oriented system, and it has frequency characteristics in the propagation path itself due to the difference by frequency of electric conductivity of the propagation path. Accordingly, the pulse waveform emitted from the transmitting point cannot be transmitted to the receiving point with accuracy, but is displayed in the form of ECD abnormality. This is a problem which affects the whole system and cannot be solved easily.

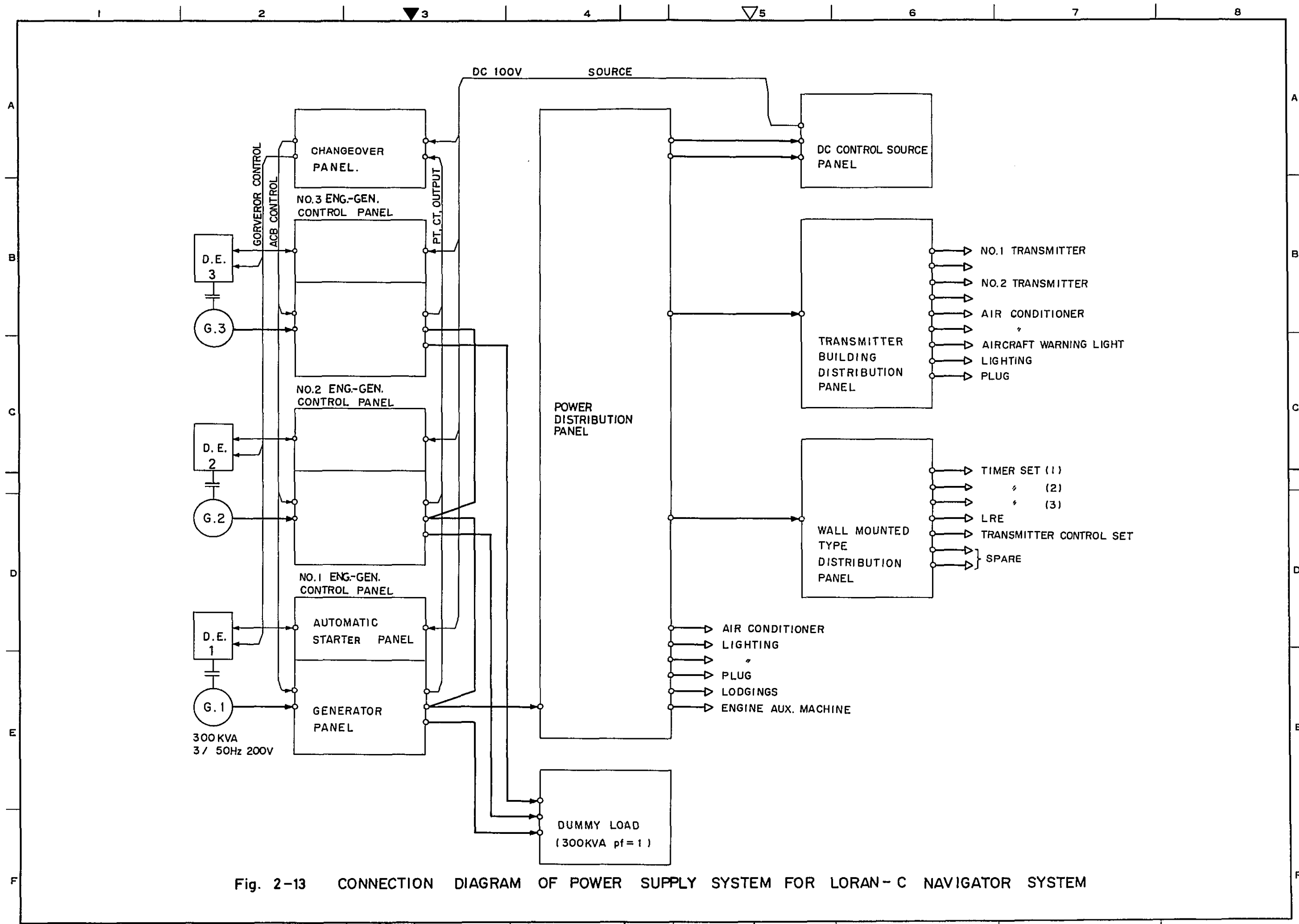


Fig. 2-13 CONNECTION DIAGRAM OF POWER SUPPLY SYSTEM FOR LORAN-C NAVIGATOR SYSTEM

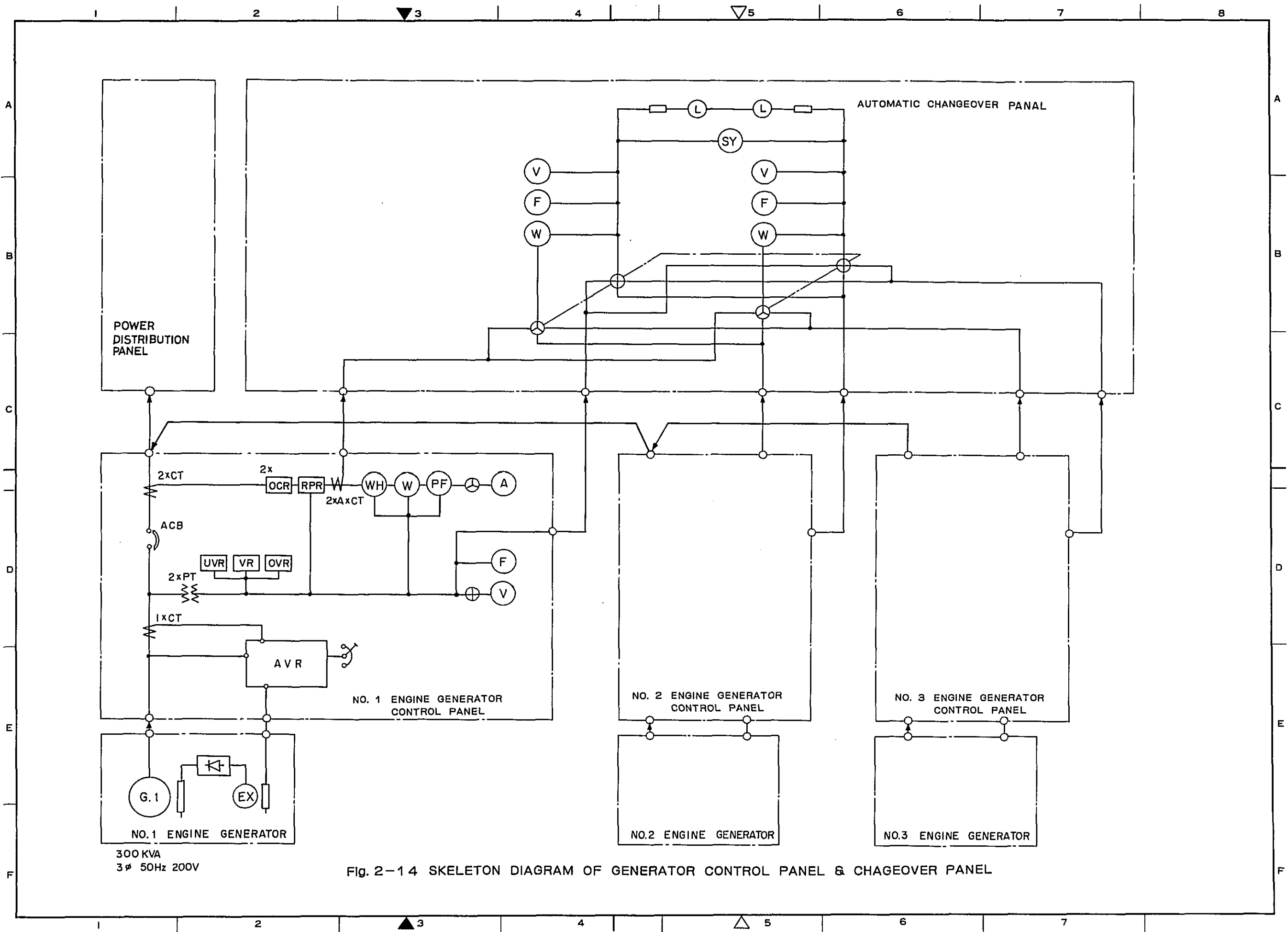


Fig. 2-14 SKELETON DIAGRAM OF GENERATOR CONTROL PANEL & CHAGEOVER PANEL

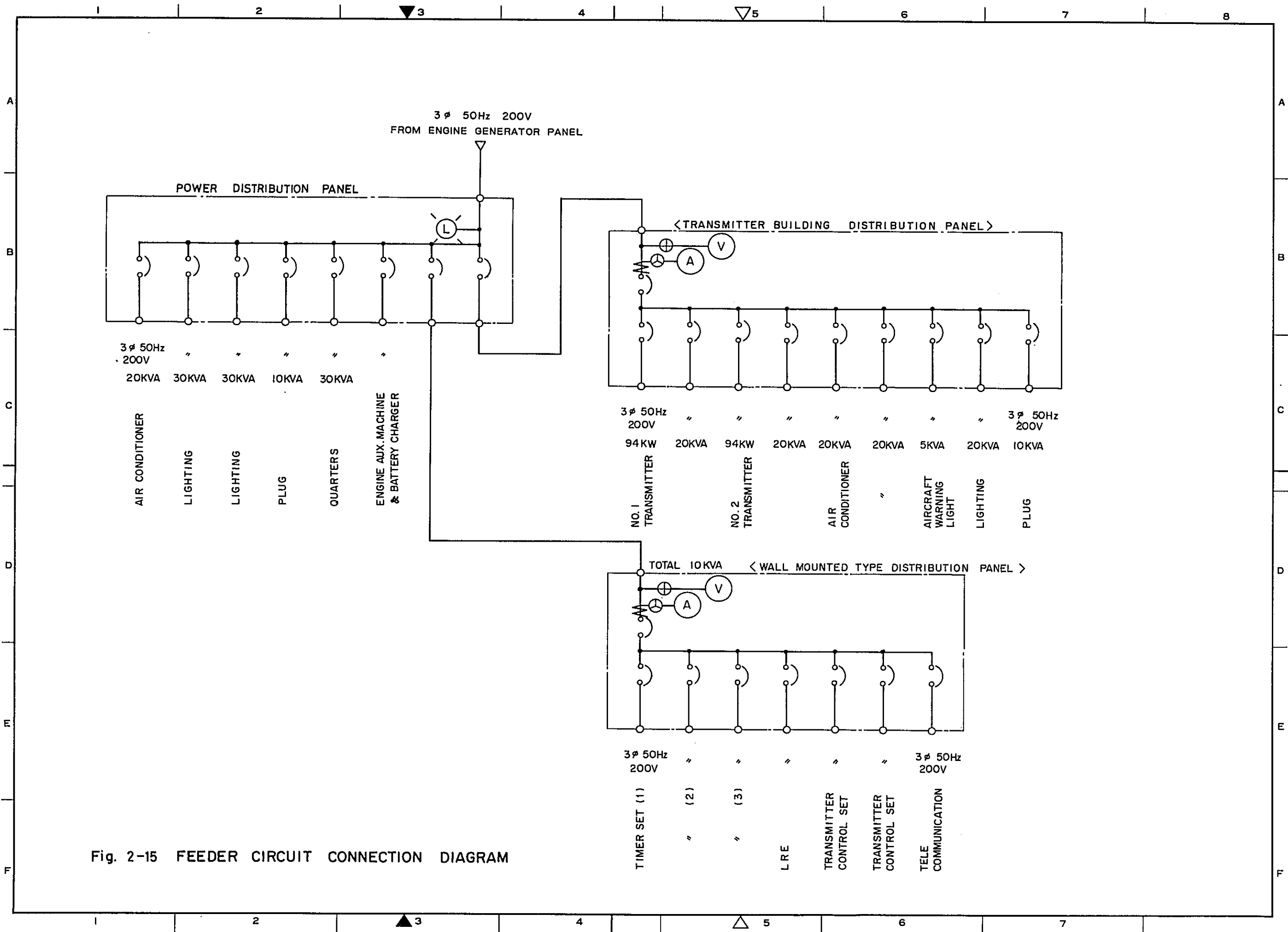


Fig. 2-15 FEEDER CIRCUIT CONNECTION DIAGRAM

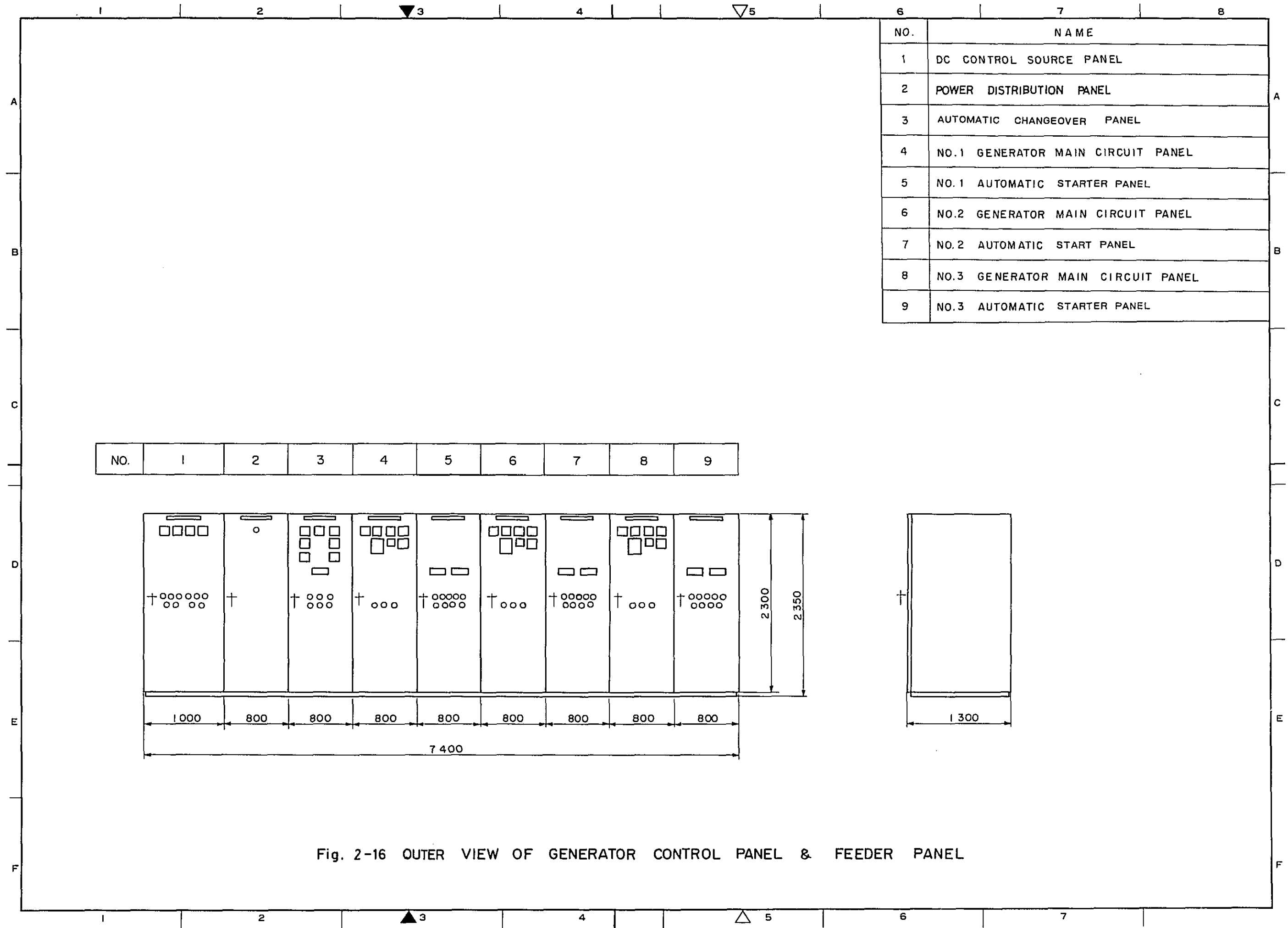
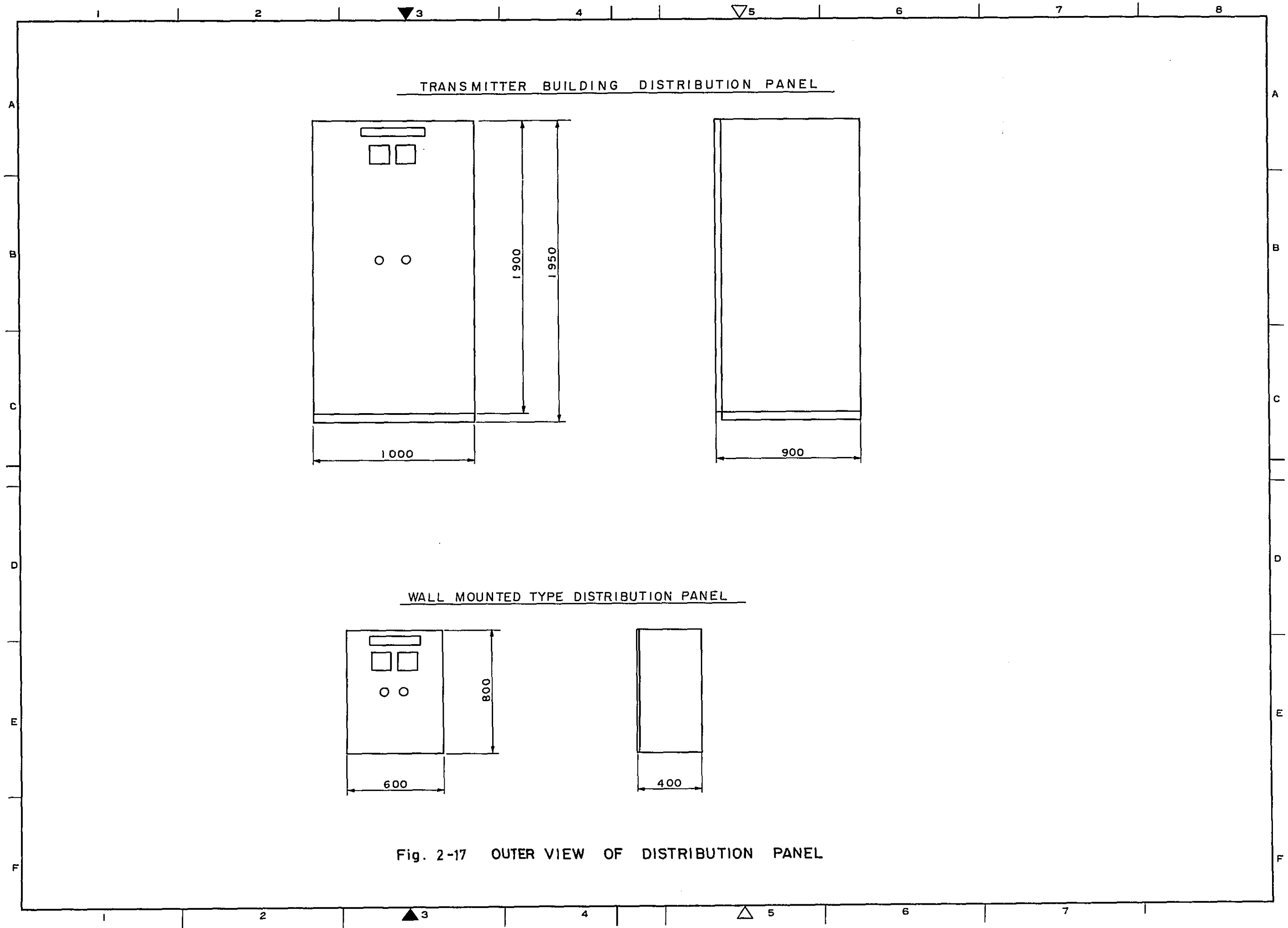


Fig. 2-16 OUTER VIEW OF GENERATOR CONTROL PANEL & FEEDER PANEL





DIESEL ENGINE		A C. GENERATOR	
TYPE	4 - CYCLES	TYPE	SYNCHRONOUS
NO. OF CYL	6	PHASE	3 $\phi$
BORE	180 m/m	VOLTAGE	200 V
STROKE	230 m/m	CURRENT	866 A
REVOLUTION	1 000 r.p.m.	REVOLUTION	1 000 r.p.m.
B. H. P.	450 P.S.	OUT PUT	300 KVA
B. M. E. P.	11.54 Kg/cm <sup>2</sup>	POWER FACTOR.	80 %
MAX. PRESS.	115 Kg/cm <sup>2</sup>	CYCLE	50 Hz
PISTON SPEED	9.2 m/s	NO. OF POLES	6
STARTING	COMP. AIR	EXCITING	
COOLING	WATER	RATING	CONTINUITY
WEIGHT	5 450 Kg	WEIGHT	2000Kg

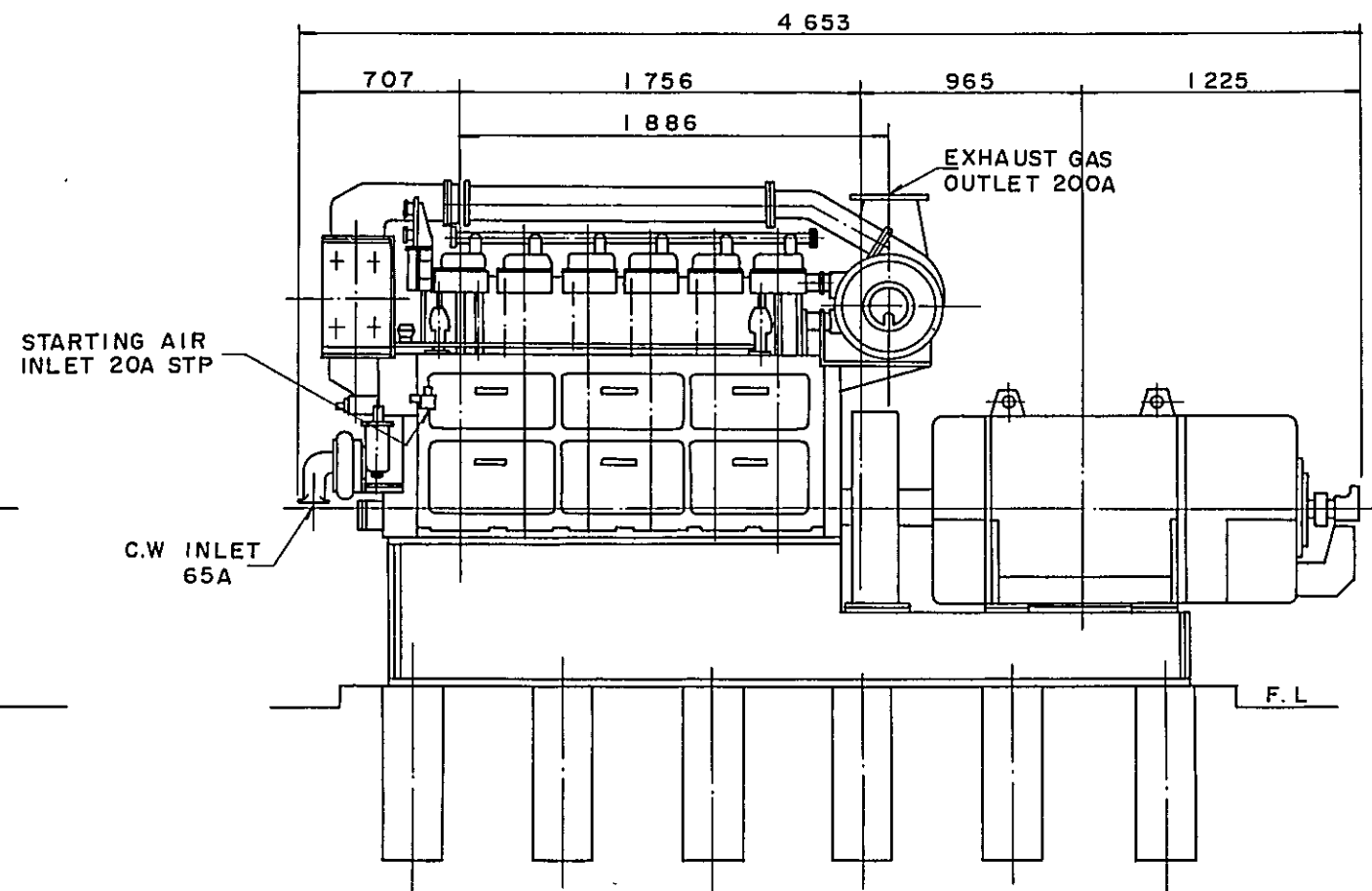
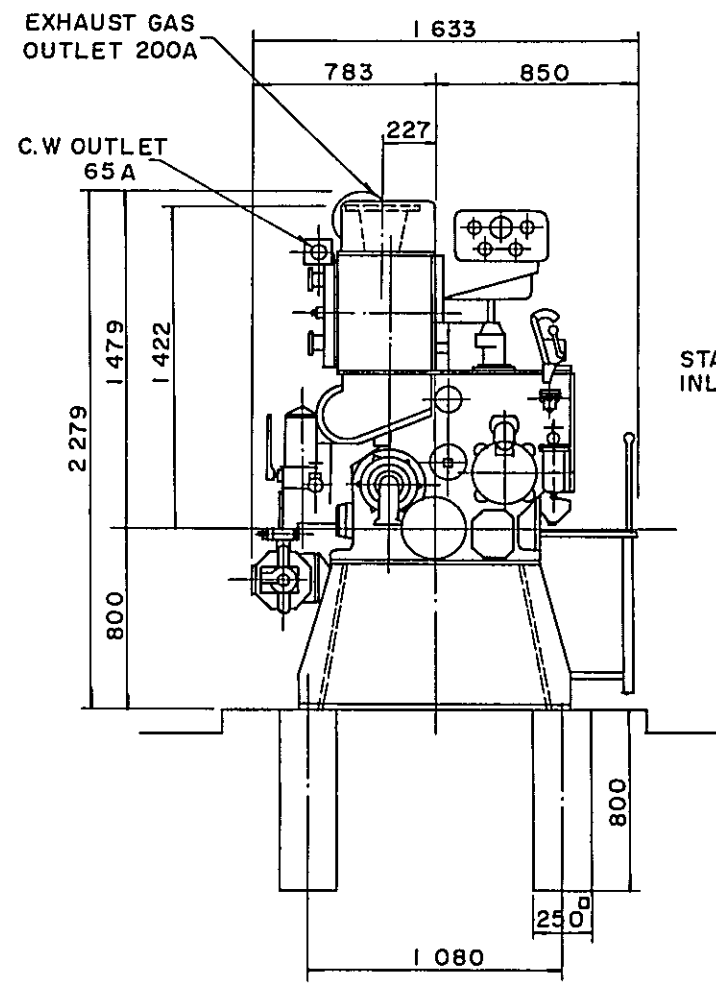
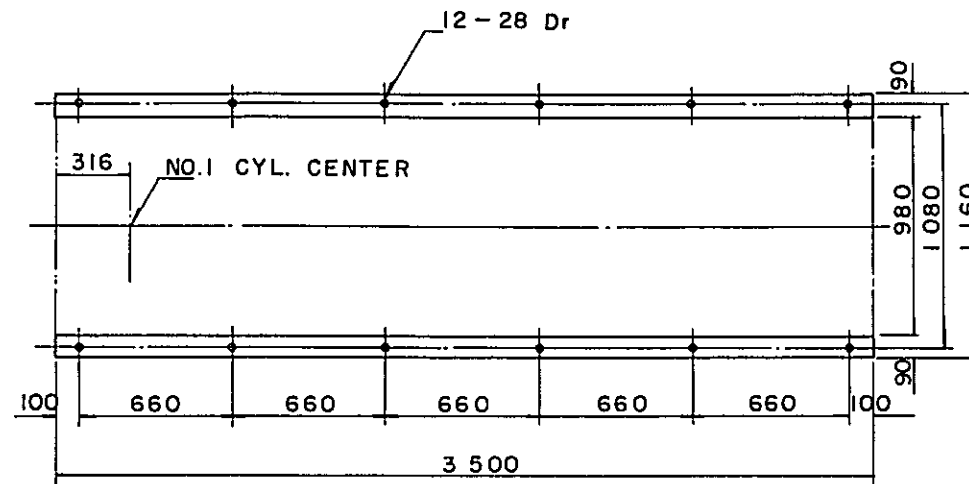
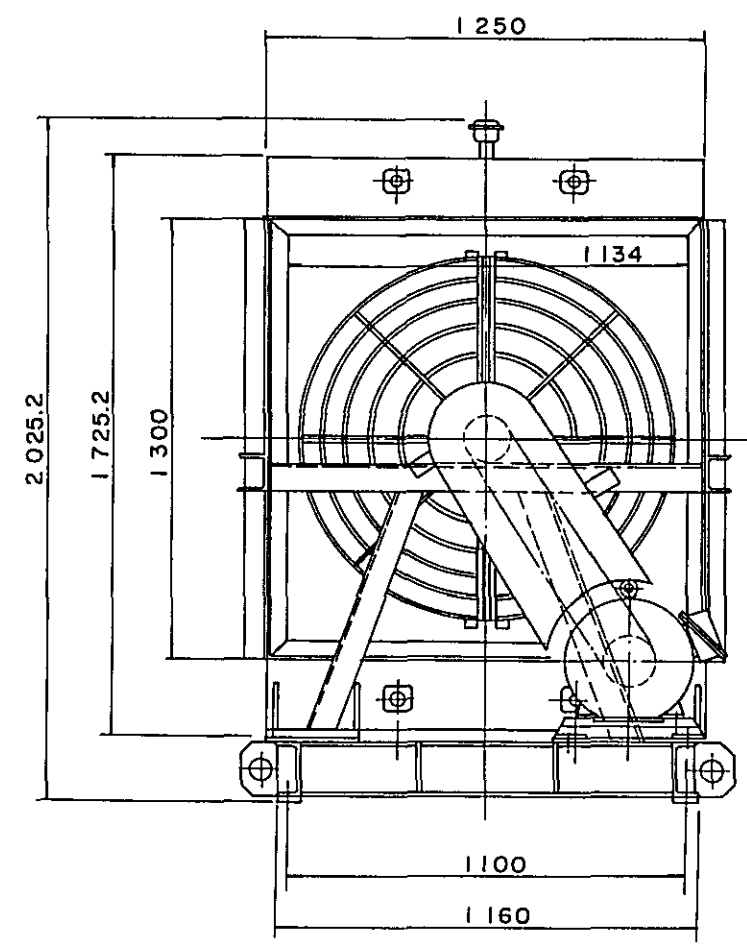
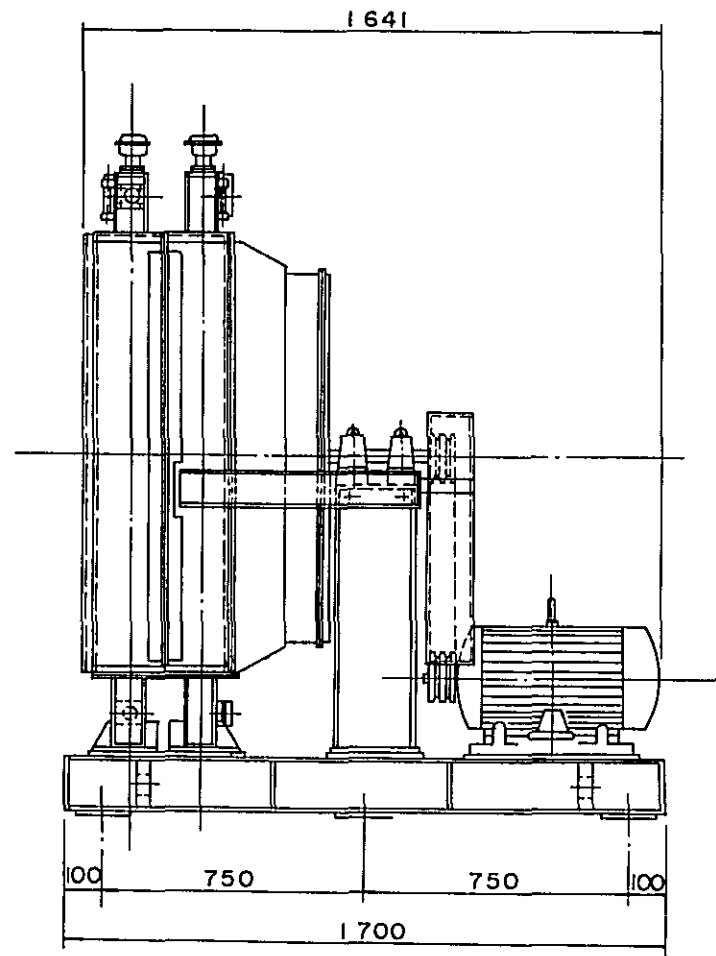
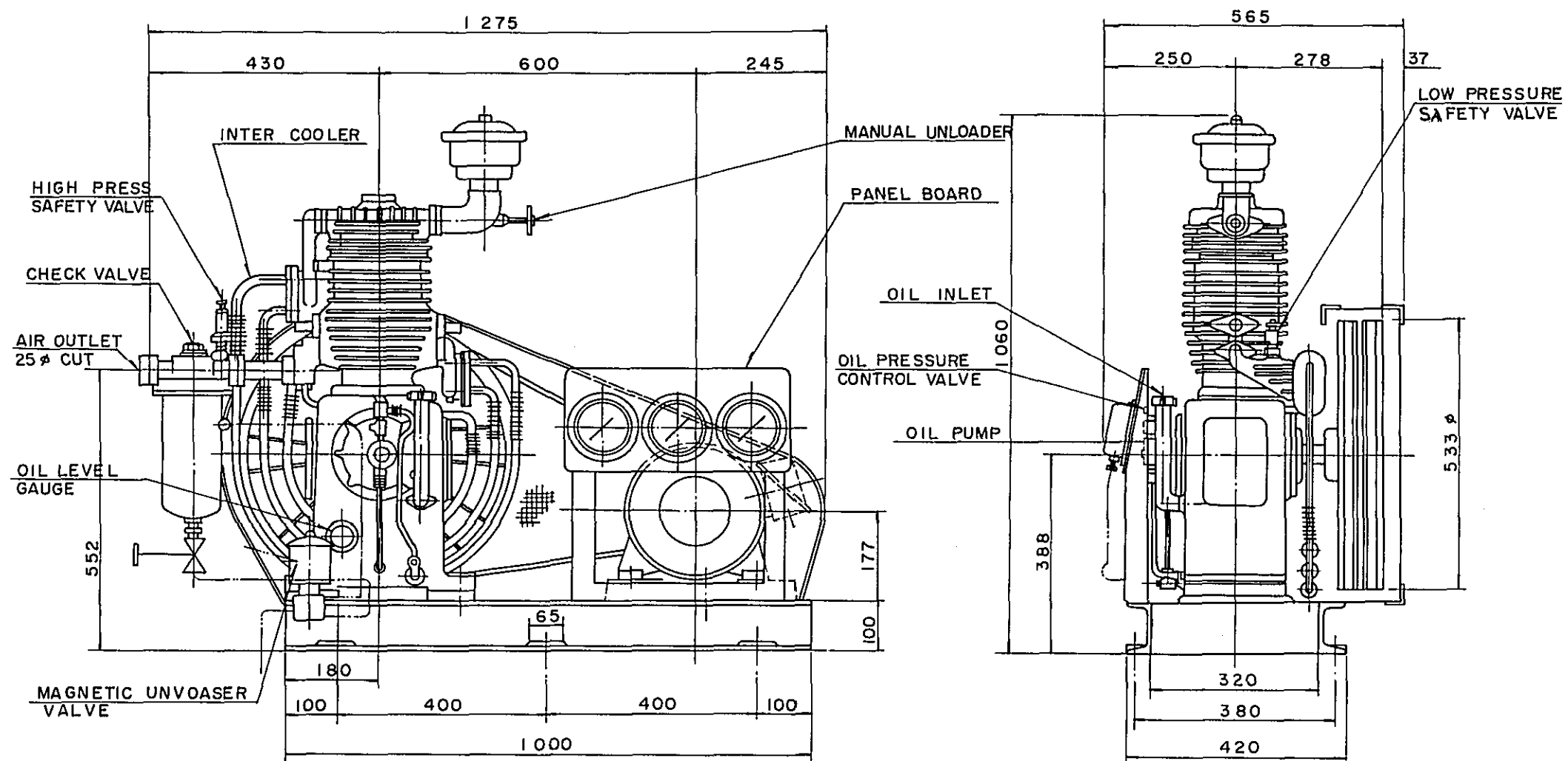


Fig. 2-18A OUTER VIEW OF ENGINE - GENERATOR



	JACKET COOLER	WATER COOLER	FAN & MOTOR	
RADIATION AREA	124.43 m <sup>2</sup>	66.47 m <sup>2</sup>	OUTER DIA.	1016 $\phi$ mm
FIN	98.61 m <sup>2</sup>	49.27 m <sup>2</sup>	AIR FLOW RATE	680 m <sup>3</sup> /min
TUBE	25.82 m <sup>2</sup>	17.20 m <sup>2</sup>	REVOLUTION	1355 RPM
			MOTOR OUT PUT	18.5 KW

Fig. 2-18B RADIATOR FOR ENGINE GENERATOR



AIR COMPRESSOR		A · C MOTOR	
TYPE	AIR COOLER DOUBLE STAGE COMPRESSION	OUT PUT	5.5 kw
BORE	HIGH PRESS 107.95 mm LOW PRESS 127 mm	NO. OF POLE	4 P
STROKE	101.6 mm	CYCLE	50 Hz
PRESS	30 kg/cm <sup>2</sup>	REVOLUTION	1500 RPM
REVOLUTION	620 RPM		
CAPACITY	47.7 M <sup>3</sup> /Hr		

Fig. 2-18C AIR COMPRESSOR

SPECIFICATIONS		
MAX. OPERATING PRESS.	30	Kg/cm <sup>2</sup>
DESIGN PRESS	32	Kg/cm <sup>2</sup>
SAFETY VALVE	32	Kg/cm <sup>2</sup>
HYDROLIC TEST		
BOTTLE	48	Kg/cm <sup>2</sup>
HEADER	64	Kg/cm <sup>2</sup>
PRESSURE SWITCH SET PRESS.		
AUTO-CHARGE	22	$\frac{ON}{OFF}$ 30 Kg/cm <sup>2</sup>
ALARM	18	Kg/cm <sup>2</sup>

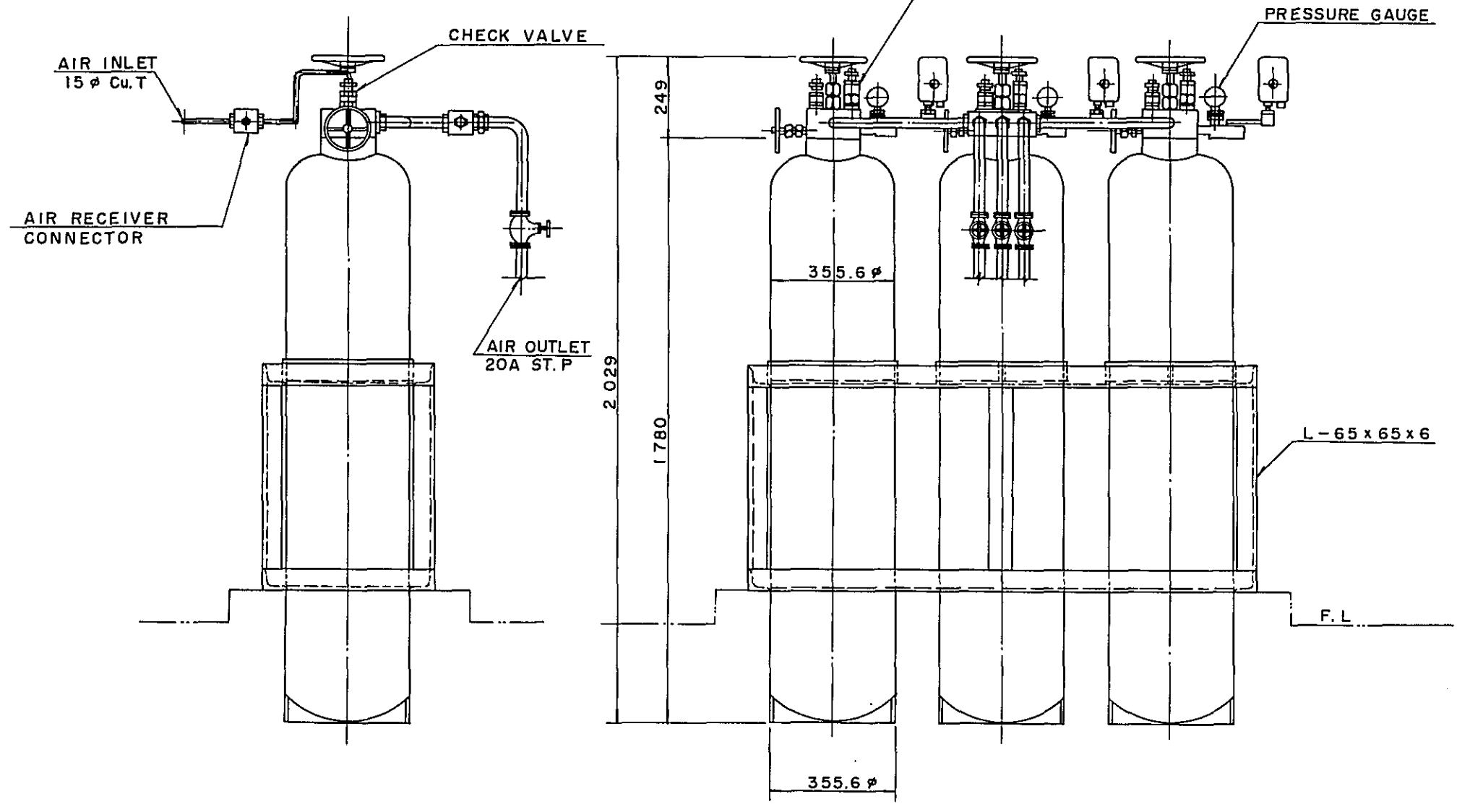
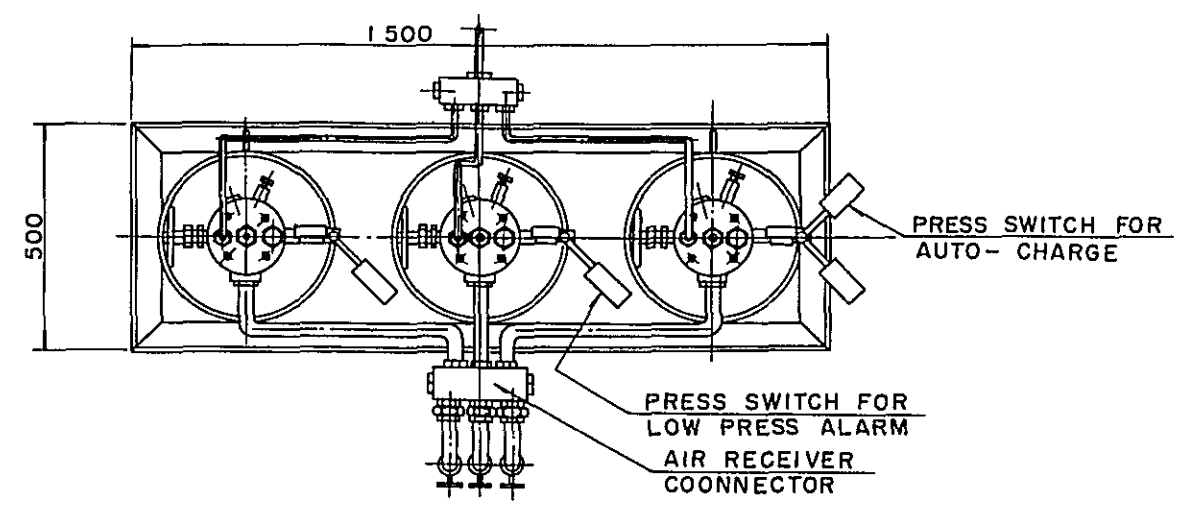


Fig. 2-18D (3-1500) AIR TANK

### 3. Accuracy of Decca system and Loran C system

#### 3-1 Accuracy of Decca system

##### 3-1-1 Introduction

The errors of the Decca Navigator system can be roughly classified into two groups: those caused by alterations in the state of radio wave propagation and those others which are indigenous to the system itself.

The first group of errors are random errors caused chiefly by changes in time of atmosphere in radio wave propagation path, while those of the latter group are errors caused from configuration of the transmitting station and performance of the equipment, and the value of these latter errors could be reduced by efforts of the operator.

##### 3-1-2 Random errors

Random errors are caused by changes in time of atmospheric condition in radio wave propagation path, changes to Decca equipment for a short time, or by errors in reading numerical value. The biggest cause of all these is the changes in time of atmospheric condition in the radio wave propagation path, and the influence is big particularly at night.

In the Decca Navigator system it is always necessary to ensure that the synchronised radio waves from the master and slave station arrive at the receiving point, maintaining a certain phase relationship.

Most of the radio wave propagation is the ground wave that propagates along the surface of the earth during daytime. The reflecting energy of the radio wave radiated toward the sky (sky-wave) is extremely small (The reflection factor at E-layer in the sky 70km high is approximately 2%) and therefore negligible. The phase deviation is also small, and errors caused by the propagation condition do not present any problem. During nighttime,

however, the activities of the E-layer about 100km high up in the sky and the ionosphere called F-layer, 200 to 400km high are remarkable, and the radio wave radiated toward to sky are refracted as it travels through the ionosphere and, reflected, return to the surface of the earth. The reflection factor at 95km high up in the sky is approximately 25%. This is because the ionosphere comprises free electron and positive and negative ionospheric layer, and its character is unstable, and the degree of reflection changes every moment, with which the phase and amplitude of the skywave that has returned to the ground also change every moment. Since the Decca system adopts continuous wave system, unlike the Loran C system which employs pulse wave, cannot utilise skywave and ground wave by distinguishing one from the other. Accordingly, as the power of skywave at the receiving points becomes strong, the skywave joins the ground wave to make composite wave, the amplitude and phase of which fluctuate to cause errors in the fixed position.

(1) Errors by skywave

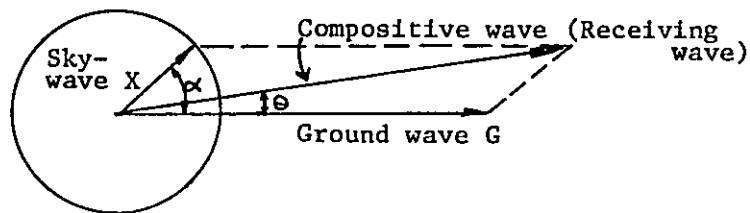


Fig. 3-1

The fluctuation of phase of the received radio wave, caused by composite wave of ground wave and skywave may be obtained in the following manner:

In Fig. 3-1 above, suppose

- G: Field intensity of the ground wave
- S: Square mean value (R.M.S.) of field intensity of the skywave
- X: Instanraneous valve of S.

$\Theta$ : Phase angle (radian) of the composite wave and ground wave

$\Theta_1$ : Instantaneous value (radian) of  $\Theta$

$\alpha$ : Phase angle of the skywave and ground wave, and here  $X > G$  and  $(X/G) > 0$ ,

then

$$\sin \Theta_1 \rightarrow \Theta_1 \doteq \frac{X \cdot \sin \alpha}{G}$$

If this is expressed in cycle, the result will be:

$$\frac{X \cdot \sin \alpha}{2X \cdot G}$$

Since the probabilities caused by all values of  $\alpha$  are considered equal, if the square mean value of  $\Theta_1$ , by the mixing of skywave S is set at  $\sigma$ ,

$$\begin{aligned} \sigma^2 &= \frac{\sum \Theta_1^2}{n} \\ &= \frac{1}{n} \sum \left( \frac{1}{2\pi} \cdot \frac{1}{G} \cdot X \sin \alpha \right)^2 \end{aligned}$$

Since again the square mean value of X is S and that of  $\sin \Theta$  is  $1/\sqrt{2}$ ,

$$\sigma = \frac{1}{\sqrt{2}} \cdot \frac{1}{2\pi} \cdot \frac{S}{G} \doteq \frac{1}{9} \cdot \frac{S}{G} \text{ (cycle)} \dots (3-1)$$

can be obtained.

Therefore, if the square mean value of synchronization errors between the master and slave stations is held at 0.01 cycle,  $S/G = 0.09$  can be obtained. This indicates that the intensity of the skywave is made less than -21 db against the intensity of the ground wave.

## (2) Lane errors

The Decca Navigator receiver receives radio waves transmitted from the master and slave station, multiplies the radio waves up to comparison frequency,



compares phases and displays phase difference on the decometer.

If the radio waves from both stations have undergone phase fluctuation by skywave, such waves are multiplied and phase compared, and the result is lane errors in the decometer, which becomes errors in fixing positions.

When two signals a and b are multiplied and phase compared — one signal has phase angle  $\theta_1$  of the composite wave of ground wave and skywave and the other signal has phase angle  $\theta_2$  of the ground wave — , the resultant phase difference  $\theta_x$  will be:

$$\theta_x = a \cdot \theta_1 - b \cdot \theta_2$$

Accordingly, the phase difference x

$$\begin{aligned} \text{is: } \sigma_x^2 &= \frac{1}{n} \quad \theta_x^2 = \frac{1}{n} \quad (a \cdot \theta_1 - b \cdot \theta_2)^2 \\ &= \frac{1}{n} \left\{ \sum a^2 \cdot \theta_1^2 + \sum b^2 \cdot \theta_2^2 - \sum 2ab \theta_1 \cdot \theta_2 \right\} \end{aligned}$$

Since  $\theta_1$  and  $\theta_2$  are considered to change arbitrarily and all their values are considered to be produced with the equal probability, the result will be:

$$\sum a \theta_1 \cdot b \theta_2 = 0$$

Therefore:

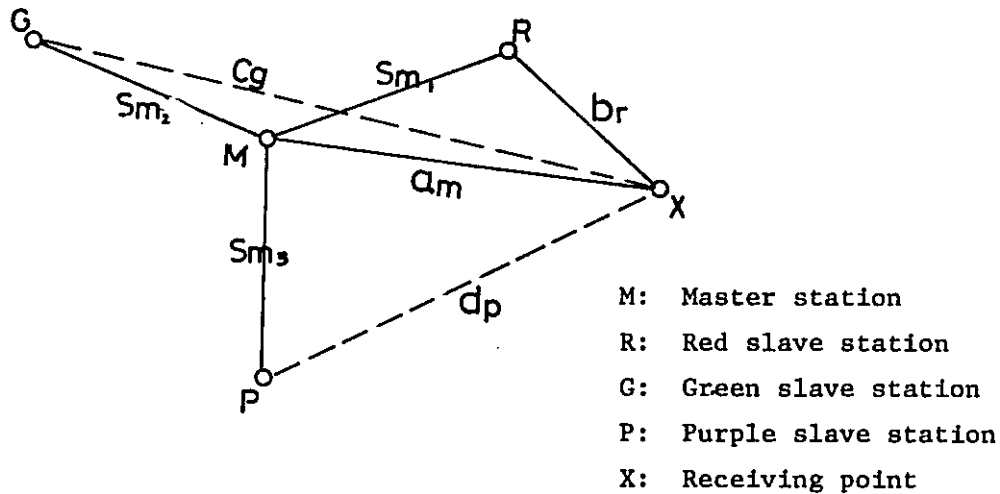
$$\sigma_x^2 = a^2 \cdot \sigma_1^2 + b^2 \cdot \sigma_2^2$$

Where  $\sigma_1$  is square mean value of  $\theta_1$

$\sigma_2$  is square mean value of  $\theta_2$

### (3) Application of the skywave error theory to Decca chains

The master and slave stations of the Decca Navigator system transmit radio wave of different frequencies having multiplying relationship, and it is therefore necessary to modify the frequency relation when skywave errors are considered.



To take the pattern of the red slave station for example, errors at the receiving point X are presumed to be those by phase deviation as shown below.

- Sm1: Phase deviation of master station frequency (6f) in synchronisation path of master/slave
- br : Phase deviation of red slave station frequency (8f) in path between red slave and receiving point
- am : Phase deviation of master station frequency (6f) in the path between master and receiving point

When the phase deviation of signal from the master station in the propagation path of master/slave stations is Sm1 cycle, the deviation is converted into amount four times that of the comparison frequency of the control receiver of a slave station. The amount of phase deviation is subject to 1/3 time conversion when it is converted into the frequency of the red slave station.

Accordingly, the phase of the signal from the red slave station has a phase deviation of 4/3 Sm1. Further,

the signal is subject to the phase deviation of  $br$  by the time it reaches the receiving point. The phase deviation of the red slave station at Point X is:

$$(br + \frac{4}{3} Sml) \text{ cycle}$$

On the other hand, the signal from the master station, which has reached the receiving point through the path of MX is subject to the phase deviation of  $Am$ .

The phase deviation  $\Theta_R$  of the red decometer at the time when the signal from both the master and slave stations at the receiving point is taken into the receiver and converted into comparison frequency, is indicated in the following formula:

$$\begin{aligned} \Theta_R &= 4Am - 3(br + \frac{4}{3} Sml) \\ &= 4Am - 3br - 4Sml \text{ cycle or lane} \dots\dots(3-2) \end{aligned}$$

When a number of observation values of  $\Theta_R$  have been obtained, the following expression is possible as dispersion of  $\Theta_R$ :

$$\begin{aligned} \sigma_R^2 &= \frac{\sum_{i=1}^N \Theta_{Ri}^2}{N} \\ &= \frac{\sum_{i=1}^N (4Am - 3br - 4Sml)^2}{N} \dots\dots(3-3) \end{aligned}$$

Where N is amount of observation value

Both  $Am$  and  $br$  are clearly independent and employ random distribution with zero as mean value, and have no interphase for phase errors.

The term of cross product of Am and br under big observation value, therefore, can be deemed as zero. Accordingly,  $\sigma_R$  is expressed as follows:

$$\sigma_R^2 = 16\sigma_{Am}^2 + 9\sigma_{br}^2 + 16\sigma_{Sm1}^2 + (0.012)^2 \dots (3-4)$$

The 0.012 in the above expression is an amount estimated for automatic synchronisation error at a slave station and follow-up error of the receiver.

Likewise, in the green pattern, we can obtain:

$$\begin{aligned} \Theta_G &= 3A_m - 2 \left( \frac{3}{2} S_{m2} + C_g \right) \\ \sigma_G^2 &= 9\sigma_{Am}^2 + 9\sigma_{Sm2}^2 + 4\sigma_{Cg}^2 + (0.009)^2 \dots (3-5) \end{aligned}$$

In the purple slave station

$$\begin{aligned} \Theta_P &= 5A_m - 6 \left( \frac{5}{6} S_{m3} + d_p \right) \\ \sigma_P^2 &= 25\sigma_{Am}^2 + 25\sigma_{Sm3}^2 + 36\sigma_{d_p}^2 + (0.015)^2 \dots (3-6) \end{aligned}$$

can be obtained.

### 3-1-3 System error

When the Decca Navigator system is utilised in measuring phase difference and the position obtained from the mean value of the thus measured value differs from the actual position, it is said that there is a system error. There are several types of system error as shown below.

#### (1) Error by propagation speed of radio wave

The propagation speed of radio wave varies according to the soil conductivity of propagation path. Generally, the speed is indicated in the following values:

In vacuum	299792 km/sec
At sea	299650 km/sec

In fresh water	299250 km/sec
Over farm	299400 km/sec
In mountain area	298800 km/sec

The propagation path between the transmitting point and the receiving point is not normally of a single property. It usually passes the portion where soil conductivity varies. In order to calculate an accurate position, the propagation speed is assumed with every classification of the conductivity, and distance is calculated also with each classification of propagation path, and thus the chart calculation is performed most effectively by the integral value of each phase value.

The chart calculation in the Decca Navigator system is carried out by dividing the propagation path into two types; that of the sea and that of land, or by further dividing land propagation path into that of big conductivity and that of small conductivity, and by applying a suitable propagation speed to the propagation path. The length of base line is relatively short in this system and this contributes to the smallness of accumulation of errors and to the satisfactory result of the calculation.

The chart calculation in the Loran C system, on the other hand, is performed on the basis of a single propagation path which results in an increase in the accumulated errors caused by the large distance between two stations, and in big errors.

- (2) Frequency stability and error of radio wave transmitted from the master and slave stations

The frequency deviation of radio wave transmitted from the master and slave stations is indicated as deviation of line of position and becomes a system error.

The deviation  $\delta(m)$  caused by frequency deviation  $\Delta f$  is expressed as follows, of the distance to the receiving point is  $D(m)$ :

$$\delta = \frac{a}{c} \cdot D \cdot \Delta f$$

Where  $C$  is propagation speed of radio wave  
 $a$  is wave length

As explained in the following paragraph, this system has a frequency oscillator of high degree of accuracy, and the errors of this system referred to in this paragraph are quite negligible.

(3) Errors by phase synchronisation between the master and slave stations

In the Decca Navigator system, the ground wave (Gf) from the master station is received at a slave station, which, in turn, transmits radio wave synchronised to the one received from the master station. If there is an error in this synchronisation, it will become an error in position fixing. During the nighttime may be mixed with skywave and affected by the fluctuation of phases, which makes it difficult to maintain the normal phase relations between the master and slave stations. This also causes an error in position fixing. The synchronisation between the master and slave station is performed by 6f transmitted from the master station, but the synchronisation error at the time of synchronisation is held within the sphere of 0.01 lane by the decometer of the user's receiver, i.e. within 0.01 Hz by comparison frequency, and this means the error is held within 0.001 Hz by 6f.

(4) Geometrical accuracy of line of position

1) Deviation error

In the Decca Navigator system, the higher the

density of lines of position, the smaller the deviation error of lines of position influenced by indicating error of the decometer. The deviation error is smallest when it is on the base line and becomes larger as it falls out farther of the line.

Suppose the width of a lane on the base line is denoted as  $W$ , the included angle between the master and slave stations, measured from the measuring point, as  $\phi$  and the error of measured value of the lane as  $\Delta l$ , the deviation error  $\Delta S$  at the point can be expressed as follows:

$$\Delta S = \Delta l \cdot W \cdot \operatorname{Cosec} \frac{\phi}{2}$$

As clearly seen from this expression, at the point where the included angle  $\phi$  becomes zero, i.e. on the base line extension, deviation error will become infinitely great and unusable, and on the base line the included angle becomes 180 degrees and the error becomes smallest.

## 2) Error by crossing angle

When accuracy of the lines of position is considered, reference must be made to the random error contained in the reading value of the decometer and the deviation error determined by the position of measuring point as described in the preceding paragraph. Therefore, error band can be considered on both sides of the line of position.

The position obtained as crossing point of the line of position by the reading value of two decometers is located within the parallelograms overlapped with two error bands as shown in Fig. 3-2 below.

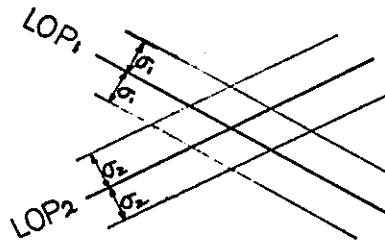


Fig. 3-2

It is, however, inconvenient to express the error by such parallelograms, and the general practice is denote the error by error circles.

Suppose the difference in distance between the measured position of a vessel and the actual position of the same vessel is expressed as  $d$ , and the standard deviation of  $d$  as  $\sigma_d$ , and this is denoted by the standard deviations  $\sigma_1$  and  $\sigma_2$  of the measured value of the line of position and the crossing angle  $Q$  of the line of position,  $\sigma_d$  is:

$$\sigma_d = \text{Cosec } \theta \sqrt{\sigma_1^2 + \sigma_2^2}$$

The radius  $R$  of the error circle denoted by distance (68% circular error field) is indicated by the following expression:

$$R = \text{Cosec } \theta \sqrt{(\sigma_1 W_1 \text{Cosec } \frac{\psi_1}{2})^2 + (\sigma_2 W_2 \text{Cosec } \frac{\psi_2}{2})^2} \dots (3-8)$$

Where  $W_i$  : Width of a lane on base line of  $LOP_i$

$\psi_1$  : Included angle between master and slave stations Viewed from the measuring point

3-1-4 Estimated accuracy of Decca system in the low latitude zone

The propagation during the nighttime of the radio wave of long wave band is subject to the magnetic field and latitude effect of the earth. The Decca Navigator Co. and organisation in the



countries having the Decca system in operation have collected data and information on the propagation of radio wave in order to establish proper operation of the Decca Navigator system which utilises radio wave of long wave band. The data thus collected have been made available to general public.

The data on estimated accuracy of the system in such low latitude zone as Malacca/Singapore straits and Lombok/Makassar straits have been prepared by the Japanese survey team on the basis of the actual data and automatic drawing by computer under the following conditions:

- 1) The curve shown in Fig. 3-3 has been used as standard deviation curve of random phase error during nighttime.

The data obtained from actual measurement at Decca stations in Japan on the distance-to-skywave intensity curve as shown in Fig. 3-4 have also been taken into consideration in slide calculation together with the latitudinal effect.

- 2) The curve has been added with the following frequency characteristics:

5f	+ 1.5 db (multiplied by 1.189)
6f	} Without any change
8f	
9f	-0.5 db (multiplied by 0.944)

- 3) The relative co-efficient of the line of position has been made at 0.75 during nighttime and 0 during daytime in calculating errors in position-fixing.
- 4) The following values have been added as fixed errors appearing on the decometer:

Red pattern	0.012 lane
Green pattern	0.009 lane
Purple pattern	0.015 lane

- 5) The daytime value of phase error has been - 9db ( $1/2.83$ ) lower than the curve of  $0^\circ$  shown in Fig. 3-4.

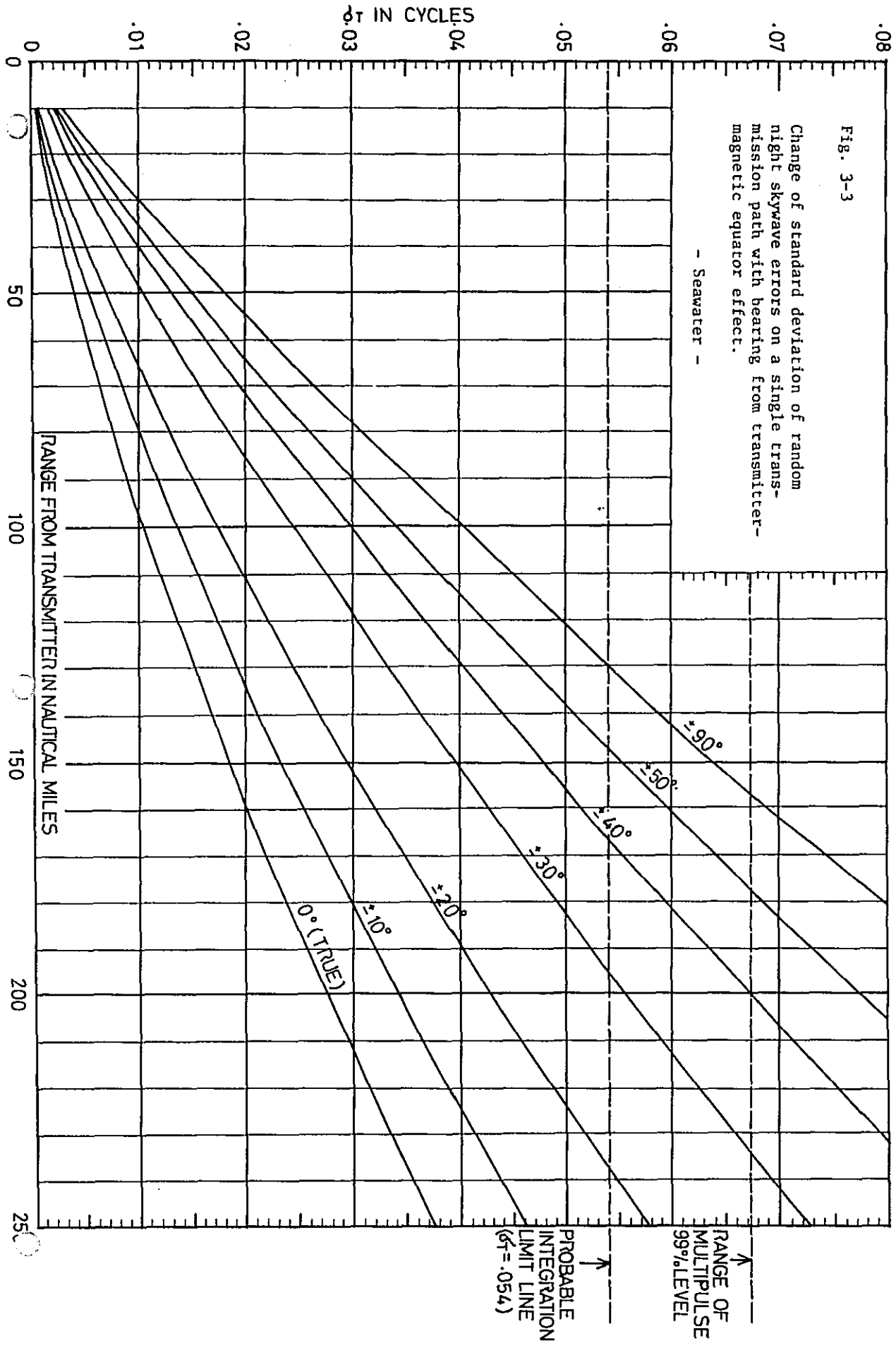


Fig. 3-3

Change of standard deviation of random night skywave errors on a single transmitter path with bearing from transmitter-magnetic equator effect.

- Seawater -

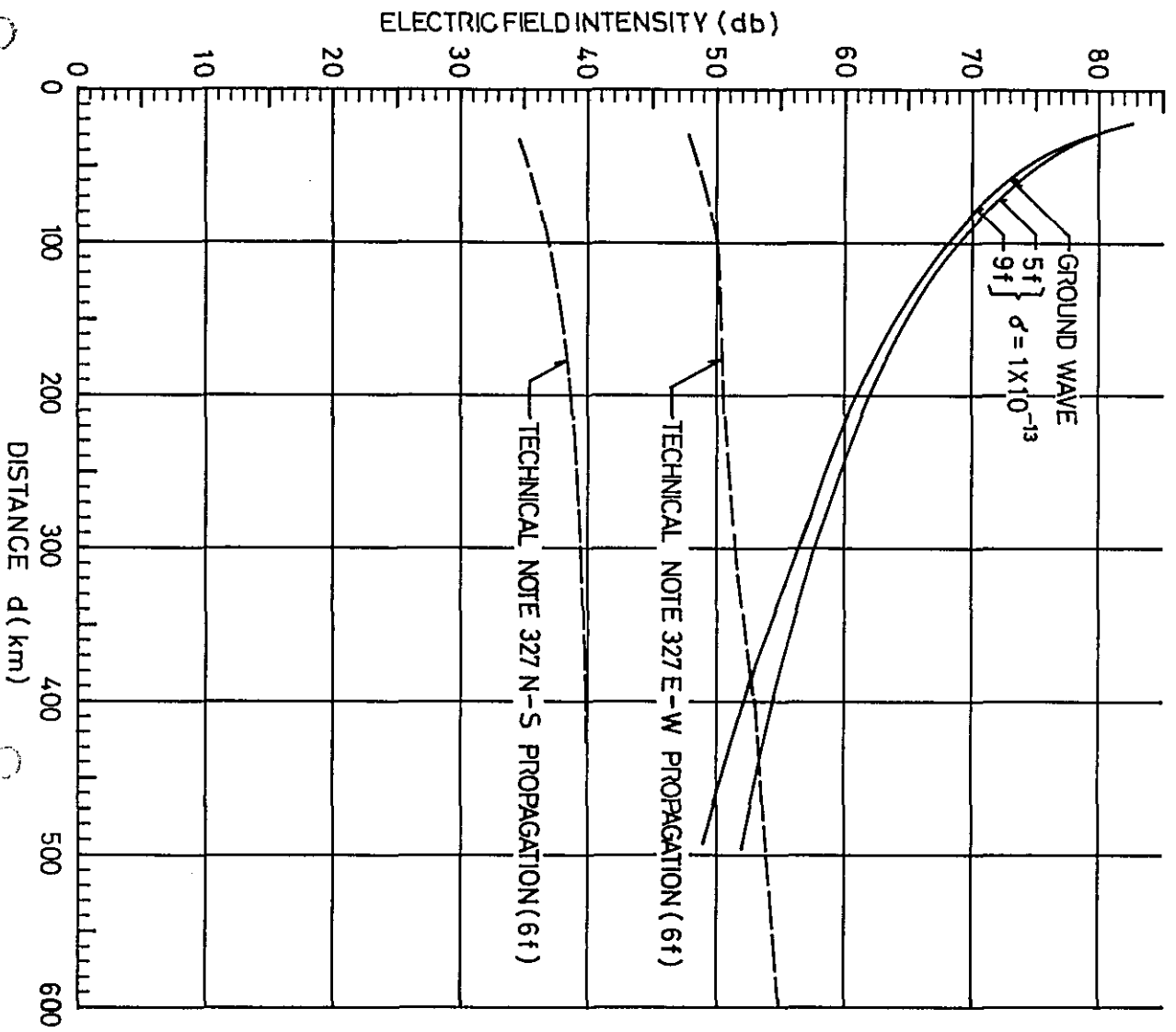


Fig. 3-4  
 Electric field intensity of  
 ground wave and skywave

## 3-2 Accuracy of Loran C system

### 3-2-1 Introduction

The fundamental matters relating to the errors of the Loran C system are similar to those of the Decca Navigator system. The only difference should be that the selection of ground wave and skywave is possible in the Loran C system which employs pulses, by utilising the third rising-up cycle of the pulse. However, transmitting stations throughout the world mingle in a single channel of frequency band of 90 to 110 KHz and particularly at night these stations mutually beat signals from other stations on many occasions. This trend will become increasingly marked in the future. This beating of signals is rated in the similar way as an extremely big noise, which would bring timing changes in the display of the receiver. In the calculation of errors these are completely disregarded and the evaluation is made in the quite ideal state which is far from the actual situation.

### 3-2-2 Estimation of accuracy of Loran C system in low latitude zone

The estimation data on the accuracy of the Loran C system have been indicated in automatic drawing by a computer taking the following conditions into account:

- a) Relation between signal-to-noise ratio and standard deviation ( $\sigma_{DT}$ ) of received signal.

The time fluctuation by noise of the secondary servo used in the Loran C receiver is, according to a report published by the National Technical Information Service (NTIS), expressed in the following expression:

$$\sigma = 1.25 \left( \frac{N}{S} \right) \frac{1}{\sqrt{n}} \cdot K_a \frac{1}{4} \dots\dots(3-9)$$

Where  $\sigma$ : r.m.s. error ( $\mu s$ )

N/S : r.m.s. noise-to-signal ratio  
at input point of sampler

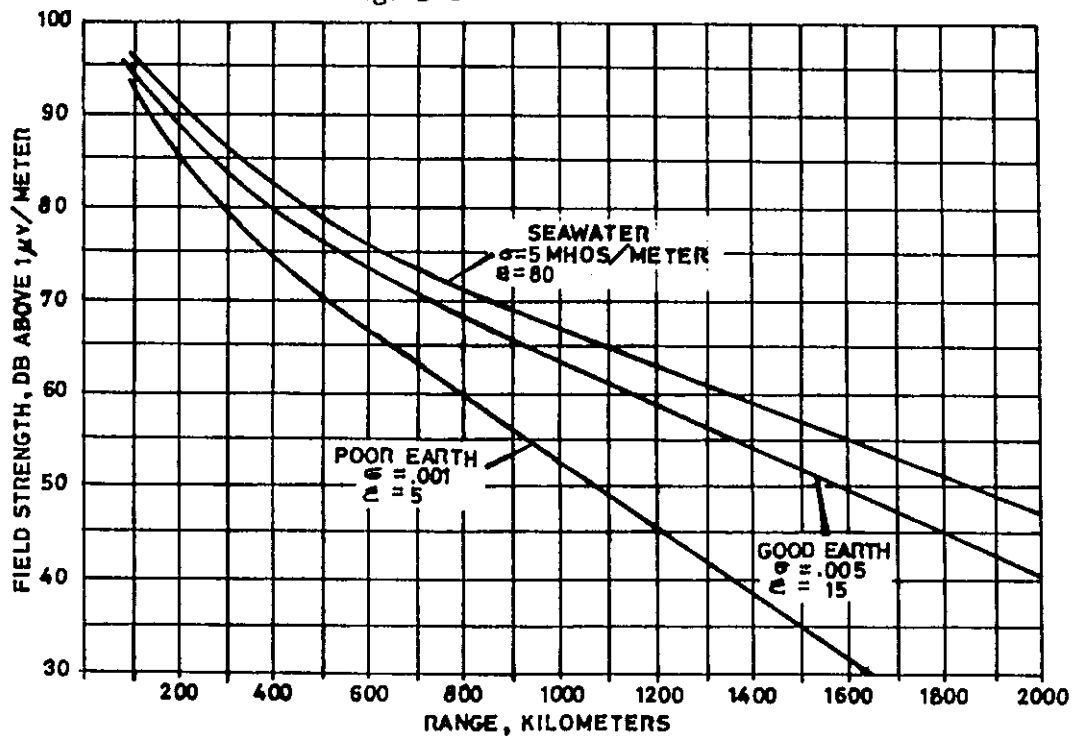
n : Number of samplings per second  
(80 in normal Loran C chains)

Ka : Accelerating constant of servo  
loop (According to NTIS  
report, ITT-make equipment Ka  
is:  $Ka = 0.08 \text{ rad/sec}^2$  )

b) Relation between distance and field intensity

According to the data published by ITT, the field intensity of Loran C (field intensity of sampling point (3rd cycle), from a transmitting station having transmission power of 400 KW) is as shown in Fig. 3-5.

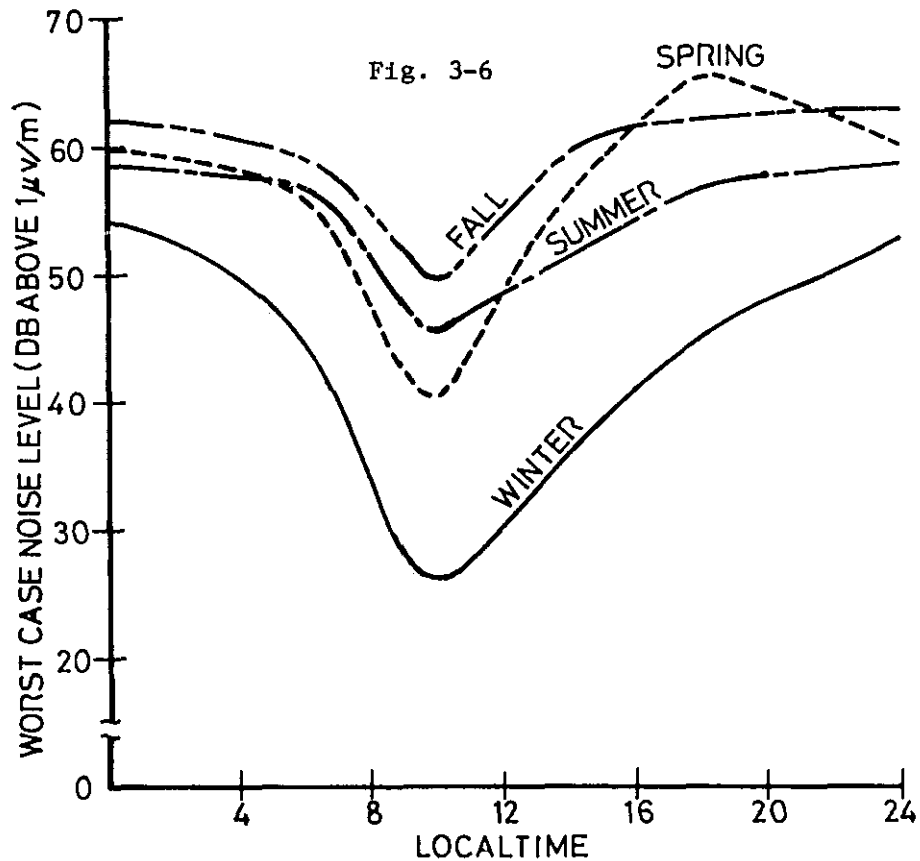
Fig. 3-5



In the calculation, a curve of  $\sigma = 0.005 \text{ m}$   
 $\epsilon = 15$  (land propagation) is used.

c) Noise in Southeast Asia

The atmospheric noise level in Southeast Asia is, according to the quotation in CCIR 322, considered to be  $M=62$  db when the band width is 20 KHz,  $M$  being the worst value.



d) Other factors to cause errors

i) Standard deviation value of synchronisation error of slave station  $0.04 \mu s$

ii) Errors in the hardware of the receiver  $0.1 \mu s$   
The receiver having a resolution of less than  $0.1 \mu s$  is only for military use. Public type receiver's error is  $0.1 \mu s$ .

iii) Improvement of noise

The degree of improvement by the noise checking by limiter has been deemed as zero.

e) Signal-to-noise ratio at sampling point

S/N at sampler input point is denoted in the following expression:

$$(S/N) \text{ db} = E - M + L \quad (\text{db}) \quad \dots (3-10)$$

Where E : Field intensity of signal (db)

M : Noise level (db)

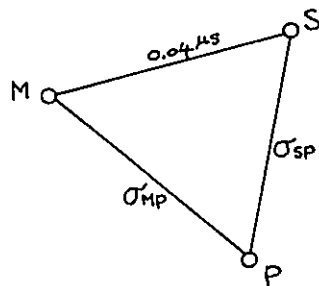
L : Improvement by limiter (db)

f) The timing changes caused in the receiver by noise in propagation path from the transmitting point to the receiving point

The timing changes in the above caption can be denoted by the following expression by using the relation of a) through e) above:

$$\begin{aligned} \sigma_d &= 1.25 \left( \frac{N}{S} \right) \frac{1}{n} \cdot K_a \frac{1}{4} \\ &= 1.25 \times \frac{1}{10 \left( \frac{E - M + L}{20} \right)} \times \frac{1}{\sqrt{80}} \times 0.08 \frac{1}{4} \quad \dots (3-11) \end{aligned}$$

g) Stability of lines of position



M : Master station  
S : Slave station  
P : Receiving point

As a result of a) through h), the standard deviation of timing fluctuation of each station is as shown in Fig.



The error of the line of position is expressed in the following expression:

$$\sigma_i = \sqrt{\sigma_{MP}^2 + 0.04^2 + \sigma_{SP}^2 + R^2} \dots (3-12)$$

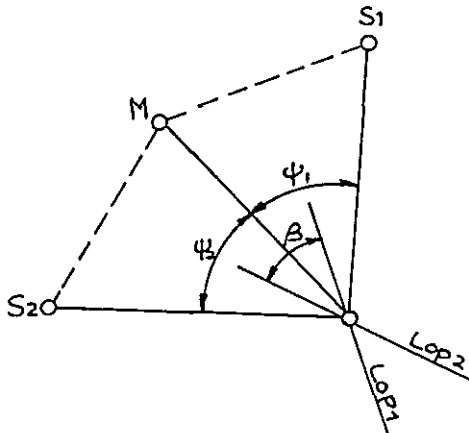
Where the R value is an error on the hardware of the receiver (including resolution of LOP) and 0.2 μs is given.

i : pair of stations

h) Calculation of error circle

The error circle (probability 68%) dr.m.s. can be expressed as follows:

$$\text{dr.m.s.} = \frac{150}{\sin\left(\frac{\psi_1 + \psi_2}{2}\right)} \sqrt{\left(\frac{\sigma_1}{\sin\frac{\psi_1}{2}}\right)^2 + \left(\frac{\sigma_2}{\sin\frac{\psi_2}{2}}\right)^2} \dots (3-13)$$



M : Master station  
 S1: Slave station 1  
 S2: Slave station 2  
 B : Angle between LOP's  
 $= \frac{\psi_1 + \psi_2}{2}$

Accuracy of Loran C : example of receiving

Expression (3) in the preceding paragraph indicates a case where the Loran C system is operated ideally, free from interference from others. In actual cases, particularly during the nighttime, interference by

mutual signals from the stations becomes very large because of the peculiarity of the Loran C system that it is operated in a single channel. This inevitably leads to the worsening of signal-to-noise ratio and the reduction in the number of samplings of signals and eventually to big timing changes.

Here is example of receiving signals from the Loran C stations in Japan.

Example 1 (Fig. 3-7) and Example 2 (Fig. 3-8) are Lissajous during 3 to 4 hours of receiving LOP value under the conditions shown in the following table:

Table 3-1. Example of receiving signal from Loran C stations

	Example 1	Example 2
Chain received		
LOP 1	SS3 - X	SS3 - X
LOP 2	SS3 - Y	SS3 - W
Distance to receiving point from:		
Master station	1300 km	1300 km
Slave 1	1200 km	1200 km
Slave 2	1200 km	2200 km
Lissajous Drawing	Fig. 3	Fig. 4
Fluctuation of LOP		
LOP 1	0.75 $\mu$ s P-P	0.62 $\mu$ s P-P
LOP 2	0.75 $\mu$ s P-P	7.63 $\mu$ s P-P

Receiving point	Akashi, Japan 34°46' N 134°56' E
Receiver	DL 91 Loran C receiver made by Decca

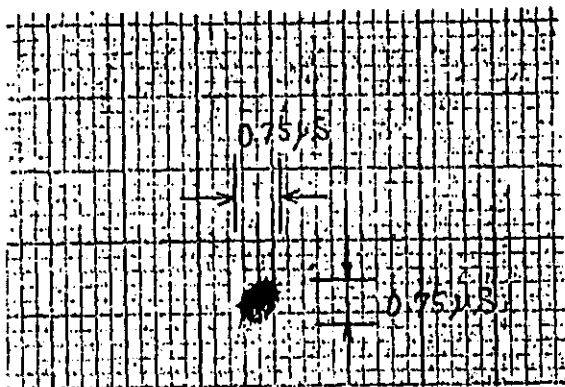
Example 1 shows a case where the distance from the master and slave stations is both within 750 nautical miles.

Example 2 shows a case where the distance from a slave station is more than 750 n.m.

Example 1 is within the best coverage of SS3 chain and indicates a time fluctuation of peak-to-peak  $0.75 \mu\text{s}$ , a big fluctuation quite different from the theoretical value.

Fig. 3-7

Loran C receiving data (SS-3)  
(by DL91 MK2 receiver)



18th March, 1977.

Time of  
measurement: 08:45 - 20:37

Axis X (LOP 1): M-X (Tokachibuto)

Axis Y (LOP 2): M-Y (Okinawa)

Scale: 8cm/10  $\mu$ s

LOP 1 Centre value 36412.0  $\mu$ s

LOP 2 " 58594.4  $\mu$ s

Receiving point:  $\phi = 34^{\circ} 46.056' N$

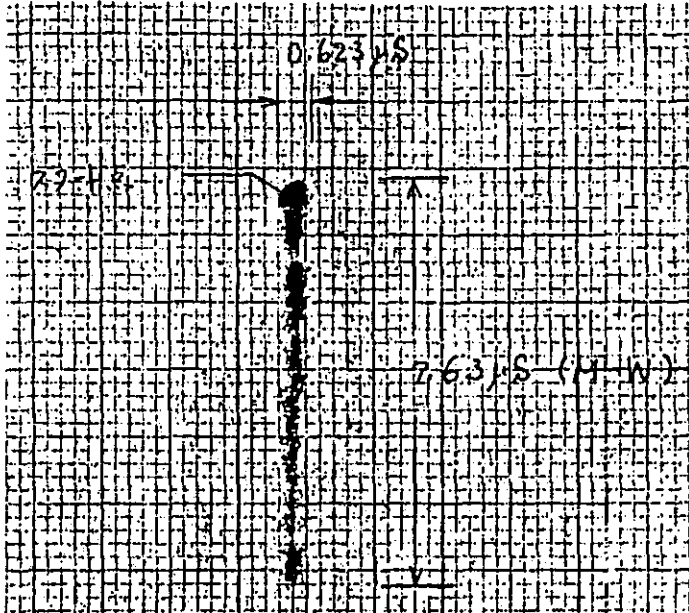
$\lambda = 134^{\circ} 56.209' E$

(Fujitsu Akashi Factory)

Fig. 3-8

Loran C receiving data (SS-3)

25th March, 1977.



Time of

measurement: 10:30 - 16:20

Axis X (LOP 1): M-X (Tokachibuto)

Axis Y (LOP 2): M-X (Marcus Is.)

Scale: 8cm/ 10  $\mu$ s

Starting point:

LOP 1 = 36411.8  $\mu$ s

LOP 2 = 18366.8  $\mu$ s

Receiving point:

$\phi = 34^{\circ}46.056' N$

$\lambda = 134^{\circ}56.209' E$

(Fujitsu Akashi Factory)

## Appendix B

### Analysis of guyed towers

#### 1-1 Introduction

A method of analysis of high guyed towers under wind loading, readily adaptable to electronic computer solution, is presented herein. The method includes the variable guy spring constants, effect of drag and lift on the guys, and such secondary effects as external moments produced at each guy level, and those produced by the distortion of the shaft. Effects of ice loads and insulators, or both, on the guys are also examined.

The analysis presented for computing tower member stresses includes the effects of web member strains, initial eccentricities of tower shaft between guy levels, and increase in shear caused by shaft distortion.

An examination of two-way bending of guyed towers is also included and a method of solution presented.

#### 1-2 Assumptions

The following assumptions are made concerning high guyed towers under wind loading:

(a) Wind loads on tower shaft are known and are assumed to be uniform between guy levels; (b) the moment of inertia of the tower shaft is considered to be uniform between guy levels; (c) dead load of tower shaft for each span is concentrated, one-half at each end for beam-column action only; (d) the guys are uniformly loaded by the wind or by a combination of wind and ice; (e) the velocity of the wind acting on a guy is the velocity at its average height; (f) guy curve is a parabola for all loading conditions; (g) drag and lift coefficients for a

guy are as indicated by Diehl; and (h) wind is blowing parallel to the ground.

1-3 Normal position of guy

Fig.1 shows a guy with no wind blowing and at normal temperature,  $t_0$ . If the total weight of the guy is  $W$  kips, its approximate length  $L$ , in feet, is given by

$$L = a \left( \sec \omega + \frac{W}{24H^2 \sec^3 \omega} \right) \dots \dots \dots (1)$$

in which  $H$  is the horizontal component of the tension in the guy in kips.

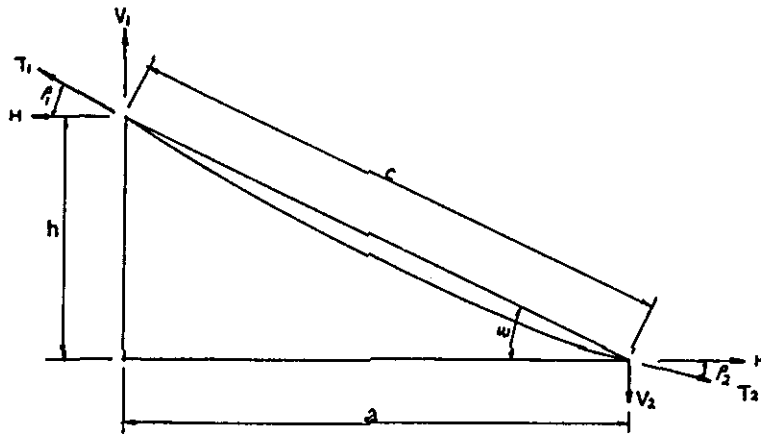


FIG. 1. - ELEVATION OF GUY IN NORMAL POSITION

For erection purposes, the tension at the anchorage,  $T_2$ , is known and  $H$  can be computed from

$$H = \frac{\cos \omega}{2} [W \sin \omega + \sqrt{4 T_2^2 - W^2 \cos^2 \omega}] \dots \dots (2)$$

It may be shown for a parabola that

$$\tan \rho_1 = \tan \omega + \frac{W}{2 H} , \dots \dots \dots (3a)$$

$$\tan \rho_2 = \tan \omega + \frac{W}{2 H} , \dots \dots \dots (3b)$$

$$\Delta_g = \frac{H a}{A_g E_g} \left( \sec^2 \omega + \frac{W^2}{12 H^2} \right), \dots\dots\dots (3c)$$

in which  $\Delta$  = stretch of the guy, in feet;  $A_g$  = the metallic area of the guy in square inches; and  $E_g$  = the modulus of elasticity of the guy in kips per square inch. The unstressed length of the guy,  $L_0$ , at normal temperature is then

$$L_0 = L - \Delta_g, \dots\dots\dots (4)$$

At a temperature of  $t$  degrees C, the unstressed length,  $L_t$ , is

$$L_t = L_0 [1.0 + .0000125(t-t_0)] \dots\dots\dots (5)$$

1-4 Effect of wind and tower motion on guy

Fig.2 shows the forces acting on a guy. The projection of these forces, on a horizontal plane, make an angle of  $\phi$  with the direction of wind. Point B represents the point of attachment to the tower which, in this case, is assumed not to have moved. Positive directions of the forces are shown in Fig.2. The total weight,  $W$ , acts vertically down; the total drag,  $d_0$ , acts parallel to the  $y$  axis; and the lift,  $l_1$ , is parallel to  $BD$  and normal to  $d_0$ .  $\theta$ , the true angle between the guy chord and the wind, is given by

$$\cos \theta = \cos \phi \cos \omega \dots\dots\dots (6)$$

Let  $l$  and  $l_h$  represent the components of the lift,  $l_1$ , in the  $z$  and  $x$  directions, respectively. Then

$$l = l_1 \sin \rho, \dots\dots\dots (7a)$$

$$l_h = l_1 \cos \rho, \dots\dots\dots (7b)$$

in which

$$\sin \rho = \frac{\sin \omega}{\sin \theta}, \text{ and } \dots\dots\dots (8a)$$

$$\cos \rho = \frac{\sin \phi \cos \omega}{\sin \theta} \dots\dots\dots (8b)$$



Assuming the velocity pressure to be given by

$$vp = 0.625 v^2 \times 10^{-6} \dots\dots\dots (9)$$

the total drag,  $d_o$ , and lift,  $l_1$ , on a guy are approximately,

$$d_o = 2.133 (Cdv^2) \cdot C_D \cdot 10^{-7} \text{ tons, and } \dots (10a)$$

$$l_1 = 2.133 (Cdv^2) \cdot C_L \cdot 10^{-7} \text{ tons, } \dots\dots\dots (10b)$$

in which  $C$  = chord length of guy in feet,  $d$  = diameter of guy in inches,  $v$  = wind velocity in miles per hour,  $C_D$  = drag coefficient, and  $C_L$  = lift coefficient.

It should be noted that  $l_1$  is negative when  $\phi$  is in the first or fourth quadrant. Hence, the sign of  $l_1$  is opposite to that of  $\cos \phi$ .

Diehl<sup>1</sup> indicates values of  $C_D$  and  $C_L$  by curves for values of  $\theta$  varying from  $0^\circ$  to  $90^\circ$ . For computer use, it is expedient to express the values of  $C_D$  and  $C_L$  in polynomial form as

$$C_D = a_0 + a_1x + a_2x^2 + a_3x^3 + a_4x^4 \dots\dots\dots (11)$$

$$C_L = b_0 + b_1x + b_2x^2 + b_3x^3 + b_4x^4$$

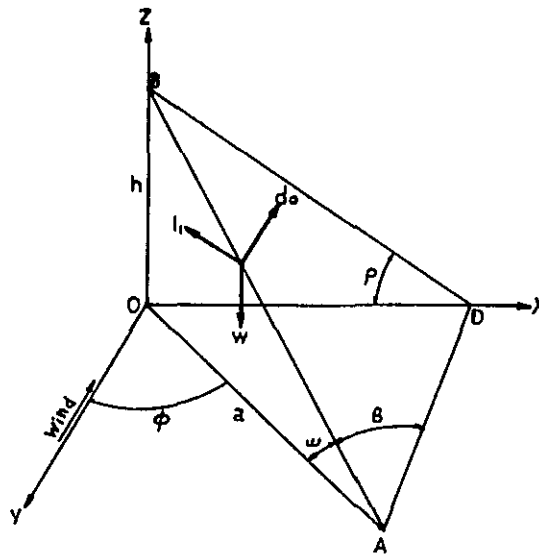


FIG. 2. - LOADS ON GUY

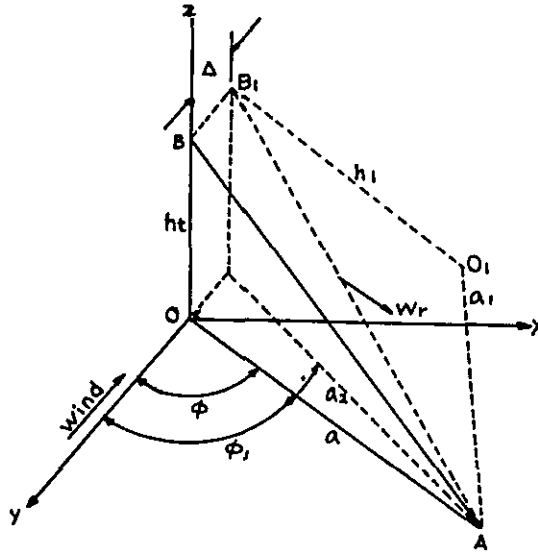


FIG. 3. - GEOMETRY OF GUY IN DEFLECTED POSITION

in which  $x = |\cos \theta|$

For  $x \leq 0.575$ :  $a_0 = 1.18457$ ;  $a_1 = 0.07816$ ;  $a_2 = -1.51543$ ;  $a_3 = -1.73395$ ;  $a_4 = 2.56634$ ;  $b_0 = 0.00008$ ;  $b_1 = 1.45668$ ;  $b_2 = -2.73481$ ;  $b_3 = 5.36663$ ; and  $b_4 = -4.75092$ .

For  $x > 0.575$ :  $a_0 = 1.20931$ ;  $a_1 = -0.08774$ ;  $a_2 = -1.33619$ ;  $a_3 = -0.82684$ ;  $a_4 = 1.06662$ ;  $b_0 = 1.40075$ ;  $b_1 = -4.20644$ ;  $b_2 = 6.00561$ ;  $b_3 = -2.24738$ ; and  $b_4 = -0.94991$ .

In Fig.3, the tower has deflected a distance  $\Delta$  ft in the direction of the wind at the point of guy attachment. Because of the wind loads, the guy lies in a new plane that contains the resultant,  $W_r$ , of all the forces acting on the guy. This new guy plane is represented by the triangle  $B_1 O_1 A$  in the figure. The guy is assumed to be a parabola lying in this plane with  $B_1 O_1$  parallel to  $W_r$  and  $O_1 A$  normal to  $W_r$ .  $W_r$  is given by

$$W_r = \sqrt{l_h^2 + d_o^2 + (W-1)^2} \dots\dots\dots (12)$$

Thus

$$a_2 = \sqrt{(a \sin \phi)^2 + (a \cos \phi + \Delta)^2} \dots\dots\dots (13a)$$

$$\sin \phi_1 = \frac{a \sin \phi}{a_2} \dots\dots\dots (13b)$$

and  $\cos \phi_1 = \frac{a \cos \phi + \Delta}{a_2} \dots\dots\dots (13c)$

It may be shown that

$$h_1 = \frac{(W-1)h_t - a_2(l_h \sin \phi_1 + d_o \cos \phi_1)}{W_r}, \dots (14a)$$

$$a_1 = \sqrt{a_2^2 + h_1^2 - h_t^2}, \dots\dots\dots (14b)$$

and  $\tan \omega_1 = \frac{h_1}{a_1}, \dots\dots\dots (14c)$

in which  $h_t$  is the height of the guy at temperature,  $t$ .  
The value of  $h_t$  is given by

$$h_t = h [1.0 + .0000125 (t-t_o)] \dots\dots\dots (15)$$

for steel structures.

The direction cosines of lines  $B_1O_1$  and  $O_1A$  are

$B_1O_1$	$O_1A$
$\cos \alpha_1 = \frac{l_h}{W_r},$	$\cos \alpha_2 = -\tan \omega_1 \cos \alpha_1 + \frac{a_2}{a_1} \sin \phi_1,$
$\cos \beta_1 = \frac{d_o}{W_r},$	$\cos \beta_2 = -\tan \omega_1 \cos \beta_1 + \frac{a_2}{a_1} \cos \phi_1, \dots (16)$
$\cos \gamma_1 = -\frac{W-1}{W_r},$	$\cos \gamma_2 = -\tan \omega_1 \cos \gamma_1 - \frac{h_t}{a_1}$

Fig.4 shows the forces at the tower produced by a guy under wind load, and Fig.5 shows the forces at the anchorage. At the tower, the vertical load produced

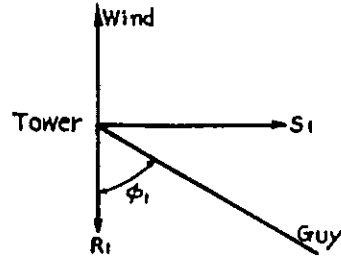


FIG. 4. - GUY FORCES AT TOWER

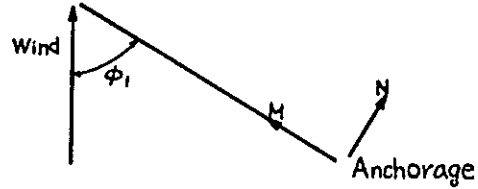


FIG. 5. - GUY FORCES AT ANCHORAGE

by the guy is  $Z_1$  and the tension in the guy is  $T_3$ . At the anchorage, the vertical uplift is  $Z_2$  and the guy tension is  $T_4$ .

If  $H_1$  is the tension in the guy of Fig.3 comparable to  $H$  of Fig.1, it is possible to write

$$\tan \rho'_1 = \tan \omega_1 + \frac{W_r}{2H_1} \dots\dots\dots (17a)$$

$$\tan \rho'_2 = \tan \omega_1 - \frac{W_r}{2H_1} \dots\dots\dots (17b)$$

$$V'_1 = H_1 \tan \rho'_1 \dots\dots\dots (17c)$$

$$V'_2 = H_1 \tan \rho'_2 \dots\dots\dots (17d)$$

$$T_3 = H_1 \sec \rho'_1 \dots\dots\dots (17e)$$

$$T_4 = H_1 \sec \rho'_2 \dots\dots\dots (17f)$$

$$R_1 = H_1 \cos \beta_2 + V'_1 \cos \beta_1 \dots\dots\dots (17g)$$

$$S_1 = H_1 \cos \alpha_2 + V'_1 \cos \alpha_1 \dots\dots\dots (17h)$$

$$Z_1 = H_1 \cos \gamma_2 - V'_1 \cos \gamma_1 \dots\dots\dots (17i)$$

$$M = H_1 (\sin \phi_1 \cos \alpha_2 + \cos \phi_1 \cos \beta_2) + V'_2 (\sin \phi_1 \cos \alpha_1 + \cos \phi_1 \cos \beta_1) \dots (17j)$$

$$N = H_1 (\sin \phi_1 \cos \beta_2 - \cos \phi_1 \cos \alpha_2) + V'_2 (\sin \phi_1 \cos \beta_1 - \cos \phi_1 \cos \alpha_1) \dots (17k)$$

and  $Z_2 = -H_1 \cos \gamma_2 - V'_2 \cos \gamma_1 \dots (17l)$

Note that  $V'_1$  is parallel to  $W_r$  and  $H_1$  is normal to  $W_r$ .

For any particular value of  $\Delta$  and temperature,  $t$ , the value of  $H_1$  is determined by trial as follows:

1. Assume a value for  $H_1$ ,

2. Compute  $L_1 = a_1 (\sec \omega_1 + \frac{W_r^2}{24 H_1^2 \sec^3 \omega_1}) \dots (18)$

3. Compute  $\Delta'_g = \frac{H_1 a_1}{A_g E_g} (\sec^2 \omega_1 + \frac{W_r^2}{12 H_1^2}) \dots (19a)$

4. Compute  $L'_t = L_1 - \Delta'_g \dots (19b)$

5. Compare the value of  $L'_t$  given by Eq. 19b with that given by Eq. 5. Because the unstressed length of the guy is invariant, these two values should be the same. If the values do not agree, assume a new value for  $H_1$  and repeat the calculations until satisfactory agreement is reached.

Having obtained a value for  $H_1$ , forces at the tower, anchorage, and the guy tensions may be found by application of Eqs. 17c to 17l, inclusive.

This same procedure is applied to all the guys at one level. Having determined the forces at the tower for

each of the guys, resultants can be found by superposition: Thus

$$R = \sum R_1, \dots\dots\dots (20)$$

and  $Z = \sum Z_1, \dots\dots\dots (21)$

in which R = the net guy reaction in a direction opposed to the wind at the guy level in question and Z = the total vertical, down load produced by the guys at the tower. Because the resultant, Z, of the Z<sub>1</sub> forces is eccentric to the centroid of the tower shaft, an external moment,  $\bar{M}$ , will be introduced at the guy level. If e is the distance of the application of the load Z<sub>1</sub> to the centroid of the tower shaft in the direction of the wind,

$$\bar{M} = \sum Z_1 e \dots\dots\dots (22)$$

Because  $\bar{M}$  is considered to be positive when it produces compression on the windward side of the tower, windward guys will have positive e values and lee guys, negative values.

In Fig. 6, values of R are plotted for tower deflection values  $\Delta$ .

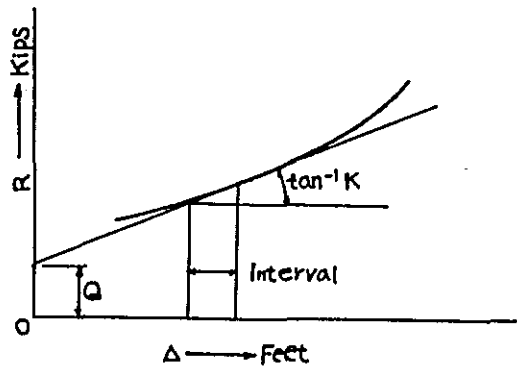


FIG. 6. R- $\Delta$  CURVE FOR GUYS AT ONE LEVEL

If it is assumed that the change in R is linear for two successive values of  $\Delta$ , then

$$R = K\Delta + Q \quad \dots\dots\dots (23)$$

for the selected interval. The values of K and Q are simply computed from the values of R at the lower and upper bounds of the  $\Delta$  interval. Thus, the two constants, K and Q, associated with each value of  $\Delta$ , (e.g., the upper bound of the interval) define the value of R for that interval. Because the slope of the R- $\Delta$  curve changes from interval to interval, values of K and Q will vary with  $\Delta$ .

Similarly,

$$\bar{M} = B \Delta + E, \quad \dots\dots\dots (24)$$

$$Z = O \Delta + J, \quad \dots\dots\dots (25)$$

#### 1-5 Tower analysis

Fig.7 shows the forces acting on two spans of a multiguyed tower.  $W_n$  and  $W_{n+1}$  = uniformly distributed wind loads;  $M_{n-1}$ ,  $M'_n$ ,  $M_n$ , and  $M'_{n+1}$  = the internal resisting moments;  $\bar{M}_n$  = the external moment produced by the guys;  $P_{n+1}$  = the total force acting down above guy level n+1 including the vertical Z loads at this guy level; and  $P_n$  = the similar load above guy level n. Positive directions of the loads and moments are shown.

To maintain continuity at joint n, Timoshenko established the relationship

$$M'_n \frac{l_n}{3EI_n} \psi(u_n) + M_{n-1} \frac{l_n}{6EI_n} \phi(u_n) + W_n \frac{l_n^2}{24EI_n} \chi(u_n) - \frac{\delta'}{l_n}$$

$$\begin{aligned}
& + M_n \frac{l_{n+1}}{3EI_{n+1}} \psi(u_{n+1}) + M'_{n+1} \frac{l_{n+1}}{6EI_{n+1}} \phi(u_{n+1}) \\
& + W_{n+1} \frac{l_{n+1}^2}{24EI_{n+1}} \chi(u_{n+1}) + \frac{\delta'_{n+1}}{l_{n+1}} = 0 \dots (26)
\end{aligned}$$

in which  $I_n, I_{n+1}$ , = the moment of inertia of beams of span  $n$  and  $n+1$ , and  $E$  = the modulus of elasticity of the tower shaft,

$$u = \frac{\ell}{2} \sqrt{\frac{P}{EI}} \dots\dots\dots (27)$$

$$\phi(u) = \frac{3}{u} \left( \frac{1}{\sin 2u} - \frac{1}{2u} \right) \dots\dots\dots (28)$$

$$\psi(u) = \frac{3}{2u} \left( \frac{1}{2u} - \frac{1}{\tan 2u} \right) \dots\dots\dots (29)$$

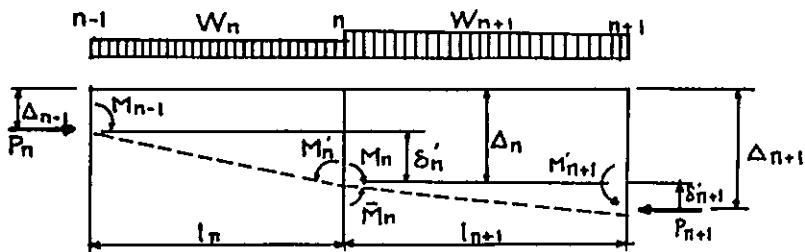


FIG. 7. FORCES ON TWO CONTINUOUS SPANS OF TOWER SHAFT



and 
$$\chi(u) = \frac{3(\tan u - u)}{u^3} \dots\dots\dots (30)$$

Because 
$$\left. \begin{aligned} M'_n &= M_n + \bar{M}_n, \\ M'_{n+1} &= M_{n+1} + \bar{M}_{n+1}, \\ \delta'_n &= \Delta_n - \Delta_{n-1}, \text{ and} \\ \delta'_{n+1} &= \Delta_{n+1} - \Delta_n, \end{aligned} \right\} \dots\dots\dots (31)$$

Eq. 26 may be written

$$\begin{aligned} &4M_{n-1} \frac{l_n}{I_n} \phi(u_n) + 8M_n \left[ \frac{l_n}{I_n} \psi(u_n) + \frac{l_{n+1}}{I_{n+1}} \psi(u_{n+1}) \right] \\ &+ 4(M_{n+1} + \bar{M}_{n+1}) \frac{l_{n+1}}{I_{n+1}} \phi(u_{n+1}) \\ &+ 8\bar{M}_n \frac{l_n}{I_n} \psi(u_n) + W_n \frac{l_n^2}{I_n} \chi(u_n) + W_{n+1} \frac{l_{n+1}^2}{I_{n+1}} \chi(u_{n+1}) \\ &= 24E \left[ \frac{\Delta_n - \Delta_{n-1}}{l_n} - \frac{\Delta_{n+1} - \Delta_n}{l_{n+1}} \right] \dots\dots\dots (32) \end{aligned}$$

Eq. 32 is the typical continuity equation.

Fig.8 shows free body diagrams of the spans of Fig.7 with applied forces as indicated. For equilibrium,  $V'_n$  and  $V_n$  are given by

$$\left. \begin{aligned} V'_n &= \frac{W_n}{2} + \frac{M_{n-1} - M'_n}{l_n} + \frac{P_n}{l_n} (\Delta_n - \Delta_{n-1}), \\ V_n &= \frac{W_{n+1}}{2} + \frac{M'_{n+1} - M_n}{l_{n+1}} - \frac{P_{n+1}}{l_{n+1}} (\Delta_{n+1} - \Delta_n), \end{aligned} \right\} \dots (33)$$

Because  $R_n = V'_n + V_n$ , and using the first two values of Eq. 32, the value of  $R_n$  is given by

$$R_n = \frac{1}{2} (W_n + W_{n+1}) + \frac{M_{n-1}}{l_n} - M_n \left( \frac{1}{l_n} + \frac{1}{l_{n+1}} \right) + \frac{M_{n+1}}{l_{n+1}} - \frac{\bar{M}_n}{l_n} + \frac{\bar{M}_{n+1}}{l_{n+1}} + \frac{P_n}{l_n} (\Delta_n - \Delta_{n-1}) - \frac{P_{n+1}}{l_{n+1}} (\Delta_{n+1} - \Delta_n) \dots (34)$$

Eq. 34 is the typical interior reaction equation.

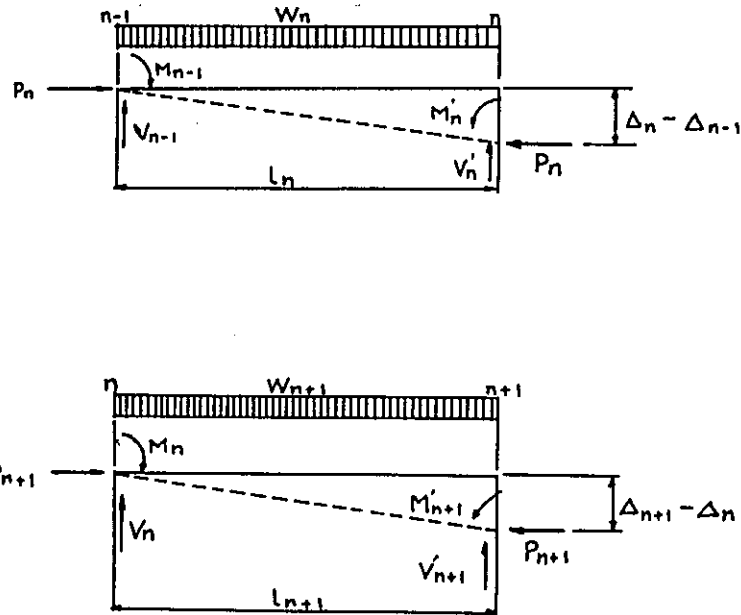


FIG. 8 . - FREE BODY DIAGRAMS OF TWO CONTINUOUS SPANS OF TOWER SHAFT

For a tower with m spans, the continuity and reaction equations, Eqs. 32 and 34 must be modified for the end spans. For continuity at support 1, Eq.32 becomes

$$4M_0 \frac{l_1}{I_1} \phi(u_1) + 8M_1 \left[ \frac{l_1}{I_1} \psi(u_1) + \frac{l_2}{I_2} \psi(u_2) \right] + 4(M_2 + \bar{M}_2) \frac{l_2}{I_2} \phi(u_2) + 8\bar{M}_1 \frac{l_1}{I_1} \psi(u_1) + W_1 \frac{l_1^2}{I_1} \chi(u_1) + W_2 \frac{l_2^2}{I_2} \chi(u_2) = 24E \left[ \frac{\Delta_1}{I_1} - \frac{\Delta_2 - \Delta_1}{I_2} \right] \dots (35)$$

and at support m-1, the term  $M_{m+1}$  is omitted. For the reaction at the first support, Eq. 34 becomes

$$R_1 = \frac{1}{2} (W_1 + W_2) + \frac{M_0}{l_1} - M_1 \left( \frac{1}{l_1} + \frac{1}{l_2} \right) + \frac{M_2}{l_2} - \frac{\bar{M}_1}{l_1} + \frac{\bar{M}_2}{l_2} + \frac{P_1}{l_1} \Delta_1 - \frac{P_2}{l_2} (\Delta_2 - \Delta_1) , \dots \dots \dots (36)$$

and for the reaction at m

$$R_m = \frac{1}{2} (W_m) + \frac{M_{m-1}}{l_m} - \frac{\bar{M}_m}{l_m} + \frac{P_m}{l_m} (\Delta_m - \Delta_{m-1}) \dots (37)$$

If the tower is hinged at the base,  $M_0 = 0$  in the above equations. If the base is fixed there is no angle change and

$$M_0 = \frac{l_1}{3EI_1} \psi(u_1) + M'_1 \frac{l_1}{6EI_1} \phi(u_1) + W_1 \frac{l_1^2}{24EI_1} \chi(u_1) + \frac{\Delta_1}{l_1} = 0 \dots \dots \dots (38a)$$

or

$$8M_0' \frac{l_1}{I_1} \psi(u_1) + 4(M_1 + \bar{M}_1) \frac{l_1}{I_1} \phi(u_1) + W_1 \frac{l_1^2}{I_1} \chi(u_1) + 24E \frac{\Delta_1}{l_1} = 0 \dots \dots \dots (38b)$$

For a tower with m guy levels, 2 m equations can be written for a fixed base and 2 m-1 equations can be written for a hinged base. The unknowns in these equations are  $M_0, M_1, \dots, M_{m-1}$ , and  $R_1, R_2, \dots, R_m$ .

The above equations contain values of the tower deflections  $\Delta_1, \Delta_2$ , etc., that are also unknown, thereby increasing the number of unknowns to 3 m for a fixed base and 3 m-1 for a hinged base. If

use is made of the constants K, Q, B, E, O, and J, the  $\Delta$  values can be eliminated, thus reducing the number of unknowns to the same number of available equations.

From Eqs. 23, 24, and 25,

$$\begin{aligned} \Delta_1 &= \frac{R_1 - Q_1}{K_1} & \bar{M}_1 &= \frac{B_1}{K_1} (R_1 - Q_1) + E_1 \\ & & & \dots (39) \\ \Delta_2 &= \frac{R_2 - Q_2}{K_2} & \bar{M}_2 &= \frac{B_2}{K_2} (R_2 - Q_2) + E_2 \\ & \text{etc.} & & \text{etc.} \end{aligned}$$

in which  $\Delta_1$  = the deflection at guy level 1,  $\Delta_2$  = the deflection at guy level 2, etc. By means of Eqs. 39 and the first two of Eqs. 31 the general continuity equation, Eq. 32 becomes

$$\begin{aligned} & 4M_{n-1} \frac{1_n}{I_n} \phi(u_n) + 8M_n \left[ \frac{1_n}{I_n} \psi(u_n) + \frac{1_{n+1}}{I_{n+1}} \psi(u_{n+1}) \right] \\ & + 4 \frac{1_{n+1}}{I_{n+1}} \phi(u_{n+1}) \left[ M_{n+1} + \frac{B_{n+1}}{K_{n+1}} (R_{n+1} - Q_{n+1}) + E_{n+1} \right] \\ & + 8 \frac{1_n}{I_n} \psi(u_n) \left[ \frac{B_n}{K_n} (R_n - Q_n) + E_n \right] \\ & + W_n \frac{1_n^2}{I_n} \chi(u_n) + W_{n+1} \frac{1_{n+1}^2}{I_{n+1}} \chi(u_{n+1}) \\ & = 24E \left\{ \left( \frac{1}{I_n} + \frac{1}{I_{n+1}} \right) \left( \frac{R_n - Q_n}{K_n} \right) - \frac{1}{I_n} \left( \frac{R_{n-1} - Q_{n-1}}{K_{n-1}} \right) \right. \\ & \quad \left. - \frac{1}{I_{n+1}} \left( \frac{R_{n+1} - Q_{n+1}}{K_{n+1}} \right) \right\} \dots \dots \dots (40) \end{aligned}$$

and the general interior reaction equation, Eq. 34, becomes

$$\begin{aligned}
R_n = & \frac{1}{2} (W_n + W_{n+1}) - M_n \left( \frac{1}{l_n} + \frac{1}{l_{n+1}} \right) + \frac{M_{n-1}}{l_n} + \frac{M_{n+1}}{l_{n+1}} \\
& - \frac{1}{l_n} \left[ \frac{B_n}{K_n} (R_n - Q_n) + E_n \right] + \frac{1}{l_{n+1}} \left[ \frac{B_{n+1}}{K_{n+1}} (R_{n+1} - Q_{n+1}) + E_{n+1} \right] \\
& + \left[ \frac{P_n}{l_n} + \frac{P_{n+1}}{l_{n+1}} \right] \left[ \frac{R_n - Q_n}{K_n} \right] - \frac{P_n}{l_n} \left[ \frac{R_{n-1} - Q_{n-1}}{K_{n-1}} \right] - \frac{P_{n+1}}{l_{n+1}} \left[ \frac{R_{n+1} - Q_{n+1}}{K_{n+1}} \right]
\end{aligned}$$

..... (41)

Guy constants  $O_1, J_1, \text{ etc.}$ , are used to determine values of  $P_1, P_2, \text{ etc.}$ , as will be described hereafter.

In a similar manner, values of  $\Delta$  can be eliminated from the end span equations.

In many cases, the span above the top guy is cantilevered and, in some instances, this cantilevered span is loaded with an antenna pull-off with an additional moment and vertical load applied at the top of the tower. Assuming a cantilever above the  $m^{\text{th}}$  guy level, as indicated in Fig. 9, and neglecting the effect on the moments caused by the force  $T$  in span  $l_c$ , the value of  $\Delta_c$  is given by

$$\Delta_c = \Delta_m + \frac{1}{EI_c} \left[ \frac{THl_c^3}{3} + \frac{Wc l_c^3}{8} + \frac{TM l_c^2}{2} \right] - l_c \theta_m \dots (42)$$

in which  $\theta_m$  is the angle change at  $m$  and  $I_c$  is the moment of inertia of the cantilevered span. In the usual design cases,  $\theta_m$  is small and will therefore

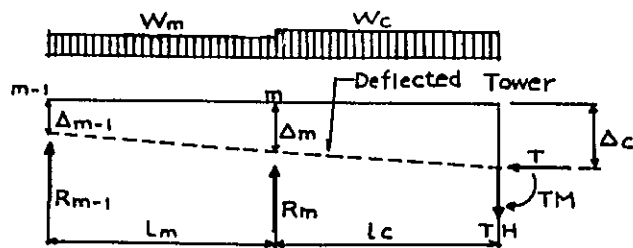


FIG. 9 . - LOADS ON CANTILEVERED SPAN OF TOWER

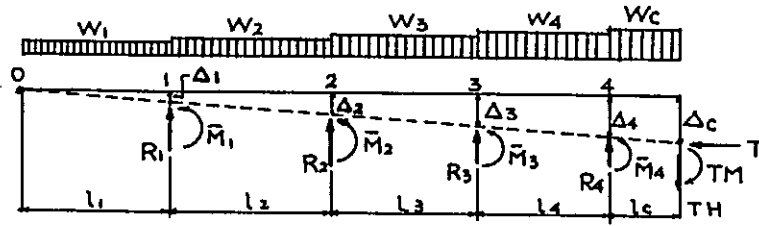


FIG. 10. - FOUR-SPAN TOWER WITH CANTILEVER

be considered herein to be = 0. A method for including the actual value of  $\theta_m$  is presented subsequently.

For  $\theta_m = 0$ , Eq. 42 becomes

$$\Delta_c = \Delta_m + \xi \dots \dots \dots (43)$$

in which

$$\xi = \frac{l_c^2}{24EI_c} [l_c(8TH + 3W_c) + 12TM] \dots (44)$$

The cantilever moment, G, at m is given by

$$G = W_c \frac{l_c}{2} + THl_c + TM + \xi (T + 0.5D_c) \dots (45)$$

in which  $D_c$  is the total weight of the cantilever.

As an example, equations for a 4-span tower with a hinged base and cantilever with pull-off, as shown in Fig.10, are as follows:

$$R_1 = \frac{1}{2}(W_1+W_2) - M_1\left(\frac{1}{l_1} + \frac{1}{l_2}\right) + \frac{M_2}{l_2} - \frac{1}{l_1}\left[\frac{B_1}{K_1}(R_1-Q_1)+E_1\right] \\ + \frac{1}{l_2}\left[\frac{B_2}{K_2}(R_2-Q_2)+E_2\right] + \left(\frac{P_1}{l_1} + \frac{P_2}{l_1}\right)\left(\frac{R_1-Q_1}{K_1}\right) - \frac{P_2}{l_2}\left(\frac{R_2-Q_2}{K_2}\right) \dots (46)$$

$$\begin{aligned}
R_2 = & \frac{1}{2}(W_2+W_3) - M_2\left(\frac{1}{1_2} + \frac{1}{1_3}\right) + \frac{M_1}{1_2} + \frac{M_3}{1_3} - \frac{1}{1_2}\left[\frac{B_2}{K_2}(R_2-Q_2)+E_2\right] \\
& + \frac{1}{1_3}\left[\frac{B_3}{K_3}(R_3-Q_3)+E_3\right] + \left(\frac{P_2}{1_2} + \frac{P_3}{1_3}\right)\left(\frac{R_2-Q_2}{K_2}\right) \\
& - \frac{P_2}{1_2}\left(\frac{R_1-Q_1}{K_1}\right) - \frac{P_3}{1_3}\left(\frac{R_3-Q_3}{K_3}\right) \dots\dots\dots (47)
\end{aligned}$$

$$\begin{aligned}
R_3 = & \frac{1}{2}(W_3+W_4) - M_3\left(\frac{1}{1_3} + \frac{1}{1_4}\right) + \frac{M_2}{1_3} - \frac{G}{1_4} - \frac{1}{1_3}\left[\frac{B_3}{K_3}(R_3-Q_3)+E_3\right] \\
& + \frac{1}{1_4}\left[\frac{B_4}{K_4}(R_4-Q_4)+E_4\right] + \left(\frac{P_3}{1_3} + \frac{P_4}{1_4}\right)\left(\frac{R_3-Q_3}{K_3}\right) \\
& - \frac{P_3}{1_3}\left(\frac{R_2-Q_2}{K_2}\right) - \frac{P_4}{1_4}\left(\frac{R_4-Q_4}{K_4}\right) \dots\dots\dots (48)
\end{aligned}$$

$$\begin{aligned}
R_4 = & \frac{W_4}{2} + W_c + TH + \frac{M_3+G}{1_4} - \frac{1}{1_4}\left[\frac{B_4}{K_4}(R_4-Q_4) + E_4\right] \\
& + \frac{P_4}{1_4}\left(\frac{R_4-Q_4}{K_4} - \frac{R_3-Q_3}{K_3}\right) \dots\dots\dots (49)
\end{aligned}$$

$$\begin{aligned}
8M_1\left[\frac{1_1}{I_1}\psi(u_1)+\frac{1_2}{I_2}\psi(u_2)\right] + 4\frac{1_2}{I_2}\phi(u_2)\left[M_2+\frac{B_2}{K_2}(R_2-Q_2)\right] + E_2 \\
+ 8\frac{1_1}{I_1}\psi(u_1)\left[\frac{B_1}{K_1}(R_1-Q_1)+E_1\right] + W_1\frac{1_1^2}{I_1}\chi(u_1) + W_2\frac{1_2^2}{I_2}\chi(u_2) \\
= 24E\left\{\left(\frac{1}{1_1} + \frac{1}{1_2}\right)\left(\frac{R_1-Q_1}{K_1}\right) - \frac{1}{1_2}\left(\frac{R_2-Q_2}{K_2}\right)\right\} \dots (50)
\end{aligned}$$

$$\begin{aligned}
4M_1\frac{1_2}{I_2}\phi(u_2)+8M_2\left[\frac{1_2}{I_2}\psi(u_2)+\frac{1_3}{I_3}\psi(u_3)\right]+4\frac{1_3}{I_3}\phi(u_3)\left[M_3+\frac{B_3}{K_3}(R_3-Q_3)+E_3\right] \\
+ 8\frac{1_2}{I_2}\psi(u_2)\left[\frac{B_2}{K_2}(R_2-Q_2)+E_2\right] + W_2\frac{1_2^2}{I_2}\chi(u_2) + W_3\frac{1_3^2}{I_3}\chi(u_3) \\
= 24E\left\{\left(\frac{1}{1_2} + \frac{1}{1_3}\right)\left(\frac{R_2-Q_2}{K_2}\right) - \frac{1}{1_2}\left(\frac{R_1-Q_1}{K_1}\right) - \frac{1}{1_3}\left(\frac{R_3-Q_3}{K_3}\right)\right\} \dots (51)
\end{aligned}$$

and

$$\begin{aligned}
& 4M_2 \frac{1_3}{I_3} \phi(u_3) + 8M_3 \left[ \frac{1_3}{I_3} \psi(u_3) + \frac{1_4}{I_3} \phi(u_4) \right] \\
& + 4 \frac{1_4}{I_4} \phi(u_4) \left[ -G + \frac{B_4}{K_4} (R_4 - Q_4) + E_4 \right] \\
& + 8 \frac{1_3}{I_3} \psi(u_3) \left[ \frac{B_3}{K_3} (R_3 - Q_3) + E_3 \right] \\
& + W_3 \frac{1_3^2}{I_3} \chi(u_3) + W_4 \frac{1_4^2}{I_4} \chi(u_4) \\
& = 24E \left\{ \left( \frac{1}{I_3} + \frac{1}{I_4} \right) \left( \frac{R_3 - Q_3}{K_3} \right) - \frac{1}{I_3} \left( \frac{R_2 - Q_2}{K_2} \right) - \frac{1}{I_4} \left( \frac{R_4 - Q_4}{K_4} \right) \right\} \dots (52)
\end{aligned}$$

The P values in the above equations are determined as follows: Let  $D_1$  = dead load of span 1,  $D_2$  = dead load of span 2, etc. Because  $Z_1 = O_1 \Delta_1 + J_1$ ,  $Z_2 = O_2 \Delta_2 + J_2$ , etc. Then  $P_4 = T + D_c + Z_4 + 5D_4$ ,  $P_3 = P_4 + Z_3 + .5(D_3 + D_4)$ ,  $P_2 = P_3 + Z_2 + .5(D_2 + D_3)$  and  $P_1 = P_2 + Z_1 + .5(D_1 + D_2)$ .

In Eqs. 46-52, the unknowns are  $R_1, R_2, R_3, R_4, M_1, M_2$ , and  $M_3$ . The values of the unknowns are found by a solution of the seven simultaneous equations. Having determined the reactions, the deflections and remaining moments can be computed by means of Eqs. 23, 24, and 25.

#### 1-6 Notation

The following symbols have been adopted for use in this paper:

- $a$  = horizontal projection of guy in normal position;
- $a_1$  = projection of guy normal to resultant of guy loads;
- $a_2$  = horizontal projection of guy chord with tower motion;



$a_0, a_1, \dots$  = coefficients in polynomial expression for drag coefficient;

$B_n$  = a constant for guys at guy level  $n$ ;

$b_0, b_1, \dots$  = coefficients in polynomial expression for lift coefficient;

$C$  = chord length of guy;

$C_D$  = coefficient for drag force on guy;

$C_L$  = coefficient for lift force on guy;

$D_C$  = dead load of cantilever span of tower shaft;

$D_n$  = dead load of span  $n$  of tower shaft;

$DI_n$  = weight of insulator strings at guy level  $n$ ;

$d$  = diameter of guy;

$d_0$  = total drag force on guy;

$E$  = modulus of elasticity of tower shaft;

$E_g$  = modulus of elasticity of guy;

$E_n$  = a constant for guys at guy level  $n$ ;

$e$  = moment arm for vertical component of guy force about centroid of tower shaft;

$H$  = horizontal component of tension in guy for guy in normal position;

$H_1$  = component of tension in guy parallel to  $a_1$ ;

$h$  = height of guy above anchorage at normal temperature, also panel height of web members of triangular tower;

$h_t$  = height of guy above anchorage at temperature  $t$ ;

$h_1$  = projection of guy parallel to  $W_r$ ;

$I_C$  = moment of inertia of cantilever span of tower shaft;

$I_n$  = moment of inertia of span  $n$  of tower shaft;

$J_n$  = a constant for guys at guy level  $n$ ;

$K_n$  = a constant for guys at guy level  $n$ ;

$L$  = stretched length of guy in normal position;

$L_1$  = stretched length of guy under wind load at temperature  $t$ ;  
 $L_0$  = no stress length of guy in normal position;  
 $L_1$  = no stress length of guy in normal position at temperature  $t$ ;  
 $L'_t$  = no stress length of guy under wind load at temperature  $t$ ;  
 $l$  = vertical component of lift on guy;  
 $l_1$  = total lift on guy;  
 $l_h$  = horizontal component of lift on guy;  
 $l_n$  = length of span  $n$  of tower shaft;  
 $M$  = horizontal guy force at anchorage in guy direction under wind loading;  
 $M_n$  = internal resisting moment in tower shaft immediately above guy level  $n$ ;  
 $M'_n$  = internal resisting moment in tower shaft immediately below guy level  $n$ ;  
 $m$  = top guy level of tower;  
 $N$  = horizontal guy force at anchorage normal to  $M$  under wind loading;  
 $n$  = guy level number;  
 $O_n$  = a constant for guys at guy level  $n$ ;  
 $P_n$  = total vertical load on tower shaft at guy level  $n$ ;  
 $Q_n$  = a constant for guys at guy level  $n$ ;  
 $Q_1$  = shear in triangular tower in direction 1;  
 $Q_2$  = shear in triangular tower in direction 2;  
 $R_n$  = guy reaction at guy level  $n$ ;  
 $S_1$  = component of guy force at tower normal to wind direction;  
 $s$  = width of face of triangular tower;  
 $T$  = vertical component of pull-off load at tower top;  
 $T_1$  = erection tension in guy at tower at normal temperature;

$T_2$  = erection tension in guy at anchorage at normal temperature;  
 $T_3$  = guy tension at tower under wind loading;  
 $T_4$  = guy tension at anchorage under wind loading;  
 $T_H$  = horizontal component of pull-off load at tower top;  
 $T_M$  = moment at tower top caused by pull-off load;  
 $t$  = temperature;  
 $t_0$  = normal temperature  
 $V_n$  = shear immediately above guy level  $n$ ;  
 $V'_n$  = shear immediately below guy level  $n$ ;  
 $V_1$  = vertical component of guy tension at tower, guy in normal position;  
 $V'_1$  = component of guy tension at tower parallel to  $W_r$ ;  
 $V'_2$  = component of guy tension at anchorage parallel to  $W_r$ ;  
 $v$  = wind velocity;  
 $v_p$  = velocity pressure of wind;  
 $W$  = total weight of guy;

\*\*\* TOWER DATA (1) \*\*\*

SPAN	BASE H.	LENGTH	HEIGHT	I	SECT. AREA	WEIGHT	DRAG AREA	C
G-B	300.00							
1		2700.00	3000.00	77600.	46.56	4.05	46.460	
2		2700.00	5700.00	77600.	46.56	4.05	46.460	
3		2700.00	8400.00	77600.	46.56	4.05	46.460	
4		2600.00	11000.00	77600.	46.56	3.90	46.460	
5		0.00	11000.00	100.	1.00	0.00	0.000	

MODULUS OF ELASTICITY OF TOWER SHAFT = 2000.

TEMPERATURE = 30.0      NORMAL TEMP. = 30.0

\*\*\* LOCATION DATA \*\*\*

LEVEL	GUY		VERT.	HORIZ.	..... REFERENCE .....		
	SET	TRUE BEG.	HT	A	HANC	A1	LEVER ARM
1	1	60.000	2950.0	6959.0	50.0	7000.0	41.0
1	2	180.000	2950.0	6959.0	50.0	7000.0	41.0
1	3	300.000	2950.0	6959.0	50.0	7000.0	41.0
2	1	60.000	5650.0	6959.0	50.0	7000.0	41.0
2	2	180.000	5650.0	6959.0	50.0	7000.0	41.0
2	3	300.000	5650.0	6959.0	50.0	7000.0	41.0
3	1	60.000	8350.0	6959.0	50.0	7000.0	41.0
3	2	180.000	8350.0	6959.0	50.0	7000.0	41.0
3	3	300.000	8350.0	6959.0	50.0	7000.0	41.0
4	1	0.000	10970.0	11929.0	30.0	12000.0	71.0
4	2	22.500	10970.0	11929.0	30.0	12000.0	71.0
4	3	45.000	10970.0	11929.0	30.0	12000.0	71.0
4	4	67.500	10970.0	11929.0	30.0	12000.0	71.0
4	5	90.000	10970.0	11929.0	30.0	12000.0	71.0
4	6	112.500	10970.0	11929.0	30.0	12000.0	71.0
4	7	135.000	10970.0	11929.0	30.0	12000.0	71.0
4	8	157.500	10970.0	11929.0	30.0	12000.0	71.0
4	9	180.000	10970.0	11929.0	30.0	12000.0	71.0
4	10	202.500	10970.0	11929.0	30.0	12000.0	71.0
4	11	225.000	10970.0	11929.0	30.0	12000.0	71.0
4	12	247.500	10970.0	11929.0	30.0	12000.0	71.0
4	13	270.000	10970.0	11929.0	30.0	12000.0	71.0
4	14	292.500	10970.0	11929.0	30.0	12000.0	71.0
4	15	315.000	10970.0	11929.0	30.0	12000.0	71.0
4	16	337.500	10970.0	11929.0	30.0	12000.0	71.0

DECCA 110 METERS TOWER

\*\* GUY DIMENSION \*\*\*

LEVEL	SER	TENSION	WIRE WEIGHT (T/CM)		DIAM.	SECT. AREA	E	BREAK-UP INSULATOR		
			NO ICE	WITH ICE				NO.	LENGTH	WEIGHT
1	1	5.06	0.1163E-03	0.1163E-03	2.20	2.90	1600.00	0	0.00	0.00
1	2	5.06	0.1163E-03	0.1163E-03	2.20	2.90	1600.00	0	0.00	0.00
1	3	5.06	0.1163E-03	0.1163E-03	2.20	2.90	1600.00	0	0.00	0.00
2	1	4.03	0.1018E-03	0.1018E-03	2.20	2.90	1600.00	0	0.00	0.00
2	2	4.03	0.1018E-03	0.1018E-03	2.20	2.90	1600.00	0	0.00	0.00
2	3	4.03	0.1018E-03	0.1018E-03	2.20	2.90	1600.00	0	0.00	0.00
3	1	4.39	0.8810E-04	0.8810E-04	2.20	2.90	1600.00	0	0.00	0.00
3	2	4.39	0.8810E-04	0.8810E-04	2.20	2.90	1600.00	0	0.00	0.00
3	3	4.39	0.8810E-04	0.8810E-04	2.20	2.90	1600.00	0	0.00	0.00
4	1	0.40	0.9650E-05	0.9650E-05	1.26	0.97	1600.00	0	0.00	0.00
4	2	0.40	0.9650E-05	0.9650E-05	1.26	0.97	1600.00	0	0.00	0.00
4	3	0.40	0.9650E-05	0.9650E-05	1.26	0.97	1600.00	0	0.00	0.00
4	4	0.40	0.9650E-05	0.9650E-05	1.26	0.97	1600.00	0	0.00	0.00
4	5	0.40	0.9650E-05	0.9650E-05	1.26	0.97	1600.00	0	0.00	0.00
4	6	0.40	0.9650E-05	0.9650E-05	1.26	0.97	1600.00	0	0.00	0.00
4	7	0.40	0.9650E-05	0.9650E-05	1.26	0.97	1600.00	0	0.00	0.00
4	8	0.40	0.9650E-05	0.9650E-05	1.26	0.97	1600.00	0	0.00	0.00
4	9	0.40	0.9650E-05	0.9650E-05	1.26	0.97	1600.00	0	0.00	0.00
4	10	0.40	0.9650E-05	0.9650E-05	1.26	0.97	1600.00	0	0.00	0.00
4	11	0.40	0.9650E-05	0.9650E-05	1.26	0.97	1600.00	0	0.00	0.00
4	12	0.40	0.9650E-05	0.9650E-05	1.26	0.97	1600.00	0	0.00	0.00
4	13	0.40	0.9650E-05	0.9650E-05	1.26	0.97	1600.00	0	0.00	0.00
4	14	0.40	0.9650E-05	0.9650E-05	1.26	0.97	1600.00	0	0.00	0.00
4	15	0.40	0.9650E-05	0.9650E-05	1.26	0.97	1600.00	0	0.00	0.00
4	16	0.40	0.9650E-05	0.9650E-05	1.26	0.97	1600.00	0	0.00	0.00

\*\*\* WIND DATA \*\*\*

BASIC WIND VELOCITY = 35.0 M/S  
 STANDARD HEIGHT = 1500. CM  
 ESCALATION CUTOFF HEIGHT = 11000. CM  
 ESCALATION EXPONENT = 0.143000  
 WIND INJECTION ANGLE = 180.000 DEG (TRUE BEARING)  
 MODIFICATION COEFFICIENT OF TOWER INPUT DATA BY CHANGE OF WIND ANGLE

I ..... 1.000  
 CD ..... 1.000

TOWER DATA (2)

SPAN	MOD. I	MOD. CD	WIND LOAD
1	0.7760E+05	1.820	1.863
2	0.7760E+05	1.820	2.362
3	0.7760E+05	1.820	2.718
4	0.7760E+05	1.820	2.869
5	0.1000E+03	1.000	0.000

\*\*\* LOCAL LOAD (AT GUY LEVEL) \*\*\*

LEVEL	LOCAL LOAD			EXT. MOM.	
	VERT.	WINDWARD	NORMAL	WINDWARD	NORMAL
1	1.500	0.250	0.000	0.000	0.000
2	1.510	0.300	0.000	0.000	0.000
3	1.510	0.330	0.000	0.000	0.000
4	0.670	0.300	0.000	0.000	0.000

\*\*\* PULL OFF LOAD (AT TOWER TOP) \*\*\*

TH = 0.00 TM = 0.00 TN = 0.00 TH1 = 0.00 TM1 = 0.00

ERROR FUNCTION SQRT(-X) RESULT=SQRT(ABS(X)) PN=000032 IC=64CF SEG02

ERROR FUNCTION SQRT(-X) RESULT=SQRT(ABS(X)) PN=000032 IC=64CF SEG02

DECCA 110 METERS TOWER

\*\*\* GUY LENGTH \*\*\*

LEVEL	GUY SET	GUY ANGLE (THG)	WITH WIND (CCW)	TENSION	GUY LENGTH UNSTRESSED	CATENARY	GUY TOTAL WEIGHT	WIND VEL. ON GUY
1	1	60.000	300.000	5.060	7557.5	7566.0	0.879	35.8
1	2	180.000	180.000	5.060	7557.5	7566.0	0.879	35.8
1	3	300.000	60.000	5.060	7557.5	7566.0	0.879	35.8
2	1	60.000	300.000	4.029	8965.6	8973.9	0.913	37.9
2	2	180.000	180.000	4.029	8965.6	8973.9	0.913	37.9
2	3	300.000	60.000	4.029	8965.6	8973.9	0.913	37.9
3	1	60.000	300.000	4.391	10866.1	10877.2	0.957	39.7
3	2	180.000	180.000	4.391	10866.1	10877.2	0.957	39.7
3	3	300.000	60.000	4.391	10866.1	10877.2	0.957	39.7
4	1	0.000	0.000	0.398	16246.6	16251.3	0.157	40.7
4	2	22.500	337.500	0.398	16246.6	16251.3	0.157	40.7
4	3	45.000	315.000	0.398	16246.6	16251.3	0.157	40.7
4	4	67.500	292.500	0.398	16246.6	16251.3	0.157	40.7
4	5	90.000	270.000	0.398	16246.6	16251.3	0.157	40.7
4	6	112.500	247.500	0.398	16246.6	16251.3	0.157	40.7
4	7	135.000	225.000	0.398	16246.6	16251.3	0.157	40.7
4	8	157.500	202.500	0.398	16246.6	16251.3	0.157	40.7
4	9	180.000	180.000	0.398	16246.6	16251.3	0.157	40.7
4	10	202.500	157.500	0.398	16246.6	16251.3	0.157	40.7
4	11	225.000	135.000	0.398	16246.6	16251.3	0.157	40.7
4	12	247.500	112.500	0.398	16246.6	16251.3	0.157	40.7
4	13	270.000	90.000	0.398	16246.6	16251.3	0.157	40.7
4	14	292.500	67.500	0.398	16246.6	16251.3	0.157	40.7
4	15	315.000	45.000	0.398	16246.6	16251.3	0.157	40.7
4	16	337.500	22.500	0.398	16246.6	16251.3	0.157	40.7



DECCA 110 METERS TOWER

\*\*\* GUYS FORCE LIST \*\*\*

LEVEL	GUY	TENSION	AT ANCHORAGE			WIND	AT TOWER		AT ANCHORAGE	
			UPLIFT	M	N		NORMAL	VERT.	INITIAL TENSION	
1	1	4.66	1.32	4.11	0.06	-2.11	3.54	2.17	5.06	
1	2	7.53	2.41	6.77	-0.00	6.76	0.00	3.32	5.06	
1	3	4.66	1.32	4.11	-0.06	-2.11	-3.54	2.17	5.06	
2	1	3.72	1.72	2.63	0.09	-1.41	2.28	2.59	4.03	
2	2	7.68	4.16	5.77	-0.00	5.71	0.00	5.13	4.03	
2	3	3.72	1.72	2.63	-0.09	-1.40	-2.28	2.59	4.03	
3	1	3.85	2.22	2.18	0.12	-1.22	1.90	3.12	4.39	
3	2	9.51	6.48	5.93	0.00	5.80	0.00	7.54	4.39	
3	3	3.85	2.22	2.18	-0.12	-1.22	-1.90	3.12	4.39	
4	1	0.06	-0.03	-0.04	-0.00	-0.05	0.00	0.04	0.40	
4	2	0.29	0.12	0.13	0.04	-0.21	0.05	0.20	0.40	
4	3	0.57	0.30	0.34	0.08	-0.34	0.24	0.39	0.40	
4	4	0.86	0.48	0.56	0.11	-0.33	0.52	0.59	0.40	
4	5	1.07	0.60	0.74	0.13	-0.12	0.74	0.76	0.40	
4	6	1.18	0.66	0.85	0.11	0.21	0.79	0.86	0.40	
4	7	1.20	0.66	0.88	0.08	0.52	0.62	0.89	0.40	
4	8	1.17	0.64	0.87	0.04	0.71	0.33	0.87	0.40	
4	9	1.16	0.63	0.86	0.00	0.77	0.00	0.87	0.40	
4	10	1.17	0.64	0.87	-0.04	0.71	-0.33	0.87	0.40	
4	11	1.20	0.66	0.88	-0.08	0.52	-0.62	0.89	0.40	
4	12	1.18	0.66	0.85	-0.11	0.21	-0.79	0.86	0.40	
4	13	1.07	0.60	0.74	-0.13	-0.12	-0.74	0.76	0.40	
4	14	0.86	0.48	0.56	-0.11	-0.33	-0.52	0.59	0.40	
4	15	0.57	0.30	0.34	-0.08	-0.34	-0.24	0.39	0.40	
4	16	0.29	0.12	0.13	-0.04	-0.21	-0.05	0.20	0.40	

DECCA 110 METERS TOWER

\*\*\* TOWER OUTPUT LIST \*\*\*

WIND DIRECTION

LEV	PHI	REACTION		MOMENT		VERTICAL	
		SLOPE K	INTERCEPT O	SLOPE B	INTERCEPT E	SLOPE O	INTERCEPT J
1	1.47697	0.3922	-0.4361	6.7754	-4.4708	0.0792	7.0648
2	1.34221	0.2344	-0.6541	7.7377	-12.8216	0.1202	8.4942
3	1.20745	0.1616	-0.3242	7.8612	2.8597	0.1152	11.1564
4	1.06821	0.0388	0.4014	2.4731	138.1644	0.0307	9.1029

LEVEL	DEFLECTION	REACTION	MOMENT	MOM.PRIME	P
1	7.6	2.55	-289.02	-241.99	60.99
2	15.0	2.87	-249.30	-145.78	47.78
3	22.7	3.34	-316.83	-135.82	31.90
4	30.1	1.57	0.00	212.49	12.65

MOMENT AT BASE = 0.00      SHEAR AT BASE = 0.67      TOTAL CANTILEVER DEFLECTION = 30.055

DECCA 110 METERS TOWER

NORMAL DIRECTION

LEV	PHI	REACTION		MOMENT		VERTICAL	
		SLOPE K	INTERCEPT Q	SLOPE B	INTERCEPT E	SLOPE O	INTERCEPT J
1	1.47697	0.2133	-0.0002	3.6695	-0.0033	0.0046	7.6640
2	1.34221	0.0900	-0.0005	2.9426	-0.0160	0.0056	10.3144
3	1.20745	0.0692	0.0003	3.3327	0.0171	0.0084	13.7721
4	1.06821	0.0390	-0.0001	2.4966	-0.0087	0.0019	10.0251

LEVEL	DEFLECTION	REACTION	MOMENT	MOM.PRIME	P
1	0.0	0.00	-0.06	-0.05	60.99
2	0.0	-0.00	0.25	0.24	47.78
3	-0.0	0.00	-0.29	-0.28	31.90
4	0.0	-0.00	0.00	-0.01	12.65

MOMENT AT BASE = 0.00      SHEAR AT BASE = -0.00      TOTAL CANTILEVER DEFLECTION = 0.001

## Appendix C

### Limitation of Decca service area due to noise

#### 1 Origin and nature of noise

Most of the atmospheric noise in the world originates in thunderstorms. At a given receiving location the atmospheric noise is made up of noise from nearby centres of noise, such as local thunderstorms whose distance from the receiving location may vary from a few miles to hundreds of miles, plus noise which has been propagated from one or more of the principal centres of noise generation, such as the active thunderstorm areas in equatorial Africa, Central America and the East Indies. The location and activity of the various centres vary with time of day and season. The determination of atmospheric noise at a given receiving location is thus a series of radio propagation problems, in which the noise originating in each centre of storm activity produces a definite field intensity at the receiving locations.

#### 2 Interpretations of coverage diagrams based on noise limitations

Too rigid an interpretation should not be made of diagrams intended to show coverage due to noise limitations, owing to the wide range over which the noise level may vary from day to day and hour to hour. Such diagrams must be regarded as presenting an overall picture of the general experience of the System over a period. For this reason the useable range will be considerably greater than that indicated during quiet periods and for certain projects, when advantage can be taken of such quiet periods to fly in areas normally beyond the limiting range, the effective cover of a system may be considerably enlarged. On the other hand, in tropical regions the noise intensity over a small area may on occasions be so great that signals will be blotted out temporarily at points well within the nominal cover.

Determination of effective range  
of a Decca transmitter under given conditions

The factors controlling the effective range of a Decca transmitter are:-

- (i) The mean noise level.
- (ii) The percentage serviceability required and the amount by which the mean noise level may be exceeded during this percentage of the total time.
- (iii) The power radiated by the transmitter.
- (iv) The conductivity of the soil over which the transmission path lies.
- (v) The type of Decca receiver to be used.

A method has been evolved of denoting the value of each factor by a number so that the effective range of a transmitter can be quickly obtained from the sum of the numbers.

The procedure is as follows:-

- (a) From CCIR Figures find the noise zone corresponding to the location of the Decca Chain. For 24 hours main chains use figures for periods 2000 - 2400 and 0000 - 0400.
- (b) From Table I determine the noise level factor for the location and conditions required.
- (c) From Table II find the serviceability factor.
- (d) From Table III find the transmitter power factor.
- (e) From Table IV find the requirement factor.

Add all these together to obtain the Performance Factor and against the line with this total value in the left hand column of Table VI read (in the column headed with the appropriate soil conductivity letter) the effective range. Soil conductivities for various types of terrain are given in Table V.

It is the practice to use 85 kc/s as appropriate to the problem for planning purposes.

Example

What is the effective range of transmitter radiating 200 watts on 85 kc/s by daylight in Maracca Strait to give 98% serviceability of integration of a Mark 10 receiver over  $5 \times 10^{-14}$  e.m.u.

From C.C.I.R Noise Figures derive mean noise zone as 80.

Table I	Noise factor for day working	= 26
Table II	Serviceability factor for 98% service	= 11
Table III	Transmitter power for 200 watts (see table VII)	= 7
Table IV	Requirement factor for Mark 10 integration (Automatic Lane Setting)	= 9
	Performance factor = Total of above	<u>= 53</u>

From Table V it will be seen that the soil conductivity is Group C and looking in column C under 85 kc/s against entry 53 in the performance factor column in Table VI we find a range of 400 kms.

For survey work in choosing the "Requirement factor" it is of interest to note that (for given noise conditions) if the Decca field strength is gradually raised until there is just sufficient torque to operate the decometer, a further increase in level of 6 db will limit the decometer needle kicks to about 0.02 lane, the extent of the kicks being halved each time the field strength is doubled.

If a 95% serviceability level is adopted (requirement factor as given) torque will be maintained for 99.9% of the time and kicks of less than 0.01 lanes will be experienced at 75% of the time.

4 Limitation of range by skywave at night (Mark 10)

The effective range at night may be limited by cancellation or weakening of the groundwave signals reflected from the ionosphere.

For this reason the limit of night range is almost independent of the radiated power and depends only on the ground conductivity. The night skywave range limits are approximately as follows:-

<u>Conductivity Group</u>	<u>Limiting Range (kms)</u>
A	540
B	480
C	430
D	370
E	300

The effective range at night should be taken as the skywave limit or noise limit whichever is the lower.

5 Graph of typical conditions

Graph for the rapid solution of typical requirements is appended.

Drawing Number F.281 For 24 hour operation.

Note that in drawing F.281 during daylight periods, the coverage will be very considerably greater, as can be seen by full computation.

Table I

50% level of atmospheric noise in db  
above 1  $\mu$ v/metre for  $\pm$  30 c.p.s. bandwidth

Period 0800 - 1200 and 1200 - 1600 All Seasons Period 0400 - 0800 and 1600 - 2000 Spring and Summer		
C.C.I.R Noise Zone	Kc/s	
	85	127.5
90	37	33
80	31	27
70	25	21
60	20	15
50	14	8
40	8	2
30	3	- 4
20	- 2	- 9
10	- 6	- 15
0	- 10	- 20
Period 0000 - 0400 and 2000 - 2400 All Seasons Period 0400 - 0800 and 1600 - 2000 Autumn and Winter*		
C.C.I.R Noise Zone	Kc/s	
	85	127.5
100	40	37
90	31	28
80	23	20
70	16	12
60	9	3
50	2	- 5
40	- 4	- 12
30	- 10	- 20
20	- 15	- 29

\*See note under Section 6-3 (a)

Note: For Mark 10 operation having  $\pm$  10 c.p.s. bandwidth lower the figures above by 5 db i.e. for 40 read 35



Table II

Serviceability factor

(Difference in level between average amplitude of noise and amplitude not exceeded for given percentage of time)

Required Serviceability as Percentage of Operating Time	Serviceability Factor	
	85 Kc/s	127 Kc/s
50%	0	0
75%	4	5
90%	7	10
95%	8 1/2	12
98%	11	15
99%	12 1/2	17

Table III

Transmitter power factor

(db below 1 kw radiated power)

Radiated Power (watts)	Power Factor	Radiated Power (watts)	Power Factor
1	30	40	14
1.5	28	50	13
2	27	60	12
2.5	26	80	11
3	25	100	10
4	24	150	8
5	23	200	7
6	22	250	6
8	21	300	5
10	20	400	4
15	16	500	3
20	17	600	2
25	16	800	1
30	15	1,000	0

Table IV

Requirement factor

		REMARKS
Mark 10 Receiver	( $\pm$ 10 c.p.s. bandwidth with locked oscillators)	
Integration	0	
Automatic Lane Setting	9	
8.2f triggering	9	

Table V

Table of soil conductivity

Nature of Terrain	Column to be used in Table VI	Assumed Conductivity (e.m.u.)
Sea Water	A	$5 \times 10^{-11}$
Good Soil	B	$10^{-13}$
Poor Soil	C	$5 \times 10^{-14}$
Sandy dry flat country and rocky soil, fresh water	D	$2 \times 10^{-14}$
Desert and Mountainous	E	$10^{-14}$

Table VI

## Performance factor

(Field strength of groundwave in db above 1 $\mu$ v/metre for transmitter radiating 1 kw)										
85Kc/s						127 Kc/s				
*	A	B	C	D	E	A	B	C	D	E
80	32	32	32	32	32	32	32	32	32	32
78	37	37	37	37	35	37	37	37	37	35
76	45	45	43	42	40	45	45	42	40	39
74	58	56	56	52	48	58	56	53	50	46
72	72	71	71	64	58	72	71	66	60	55
70	90	90	88	80	72	90	90	83	75	67
69	103	101	98	90	80	102	100	90	80	72
68	116	114	109	100	88	115	113	100	90	78
67	130	128	122	111	100	128	126	110	100	85
66	140	137	131	125	120	137	134	120	110	95
65	155	152	145	137	130	151	148	135	120	105
64	180	176	168	154	140	176	172	155	135	115
63	190	184	175	162	150	185	179	165	145	125
62	205	200	190	177	165	200	195	180	155	130
61	230	225	215	195	175	225	220	200	170	140
60	250	245	235	215	190	245	235	215	185	155
59	270	264	249	226	204	265	250	225	195	165
58	290	284	269	244	219	285	270	240	210	175
57	320	313	293	263	233	310	295	260	225	185
56	350	343	323	290	258	340	325	285	240	195
55	380	373	343	308	273	365	345	300	255	205
54	410	403	373	335	298	385	370	320	270	220
53	430	423	383	343	303	415	400	345	285	230
52	460	452	412	370	327	445	425	365	302	240
51	500	492	442	397	352	470	450	390	320	250
50	540	532	480	430	380	500	480	420	340	265
49	570	562	507	452	397	525	500	440	355	275
48	600	592	537	477	417	555	530	465	375	285
47	640	632	572	507	442	590	560	490	395	300
46	675	666	606	536	466	625	590	515	415	315
45	710	701	636	561	486	655	625	540	435	330
44	750	740	675	595	515	690	660	565	455	345
43	790	780	710	625	540	725	690	590	475	360
42	825	825	755	665	575	760	725	620	498	375
41	865	855	775	680	585	795	755	650	520	390
40	900	890	810	710	610	825	785	680	545	410

\* Performance Factor      A       $5 \times 10^{-11}$  e.m.u.  
    B       $10^{-13}$  e.m.u.  
    C       $5 \times 10^{-14}$  e.m.u.  
    D       $2 \times 10^{-14}$  e.m.u.  
    E       $10^{-14}$  e.m.u.

All ranges in Kilometres

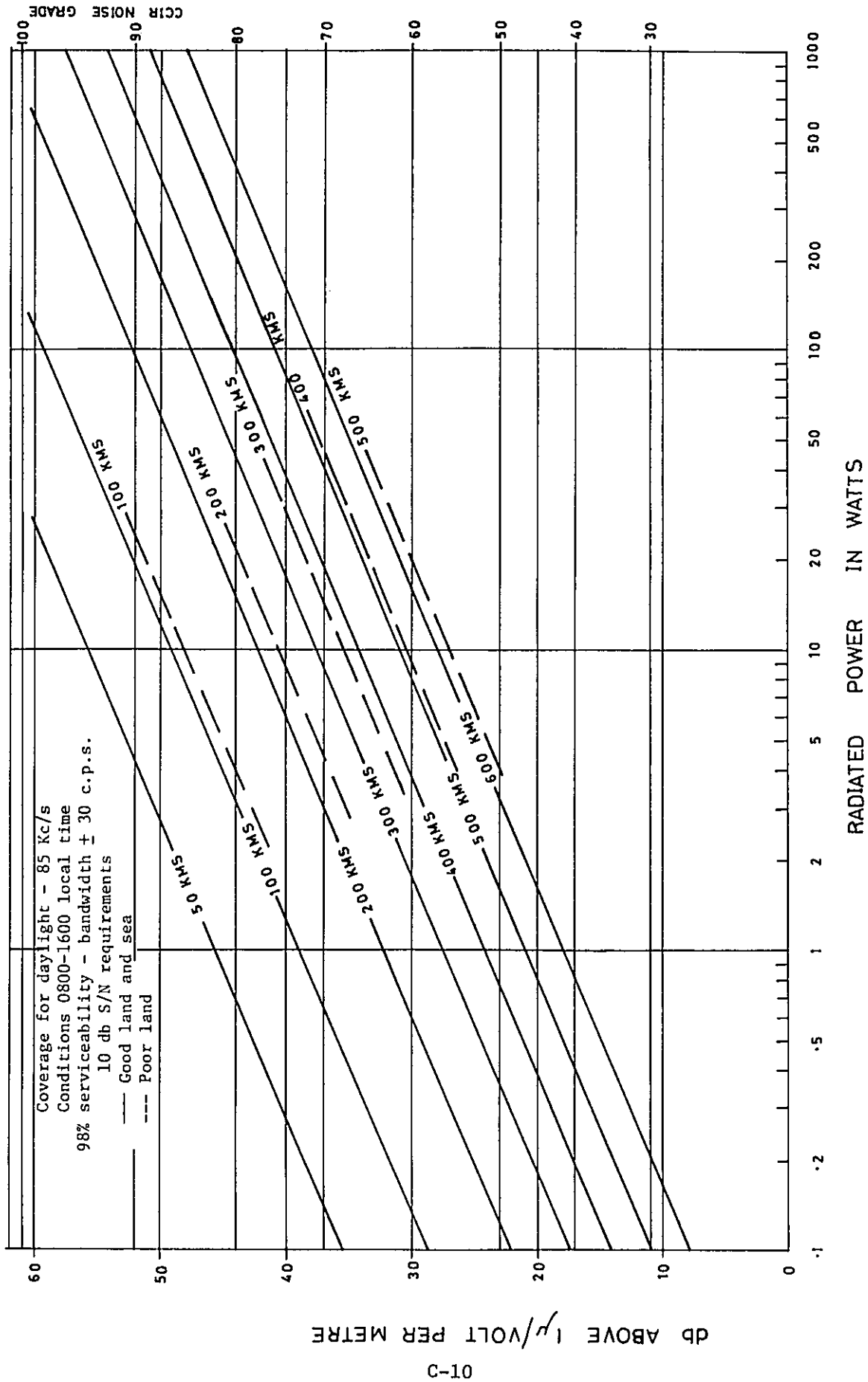
Table VII

Table for estimating radiated power in watts of a Decca station with an input power of 1.2 kilowatts.

Type and Physical Height of Aerial (in feet)		Frequency 85 Kc/s			
		Good Earth		Poor Earth	
		Single Tuned	Double Tuned	Single Tuned	Double Tuned
Umbrella	70	4	3	2	2
	100	7	6	3	3
	150	30	24	13	12
	168	36	30	18	15
	200	60	48	28	24
	300	175	150	85	78
	500	525	480	320	300
	650	750	700	525	500

Notes:

- (1) To obtain radiated power for other input powers multiply the figures shown by the ratio of required input power to 1.2 K/Watts. e.g. If input is 600 watts halve the figures shown.
- (2) To obtain radiated powers for the other main Decca chain frequencies multiply the figures derived from the Table by the following factors:  
Purple 0.7 : Red 1.7 : Green 2.2
- (3) All Mark 10 Chains are 1.2 kilowatt input power at this time and radiated about 70% of the power shown in the "Double Tuned" column.



APPENDIX D: Present and Future Maritime Traffic on Malacca/  
Singapore Straits and Lombok/Makassar Straits

		<u>Page</u>
1.	Analysis of Existing Maritime Traffic .....	D- 1
1-1	The Generated Traffic .....	D- 1
1-2	The Passing Through Traffic .....	D- 7
2.	Forecast of Future Maritime Traffic on the Straits ...	D-13
2-1	The Generated Maritime Traffic on Malacca/Singapore Straits .....	D-14
2-1-1	Forecast of Future Seaborne Cargo Movements Relating to Indonesia, Malaysia and Singapore .....	D-14
2-1-2	Forecast of Future Movement of Petroleum and Petroleum Products Relating to the Countries .....	D-18
2-1-3	Forecast of Future General Cargo Movement Relating to the Countries .....	D-21
2-1-4	Forecast of Future Average Vessel Size and Loading Factor .....	D-21
2-1-5	Growth Rate of the Sea Transport Relating to the Countries .....	D-24
2-2	The Generated Maritime Traffic on Lombok/Makassar Straits .....	D-25
2-2-1	Forecast of Future Seaborne Cargo Movements Relating to Indonesia .....	D-25
2-3	Summary of the Generated Maritime Traffic on Malacca/ Singapore Straits and Lombok/Makassar Straits .....	D-27
2-4	Forecast of Passing Through Traffic on the Straits ..	D-29
2-4-1	Forecast of Passing Through Traffic of Large Tankers .....	D-29
2-4-2	Forecast of Future Passing Through Traffic of General Cargo Vessels and General Tankers .....	D-30
2-5	Forecast of Total Vessel Traffic on the Straits ....	D-32

APPENDIX D: Maritime Traffic on Malacca/Singapore Straits and  
Lombok/Makassar Straits

1. Analysis of Existing Maritime Traffic

The maritime traffic in the peripheral water area around Indonesia, Singapore and Malaysia (called "the Countries" hereinafter) can be stratified into two groups. One is the traffic with origin and/or destination in the Countries (the generated traffic including attracted traffic), and the other is the traffic passing through the seas concerned (the passing through traffic).

1-1 The Generated Traffic

The volume of generated traffic can be estimated by the following method of:

- a) preparation of the inter-regional O-D matrices of seaborne cargo tonnage in the years of 1972 and 1973
- b) traffic assignment to typical sea routes
- c) classification of seaborne cargoes by petroleum/petroleum products and general cargoes
- d) estimation of the conversion rates from cargo tonnage to vessel traffic based on the data from Belawan Port Master Plan to derive the total volume of generated traffic.

The O-D matrix of seaborne cargo tonnage in 1973 gives the overall cargo movement in the water areas concerned. (See the attached O-D matrix) From this, the general trading pattern is analysed, and is shown below:

GENERAL TRADING PATTERN OF THE REGION

(x 1000 ton)

1973	Foreign Trade	* Domestic Trade	Total
Petroleum & Petroleum Products	76,620	15,430	92,050
General cargo	6,830	8,790	15,620
Total	83,450	24,220	107,670

\* Including trade between Indonesia and Singapore, West Malaysia.

The domestic cargo flow was also roughly assigned to sea routes.

In consequence the cargo flow for 1973 on each of the Straits was estimated as follows:

ESTIMATED DOMESTIC CARGO FLOW FOR 1973

Malacca/Singapore Straits	6.50 million ton/year
Lombok/Makassar Straits	2.50 million ton/year



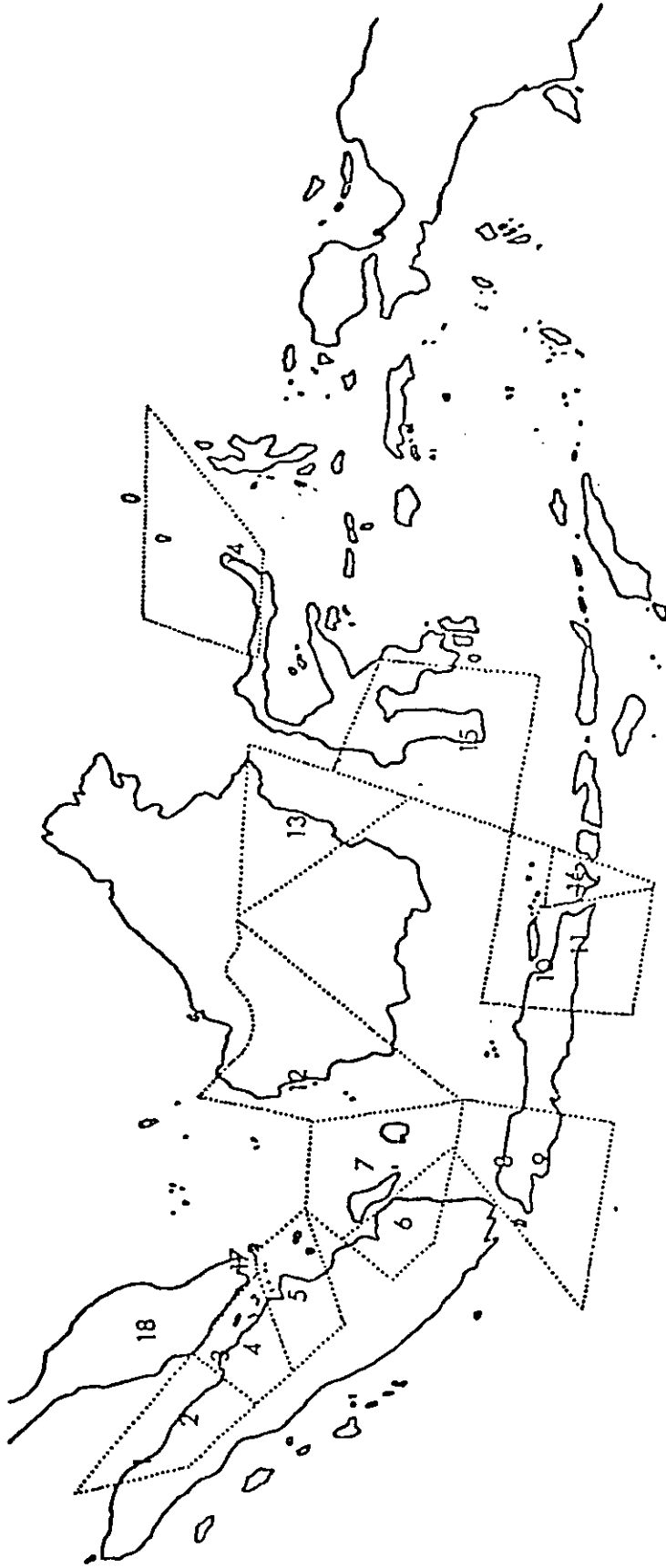
TOTAL DRY CARGO FLOWS (1973) \*100 TON

	01	02	03	04	05	06	07	08	09	10	11	12	13	14	15	16	17	18	19 TOTAL
01	10	135	13	112	26	109	6	749	10	142	2	6	3	0	1	0	849	361	281
02	103	69	41	167	27	52	5	0	0	0	0	0	0	0	0	0	472	1	290
03	0	2	63	54	4	0	0	6	7	0	0	0	5	0	0	0	351	21	16
04	4	49	68	169	35	123	1	104	85	60	0	0	0	0	0	0	2467	2	60
05	15	52	0	59	2186	175	4	5	323	0	0	0	0	0	6	0	855	2	134
06	34	15	0	5	33	2	122	145	323	209	45	6	22	0	0	48	2013	0	564
07	6	6	0	0	1	12	165	104	823	74	1	3	3	0	7	0	230	76	59
08	604	13	3	138	9	76	102	7	0	11	0	325	91	45	282	0	418	3	1261
09	477	1	25	155	218	543	503	0	1	17	0	525	3	0	8	0	2	0	993
10	1455	15	8	252	4	496	155	175	5	17	757	163	1001	200	521	70	1738	12	4547
11	587	37	3	259	7	132	8	43	64	587	451	37	67	0	21	2376	109	0	788
12	0	0	0	12	0	9	1	12	166	7	2	73	0	0	0	0	1726	38	106
13	0	0	0	0	0	4	0	101	25	254	4	0	178	0	24	14	1190	44	213
14	0	0	0	0	0	0	0	155	0	144	0	0	0	2	8	0	129	0	495
15	198	0	0	6	0	163	1	796	5	437	2	38	196	207	9	10	104	0	1846
16	0	0	0	0	0	4	0	3	0	19	576	0	2	0	0	3	5	0	35
17	2066	379	457	78	65	1141	47	3426	48	898	2	137	1235	43	134	43	0	0	2958
18	98	5	64	8	0	1	0	96	1	42	0	0	1	0	0	0	0	0	77
19	150	50	3	163	162	453	29	1306	822	3413	33	677	134	313	465	81	7769	442	6682
TOTAL	5807	828	748	1637	2777	3500	1129	7253	2708	6331	1875	1987	2941	810	1486	2645	20427	1000	22065

TOTAL DRY CARGO FLOWS (1972) \*100 TON

	01	02	03	04	05	06	07	08	09	10	11	12	13	14	15	16	17	18	19 TOTAL
01	4	99	17	93	6	62	0	617	0	145	0	0	0	0	3	0	477	338	130
02	94	93	44	157	17	44	7	1	1	0	0	0	0	0	0	0	108	0	199
03	0	3	28	53	0	1	1	4	23	0	0	25	52	0	0	0	92	3	23
04	11	46	1075	143	22	20	2	132	122	44	0	0	0	0	0	0	1316	41	397
05	35	80	3	52	1501	147	6	7	369	1	1	0	0	3	0	0	373	11	100
06	167	19	22	14	23	3	270	177	270	400	32	5	32	0	4	21	1360	2	1628
07	6	3	0	1	0	21	156	33	1708	84	1	1	0	0	2	0	151	10	69
08	711	11	50	17	6	63	10	3	0	108	26	49	109	51	249	3	505	0	664
09	4	0	16	112	100	451	1037	1	0	271	10	414	12	0	0	0	0	0	717
10	1160	9	3	36	7	584	123	48	1	2	666	171	755	168	435	82	1083	6	3677
11	276	11	1	186	4	122	15	44	87	431	045	45	41	1	20	864	72	170	3768
12	0	0	0	0	0	9	5	24	150	0	2	0	0	0	0	0	2204	170	34
13	0	0	1	0	0	1	0	46	62	175	8	0	122	1	21	2	280	0	86
14	0	0	0	0	0	0	0	124	8	43	0	0	0	1	7	0	102	19	446
15	17	1	0	0	0	10	0	254	0	126	23	23	107	48	2	3	71	0	812
16	4	0	0	0	0	5	0	2	0	46	409	0	3	0	1	4	2	0	65
17	852	164	165	60	46	698	42	3071	0	1462	0	130	167	95	35	46	0	0	1510
18	103	16	45	44	0	1	2	36	0	11	0	0	2	0	0	0	0	0	11
19	165	122	23	213	149	559	71	1314	2114	5055	100	558	429	419	673	63	5027	185	8247
TOTAL	3609	677	1493	1201	1881	2601	1770	5998	4503	8412	2123	1624	1831	787	1457	1088	13313	745	19567

MARITIME REGION MAP



1	Belawan	6	South Sumatera I	11	East Java	16	Bali
2	North Sumatera	7	South Sumatera II	12	West Kalimantan	17	Singapore
3	Dumai	8	DKI JAKARTA	13	East Kalimantan	18	West Malaysia
4	Riau I	9	West Java	14	Bitung	19	Others
5	Riau II	10	Surabaya	15	Makassar		

The international seaborne cargo in 1973 (except for Singapore and Malaysia) was 83.45 million ton/year. The exports accounted for 90.6% or 75.61 million ton/year of a total foreign trade and the imports 9.4% or 7.84 million ton/year.

The orientation and distribution are roughly given below.

East Asia	74.6%
Philippines	4.1%
Others	21.3%

As a result of the traffic assignment to the sea routes the cargo movements for foreign trade on each of the Straits in 1973 was estimated as follows:

ESTIMATED FOREIGN CARGO FLOW FOR 1973

Malacca/Singapore Straits	60.0 million ton/year
Lombok/Makassar Straits	15.0 million ton/year

By using the statistics of the seaborne cargo flow of Indonesia, 1973, a total cargo flow on both Straits can be itemized by type of trade and cargo.

ESTIMATED TOTAL CARGO FLOWS FOR 1973

Malacca/Singapore Straits	Domestic Trade	Foreign Trade	Total (Million ton)
General Cargo	1.10	5.60	6.70
Petroleum & Petroleum Products	5.40	54.40	59.80
Total (Million ton)	6.50	60.00	66.50

Lombok/Makassar Straits	Domestic Trade	Foreign Trade	Total (Million ton)
General Cargo	0.61	1.50	2.11
Petroleum & Petroleum Products	1.89	13.50	15.39
Total (Million ton)	2.50	15.00	17.50

Although vessels carrying the above cargo vary in size and type, an average size and a loading factor were derived from the actual data observed for the Belawan Port. This is summarized as follows:

Items	Average vessel size (dead weight tonnage)	Average loading factor (percentage of capacity)
General Tankers	27,000	35%
General Cargo Vessels	4,500	30%

Therefore, total generated traffic (with origin and/or destination in the Countries) in 1973 on both Straits is estimated as shown in the Table 1-1.

Table 1-1: Total Generated Traffic in 1973 on the Straits

(unit: Vessels/year)

Items	Malacca/Singapore Straits	Lombok/Makassar Straits	Total
General Tankers	6,330 (6,580)	1,630 (1,718)	11,290 (11,840)
General Cargo Vessels	4,960 (5,260)	1,560 (1,792)	3,190 (3,510)
Total	11,290 (11,840)	3,190 (3,510)	14,480 (15,350)

Note: Figures in parentheses show the estimated generated traffic in 1974.

#### 1-2 The Passing Through Traffic

For the analysis of passing through traffic, the following approach was adopted.

- a) the through traffic on the Malacca/Singapore Straits is obtained by deduction of the generated traffic derived in the previous section from a total traffic volume observed by the Port of Singapore Authority.
- b) an assumption is made that on the Lombok/Makassar Straits there is no passing through traffic except for large tankers.

#### <Passing Through Traffic on Malacca/Singapore Straits>

According to the data collected by the Port of Singapore Authority, the maritime traffic observed during each 28-day traffic survey in 1969, 1973 and 1974 is as follows:

Table 1-2: Maritime Traffic Observed by PSA

(Vessels/28 days)

1)	Year	1969 Oct.	1973 Feb./Mar.	1974 Oct.
	Total traffic	3,623	4,019	3,940

2)	By type of Vessel	1969 Oct.	1973 Feb./Mar.	1974 Oct.
	Tankers & Bulk Carriers	1,231 (34.0%)	1,115 (27.7%)	1,249 (31.7%)
	Cargo Ships	1,961 (54.1%)	2,595 (64.6%)	2,170 (55.0%)
	Passenger Ships	27 (0.7%)	38 (1.0%)	52 (1.4%)
	Others	404 (11.2%)	271 (6.7%)	469 (11.9%)

3)	By class of Gross Tonnage	1969 Oct.	1973 Feb./Mar.	1974 Oct.
	Above 30,000 ton	162 (4.5%)	276 (6.9%)	540 (13.7%)
	5,000 ~ 30,000 ton	2,344 (67.7%)	1,857 (4.62%)	1,377 (33.9%)
	75 ~ 5,000 ton	940 (25.9%)	1,882 (4.68%)	2,019 (51.3%)
	Below 75 ton	177 (4.9%)	4 (0.1%)	4 (0.1%)
	more than 180,000 ton Class Vessels in the above are:		46 (1.1%)	more than 150,000 ton Class Vessels in the above are: 39 (1.0%)

The same statistical data also indicates that tanker traffic accounts for 22.2% of the total maritime traffic in 1974.

Combining the data presented so far, the total annual vessel traffic, the generated traffic and the passing through traffic are estimated as following Table 1-3.

Table 1-3: Estimated Distribuion of Total Traffic on Malacca/Singapore Straits in 1974

(Vessels/year)

Items	Total traffic	Generated traffic	Passing through traffic
Large tankers	508	0	508
General tankers	10,894	6,751	4,134
General Cargo Vessels and Others	39,958	5,475	34,483
Total	51,360	12,226	39,134

<Passing Through Traffic on Lombok/Makassar Straits>

The maritime traffic in 1974 on the Lombok/Makassar straits is summarized in the Table 1-4.

It is assumed that there is no passing through traffic except large tankers on the straits.

Table 1-4: Estimated Distribution of Total Traffic  
on Lombok/Makassar Straits in 1974

(Vessels/year)

Items	Total traffic	Generated traffic	Passing Through traffic
Large tankers	30	0	30
General tankers	1,718	1,718	0
General cargo vessels and others	1,792	1,792	0
Total	3,540	3,510	30



Table 1-5: Summary of Maritime Traffic on Malacca/Singapore Straits

(Vessels/year)

Items	1974			1975			1976		
	Generated traffic	Passing through traffic	Total	Generated traffic	Passing through traffic	Total	Generated traffic	Passing through traffic	Total
Large tankers	-	508	508	-	528	528	-	549	549
General tankers	6,580	4,314	10,894	6,840	4,486	11,326	7,111	4,666	11,777
General cargo vessels and others	5,260	34,698	39,958	5,578	36,086	41,664	5,915	37,529	43,444
<b>Total</b>	<b>11,840</b>	<b>39,520</b>	<b>51,360</b>	<b>12,418</b>	<b>41,100</b>	<b>53,518</b>	<b>13,026</b>	<b>42,744</b>	<b>55,770</b>

Note: Annual Growth Rates referred to in Section 2 are used to derive 1975 and 1976 flows.

Table 1-6: Summary of Maritime Traffic on Lombok/Makassar Straits

(Vessels/year)

Items	1974			1975			1976		
	Generated traffic	Passing through traffic	Total	Generated traffic	Passing through traffic	Total	Generated traffic	Passing through traffic	Total
Large tankers	-	30	30	-	31	31	-	32	32
General tankers	1,718	-	1,718	1,811	-	1,811	1,909	-	1,909
General cargo vessels and others	1,792	-	1,792	2,058	-	2,058	2,365	-	2,365
<b>Total</b>	<b>3,510</b>	<b>30</b>	<b>3,540</b>	<b>3,869</b>	<b>31</b>	<b>3,900</b>	<b>4,274</b>	<b>32</b>	<b>4,306</b>

Note: Annual growth rates referred to in Section 2 are used to derive the 1975 and 1976 flows

2. Forecast of Future Maritime Traffic on the Straits

A frame of reference for the prediction of the future maritime traffic comprises the following items.

A. <Malacca/Singapore Straits>

- (a) to built a correlated model equation to estimate total seaborne cargo volume (a total of general cargo and petroleum/petroleum products) loaded and/or unloaded in Indonesia, Singapore and Malaysia in relation with Gross Domestic Product (GDP) of the respective countries.
- (b) to estimate the future movements of petroleum/petroleum products by extrapolation using a trend model.  
for Indonesia, the estimated growth rate derived from the above model can be compared with the projected growth rate given in the Tg. Priok Port Master Plan.
- (c) to estimate the general cargo movements (which have at least a destination or an origin in the Countries) by deducting the movements of petroleum and petroleum products from the total cargo movements estimated in the items (a) and (b) above.
- (d) to estimate a future average size and loading factor for vessels carrying general cargo and petroleum/petroleum products and subsequently to estimate the growth rates of the maritime traffic by type of vessel.
- (e) to estimate the passing through traffic including large tankers on the basis of the analysis of international oil movements and their growth rates.

B. <Lombok/Makassar Straits>

- (f) to built a regression model explaining total Indonesian cargo movement by the annual per capita GDP in Indonesia, subsequently to forecast total cargo movement for future traffic.
- (g) to estimate the general cargo and oil movements in Indonesia using the results derived from the above items (b) and (f).
- (h) to estimate the future maritime traffic by the same approach adopted in the items (a) ~ (e) above.

2-1 The Generated Maritime Traffic on Malacca/Singapore Straits

2-1-1 Forecast of Future Seaborne Cargo Movements Relating to Indonesia, Malaysia and Singapore.

The seaborne cargo which has at least an origin or a destination in the Countries is estimated by a multiple regression model with the independent variables of the GDP in each country and the dependent variable of a total cargo handled at ports of the Countries.

The future projected GDP in the respective countries are extracted from various national plans and government publications.

Both the future GDP and the estimated regression equation are used to forecast the future cargo volume handled in the Countries.

The data for the multiple regression model, cargo handled in each country and its GDP is collated and summarized in the following tables:

Table 2-1: Cargo Loaded and Unloaded at Ports in the Countries

Year	1968	1969	1970	1971	1972	1973	1974
Indonesia	46.0	55.6	64.4	74.1	94.4	113.9	108.5
Malaysia	24.8	26.3	28.2	27.7	27.9	29.4	28.2
Singapore	36.8	39.2	43.6	49.7	57.1	61.3	60.4
Total	107.6	121.1	136.2	151.5	179.4	204.3	197.1

- Note: 1) Iron ore loaded from the Peninsular Malaysia is excluded.  
 2) Crude petroleum transported from Brunei to Sarawak by pipes is excluded.

Table 2-2: Gross Domestic Product of the Countries

Year	1968	1969	1970	1971	1972	1973	1974
Indonesia (Bil. Rp. at 1969 Const. Price)	2,544	2,718	2,923	3,128	3,348	3,620	3,880
Malaysia (Mil. M\$ at 1970 Const. Price)	9,310	10,282	10,708	11,589	12,349	13,867	14,797
Singapore (Mil. S\$ at 1968 Const. Price)	3,971	4,502	5,107	5,747	6,514	7,239	7,731
Malaysia plus Singapore	13,281	14,784	15,815	17,336	18,863	21,106	22,528

Based on the above data, analysis of a multiple regression model was carried out and the most significant model and equation was selected as follows:

$$Y = 0.02835 X_1 + 0.00877X_2 - 84.30396 \quad (R: 0.996)$$

where, Y : cargo handled at ports in the Countries (Mil. ton)

X<sub>1</sub> : GDP of Indonesia

X<sub>2</sub> : total GDP of Malaysia and Singapore

The future GDP projected for Indonesia is taken from the "Indonesia Second Five Year Plan (PELITA II)" and for Malaysia, from the "Third Malaysia Plan". With regard to Singapore such authorized data could not be obtained, so that the future GDP of Singapore was estimated from the data used in the brief report of "Mass Transit Study, 1974".

Based on these publications the projected GDP is assumed to be as follows:

Table 2-3: Future Growth Rate of GDP in the Countries

Country	Years	Annual Growth Rate of GDP
Indonesia	1974 ~ 1979	7.5%
Malaysia	1971 ~ 1975	7.4%
	1976 ~ 1980	8.5%
	1981 ~ 1990	8.1%
Singapore	1972 ~ 1976	7.1%
	1977 ~ 1981	6.1%
	1982 ~ 1992	5.1%

Accordingly, the value of the projected GDP in the respective countries is estimated as in the Table 2-4.

Table 2-4: Projected GDP of the Countries

Year	1975	1980	1985	1990	1995	2000	2010
Indonesia (Bil. Rp. at 1969 Const. Price)	4,086	5,866	8,421	12,090	17,357	24,918	51,357
Malaysia (Mil. M\$ at 1970 Const. Price)	15,315	23,073	34,059	50,097	73,950	109,161	237,862
Singapore (Mil. S\$ at 1968 Const. Price)	8,048	11,290	14,590	18,675	23,902	30,593	50,118

By the estimated regression equation presented earlier the future total cargo volume handled in these countries can be estimated as follows:

Table 2-5: Total Maritime Cargo Volume Handled in the Countries

Year	1975	1980	1985	1990	1995	2000	2010
Total Cargo Volume handled (Mil. ton)	236.4	382.7	581.1	861.6	1265.9	1847.8	3897.3

The assumption was made that the intra-regional cargo movement which is double counted in the above table, is 10% of the total cargo handled at ports in the Countries.

Therefore, the estimated total seaborne cargo handled in the Countries has been adjusted as given in the Table 2-6 to derive the total cargo movement.

Table 2-6: Total Maritime Cargo Movement with Origin and/or Destination in the Countries

Year	1975	1980	1985	1990	1995	2000	2010
Total Cargo Movement (Mil. ton)	212.8	344.4	523.0	775.4	1,139.3	1,663.0	3,507.6

2-1-2 Forecast of Future Movement of Petroleum and Petroleum Products Relating to the Countries

For the estimation of the future movement of petroleum and petroleum products, a trend model was built using data of the past annual increases of oil volume handled at ports in each country as listed in the Table 2-7.

Table 2-7: Petroleum and Petroleum Products Handled at Ports in the Countries

(Unit: Million ton.)

Year	1968	1969	1970	1971	1972	1973	1974
Indonesia <sup>1)</sup>	23.0	29.8	34.5	37.2	45.9	59.0	62.2
Malaysia <sup>2)</sup>	11.7	11.9	12.7	14.7	11.6	11.6	11.0
Singapore <sup>3)</sup>	27.5	29.2	32.5	37.5	45.4	47.0	45.7

- Note: 1) The figures for Indonesia are quoted from the Export-Import data.
- 2) The figures for Malaysia represent a total amount of handled in Peninsular Malaysia, Sarawak and Sabah. The piped from Brunei to Sarawak is excluded.
- 3) The figures for Singapore are quoted from the data on loading-unloading at ports in Singapore.



The future seaborne oil movement of the Countries is extrapolated by a simple regression model in the case of Indonesia and, with regard to Singapore and Malaysia the total sum of the seaborne oil handled in both countries is used to obtain better correlation coefficient.

The parameters in the regression models are estimated as follows:

$$\text{Indonesia : } Y_1 = 6.693X_1 - 13,150 \quad (R = 0.982)$$

where,  $Y_1$  : Petroleum and petroleum products handled at ports in Indonesia (Million ton.)

$X_1$  : Calendar year

$$\text{Malaysia and Singapore : } Y_2 = 3.546X_1 - 6,940 \quad (R = 0.948)$$

where,  $Y_2$  : Petroleum and petroleum products handled at ports in both Malaysia and Singapore

$X_1$  : Calendar year

Thus, the future handling volume of oil at ports in the Countries is calibrated, and summarized in the Table 2-8.

Table 2-8: Forecast of Future Oil Volume Handled at Ports in the Countries

(Unit: 1000 ton)

Year	1975	1980	1985	1990	1995	2000	2010
Indonesia	68.7	102.1	135.6	169.1	202.5	236.0	302.9
Manaysia & Singapore	63.4	81.1	98.8	116.5	134.3	152.0	187.5
Total	132.1	183.2	234.4	285.6	336.8	388.0	490.4

For Indonesia, comparison of the growth rate can be made with the annual growth rate of the oil handling volume at Tg. Priok which is projected in its Port Master Plan.

Table 2-9: Oil Handling Volume Projected at Tg. Priok and that Estimated from the Model

(Unit: 1000 ton)

Year	1980	1985	1990
From the Master Plan	4,250	6,000	7,500
annual growth rate	7.1%	4.6%	
From the estimated regression equation	102,100	135,000	169,000
annual growth rate	5.8%	4.5%	

As seen in the above table, the annual growth rate derived from the Tg. Priok Port Master Plan is a little higher than that derived from the estimated regression equation for whole Indonesian ports. However, it is conceivable that the estimate for the latter should be lower in consideration of the scale of Tg. Priok Port. Therefore, the volume estimated from the equation is adopted to forecast future overall oil handling volume at ports in Indonesia.

Furthermore, in recognition of the fact that the intra-regional seaborne oil cargo movement is double counted in the total oil handling volume at ports in the Countries, it is assumed that the intra-regional oil cargo movement accounts for 10% of the total oil handling volume at ports in the Countries.

Consequently, the future oil movement which has destination and/or origin in Indonesia, Malaysia and Singapore is estimated as follows:

Table 2-10: Forecast of Future Oil Cargo Movement

Year	1975	1980	1985	1990	1995	2000	2010
Oil cargo movement (Mil. ton)	118.9	164.9	211.0	257.0	303.1	349.2	441.4

2-1-3 Forecast of the Future General Cargo Movement Relating to the Countries

The future general cargo movement is estimated by deducting the oil cargo movement from the total seaborne cargo movement forecasted in the previous sections 2-1-1 and 2-1-2. The subtraction is summarized below.

Table 2-11: Forecast of the Future General Cargo Movement

Year	1975	1980	1985	1990	1995	2000	2010
General cargo movement (Mil. ton)	93.9	179.5	312.0	518.4	836.2	1,313.8	3,066.2

2-1-4 Forecast of Future Average Vessel Size and Loading Factor

The Indonesia Five Year Plan (PELITA II) depicts the number of vessels necessary for Regular Liner Service (RLS) routes. It anticipates slightly change in ship size as indicated in the Table 2-12.

Table 2-12: Future Change in Vessel Size for RLS by PELITA II

Year	1974	1975	1976	1977	1978	1979
No. of Vessels	191	203	215	226	237	250
D.W.T.	227,500	239,250	250,000	263,500	273,750	287,750
Av. D.W.T./ Vessel	1,191	1,179	1,165	1,166	1,155	1,151

The Tg. Priok Port Master Plan indicates the future cargo volume and number of vessels as presented in the following table.

Table 2-13: Projected Number of Vessels and Cargo Volume

Year	1980	1985	1990
No. of Vessels	3,284	4,020	4,830
Cargo Tonnage (x 1000)	7,020	11,135	14,800
Av. Cargo Ton/Vessel	2,138	2,770	3,064

The Balawan Port Master Plan Report predicts that loading factor of general cargo vessels will increase on average to 50% in the future.

Therefore for general cargo vessels, the average loading factor, average cargo tonnage and average vessel size in the future are estimated as follows:

Table 2-14: Estimated Future Mutation in Items of General Cargo Vessels Relating to the Countries

Year	1975	1980	1985	1990	2000	2010
Av. Cargo Tonnage (ton/Vessel)	1,500	2,138	2,770	3,064	3,735	4,553
Av. Loading Factor (%)	30	35	40	43	45	50
Av. Vessel Size (D.W.T.)	4,500	6,110	6,925	7,125	8,300	9,100

The future loading factor of general tankers is also estimated to increase from 35% in 1975 up to 50% in the future and the size is assumed to remain constant at 27,000 DWT. The following table represents the estimated future mutation in items of general tankers.

Table 2-15: Estimated Future Mutation in Items of General Tankers Relating to the Countries

Year	1975	1980	1985	1990	2000	2010
Av. Cargo Tonnage (ton)	9,450	10,800	10,800	12,150	13,500	13,500
Av. Loading Factor (%)	35	40	40	45	50	50
Av. Vessel Size (D.W.T.)	27,000	27,000	27,000	27,000	27,000	27,000

## 2-1-5 Growth Rate of the Sea Transport Relating to the Countries

The generated vessel traffic in the peripheral seas of Indonesia, Malaysia and Singapore has been estimated in accordance with the analysis on future cargo movement and changes in characteristic of vessels as explained in the preceding sections.

Based on these assumptions, the calculation of the growth rate of the sea transport which at least has an origin and/or a destination in the Countries has been carried out and the result is given in the Table 2-16 by type of vessels.

Table 2-16: Growth Rate of the Sea Transport (1975 = 1.000)

Year	1975	1980	1985	1990	2000	2010
General Tanker	1.000	1.214	1.553	1.681	2.056	2.559
General Cargo Vessel	1.000	1.341	1.799	2.703	5.619	10.758

2-2 The Generated Maritime Traffic on Lombok/Makassar Straits

2-2-1 Forecast of Future Seaborne Cargo Movements Relating to Indonesia

The Table 2-17 gives the seaborne cargo volume dealt with in the inter-island and the international trades of Indonesia.

Table 2-17: Cargo Volume Moved for the Inter-island and International Trades

(Mil. ton)

Year	1969	1970	1971	1972	1973	1974
Inter-island Trade	31.2/2	22.9/2	26.2/2	27.6/2	33.9/2	33.0/2
International Trade	24.4	38.2	48.0	67.1	79.6	76.2
Total	40.0	49.7	61.1	80.9	96.6	92.7

"Cargo loading and unloading at Ports in Indonesia"

Source: Biro Pusat Statistik

During the same period per capita GDP of Indonesia shows the following growth.

(X1000R.P)

Year	1969	1970	1971	1972	1973	1974
Per Capita GDP at 1969 cost. Price	23.9	25.2	26.2	27.4	28.7	30.0

Making use of the above data a regression model was built relating per capita GDP to sea cargo movement.

If the figures in 1974 are precluded, to obtain a better correlation coefficient, then the following regression equation can be established.

$$Y = 12.232X - 255.797 \quad (R = 0.991)$$

where, Y : seaborne cargo movement (mil. ton)

X : per capita GDP (x 1000 R.P.)

The future per capita GDP in Indonesia is projected as in the table 2-18, so that the above equation affords the future seaborne cargo movement of Indonesia as listed in the Table 2-19.

Table 2-18: Projected Future per Capita GDP of Indonesia

(x 1,000 Rp)

Year	1975	1980	1985	1990	2000	2010
Per Capita GDP at 1969 Price	30.9	42.5	53.9	71.7	124.6	217.1

Table 2-19: Forecast of Future Seaborne Cargo Movement of Indonesia

(Mil. ton)

Year	1975	1980	1985	1990	2000	2010
Seaborne Cargo Movement	122.2	264.1	403.5	621.2	1,268.3	2,399.8

The future oil movement by vessels has been already estimated in the section 2-1-2 and listed in the Table 2-8.

Therefore, the seaborne cargo movement for Indonesia is stratified by cargo type as follows:



Table 2-20: Seaborne Cargo Movement by Cargo Type for Indonesia

Year	1975	1980	1985	1990	2000	2010
Oil Cargo Movement (Mil. ton)	61.8	91.9	122.0	152.2	212.4	272.6
General Cargo Movement (Mil. ton)	60.4	172.2	281.5	469.0	1,055.9	2,127.2

By using the loading factor and the size of vessels estimated in 2-1-4, Tables 2-14 and 2-15, the generated vessel traffic can be estimated, while the growth rate is summarized as follows:

Table 2-21: Growth Rate of the Generated Vessel Traffic Related to Indonesia

(1975 = 1.000)

Year	1975	1980	1985	1990	2000	2010
General Tankers	1.000	1.301	1.727	1.915	2.406	3.088
General Cargo Vessels	1.000	2.000	2.524	3.801	7.021	11.603

2-3 Summary of the Generated Maritime Traffic on Malacca/Singapore Straits and Lombok/Makassar Straits

The future growth rates have been estimated in the Tables 2-16 and 2-21 with regard to the maritime traffic generated and/or attracted in the peripheral seas of Indonesia, Singapore and Malaysia.

In order to predict the future generated traffic on each of the Straits, the present vessel traffic in 1975 listed in the Tables 1-3 and 1-4 is multiplied by the growth rates above.

The summary of such traffic is then given below.

Table 2-22: The Generated Maritime Traffic on the Straits

Type of Vessel		1975	1980	1985	1990	2000	2010
M/S Straits	General Tankers	6,840	8,304	10,623	11,498	14,063	17,504
	General Cargo Vessels	5,578	7,480	10,035	15,077	31,343	60,008
	Total	12,418	15,784	20,658	26,575	45,406	77,512
L/M Straits	General Tankers	1,811	2,356	3,128	3,468	4,357	5,447
	General Cargo Vessels	2,058	4,116	4,635	7,822	14,449	23,879
	Total	3,869	6,472	7,763	11,290	18,806	29,326

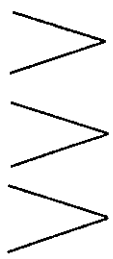
(Vessels/year)

2-4 Forecast of Passing Through Traffic on the Straits

2-4-1 Forecast of Passing Through Traffic of Large Tankers

The recession which started towards the end of 1973 had a direct impact on the world economy and on the world wide movement of crude oil and oil products. However the annual growth rate of seaborne oil in the world has been in a gradual decline as shown in the Table 2-23.

Table 2-23: Crude Oil Movement in the World

Year	Crude Oil Movement	Annual Average Rate of Growth	
1965	730 x 10 <sup>6</sup> ton	 11.0%	
1970	1,228 x 10 <sup>6</sup> ton		
1973	1,627 x 10 <sup>6</sup> ton		9.8%
1974	1,656 x 10 <sup>6</sup> ton		7.8%

It is estimated that the growth rate of seaborne oil will also be lower in the future. Assuming that the average size and loading ratio of large tankers are hardly changed in future the growth rate of their traffic is estimated as follows:

Table 2-24: Annual Growth Rate of Large Tanker's Traffic

Years	Annual Growth Rate	Growth Rate against 1975 Traffic
1975 ~ 1980	4%/year	(1.217)
1980 ~ 1985	4%/year	(1.480)
1985 ~ 1990	6%/year	(1.981)
1990 ~ 2000	6%/year	(3.547)
2000 ~ 2010	4%/year	(5.250)

2-4-2 Forecast of Future Passing Through Traffic of General Cargo Vessels and General Tankers

For lack of adequate data on through traffic of such vessels the annual growth rates of large tankers are also applied to general tankers and general cargo vessels. Furthermore, it is assumed that the future through traffic of general tankers will be of the same ship size and loading factor as the corresponding generated traffic referred to in Table 2-15, while that of general cargo vessels remains constant in either size or loading factor, 13,000 D.W.T. and 50% respectively.

The summary of the through vessel traffic on each of the Straits is shown in the Tables 2-25 and 2-26.

Table 2-25: Forecast of Future Through Traffic  
on Malacca/Singapore Straits

(Vessels/year)

Year	1975	1980	1985	1990	2000	2010
Large Tankers	528	643	781	1,046	1,873	2,772
General Tankers	4,486	5,459	6,639	8,887	15,912	23,552
General Cargo Vessels	36,086	43,917	53,407	71,486	127,997	189,452
Total	41,100	50,019	60,827	81,419	145,782	213,004

Table 2-26: Forecast of Future Through Traffic  
on Lombok/Makassar Straits

(Vessels/year)

Year	1975	1980	1985	1990	2000	2010
Large Tankers	31	38	46	61	110	163
General Tankers	-	-	-	-	-	-
General Cargo Vessels	-	-	-	-	-	-
Total	31	38	46	61	110	163

2-5 Total Vessel Traffic Forecasted on the Straits

Through the section 2-1 to 2-4, the generated and through vessel traffic on each of the Straits has been estimated by type of vessel. This data is now summarized in Tables 2-27 and 2-28.

Table 2-27: Future Vessel Traffic on Malacca/Singapore Straits

(Vessels/year)

Year	1975	1980	1985	1990	2000	2010
Large Tanker	528	643	781	1,046	1,873	2,772
General Tankers	11,326	13,763	17,262	20,385	29,975	41,056
-----	-----	-----	-----	-----	-----	-----
Generated traffic	6,840	8,304	10,623	11,498	14,063	17,504
Through traffic	4,486	5,459	6,639	8,887	15,912	23,552
General Cargo Vessels	41,664	51,397	63,442	86,563	159,340	249,460
-----	-----	-----	-----	-----	-----	-----
Generated traffic	5,578	7,480	10,035	15,077	31,343	60,008
Through traffic	36,086	43,917	53,407	71,486	127,997	189,452
Total	53,518	65,803	81,485	107,994	191,188	290,516
-----	-----	-----	-----	-----	-----	-----
Generated traffic	12,418	15,784	20,658	26,575	45,406	77,512
Through traffic	41,100	50,019	60,827	81,419	145,782	213,004

Table 2-28: Future Vessel Traffic on Lombok/Makassar Strait

(Vessels/Year)

Year	1975	1980	1985	1990	2000	2010
Large Tankers	31	38	46	61	110	163
General Tankers	1,811	2,356	3,128	3,468	4,357	5,447
Generated traffic	1,811	2,356	3,128	3,468	4,357	5,447
Through traffic	-	-	-	-	-	-
General Cargo Vessels	2,058	4,116	4,635	7,822	14,449	23,879
Generated traffic	2,058	4,116	4,635	7,822	14,449	23,879
Through traffic	-	-	-	-	-	-
Total	3,900	6,510	7,763	11,351	18,916	29,489
Generated traffic	3,869	6,472	7,763	11,290	18,806	29,326
Through traffic	31	38	46	61	110	163

REPORT ON THE ESTABLISHMENT OF ELECTRONIC AND  
OTHER NAVIGATION AID SYSTEMS PROJECT

MALACCA/SINGAPORE STRAITS &  
LOMBOK/MAKASSAR STRAITS

1978

100  
557  
500